Supplementary Materials

Computationally Assisted Lead Optimization of Novel Potent and Selective MAO-B Inhibitors

Vedanjali Gogineni [1,2]**, Manal A. Nael** [3,4,†]**, Narayan D. Chaurasiya** [5,6,†]**, Khaled M. Elokely** [3,4]**, Christopher R. McCurdy** [1,7]**, John M. Rimoldi** [1]**, Stephen J. Cutler** [1,8]**, Babu L. Tekwani** [5,6,*] **and Francisco León** [1,8,*]

[1] Department of BioMolecular Sciences, Division of Medicinal Chemistry, University of Mississippi, Oxford, MS 38677, USA; gogineni@musc.edu (V.G.); cmccurdy@cop.ufl.edu (C.R.M.); jrimoldi@olemiss.edu (J.M.R.); sjcutler@cop.sc.edu (S.J.C.)

[2] Affiliate Instructor, Drug Discovery and Biomedical Sciences, College of Pharmacy, Medical University of South Carolina, Charleston, SC 29425, USA

[3] Department of Chemistry and ICMS, Temple University, Philadelphia, PA 19122, USA; manal.nael@temple.edu (M.A.N.); kelokely@temple.edu (K.M.E.)

[4] Department of Pharmaceutical Chemistry, Faculty of Pharmacy, Tanta University, Tanta 31527, Egypt

[5] Division of Drug Discovery, Southern Research, Birmingham, AL 35205, USA; nchaurasiya@southernresearch.org

[6] National Center for Natural Products Research, Research Institute of Pharmaceutical Sciences, University of Mississippi, Oxford, MS 38677, USA

[7] Department of Medicinal Chemistry, College of Pharmacy, University of Florida, Gainesville, FL 32610, USA

[8] Department of Drug Discovery and Biomedical Sciences, College of Pharmacy, University of South Carolina, Columbia, SC 29208, USA

* Correspondence: btekwani@southernresearch.org (B.L.T.); jleon@mailbox.sc.edu (F.L.)

† These authors contributed equally to this study.

Table of Contents   **Pages**

Figure S1. ^{1}H NMR spectrum of chalcone (1a) in CDCl$_3$, 400 MHz


Figure S2. ^{13}C NMR spectrum of chalcone (1a) in CDCl$_3$, 100 MHz
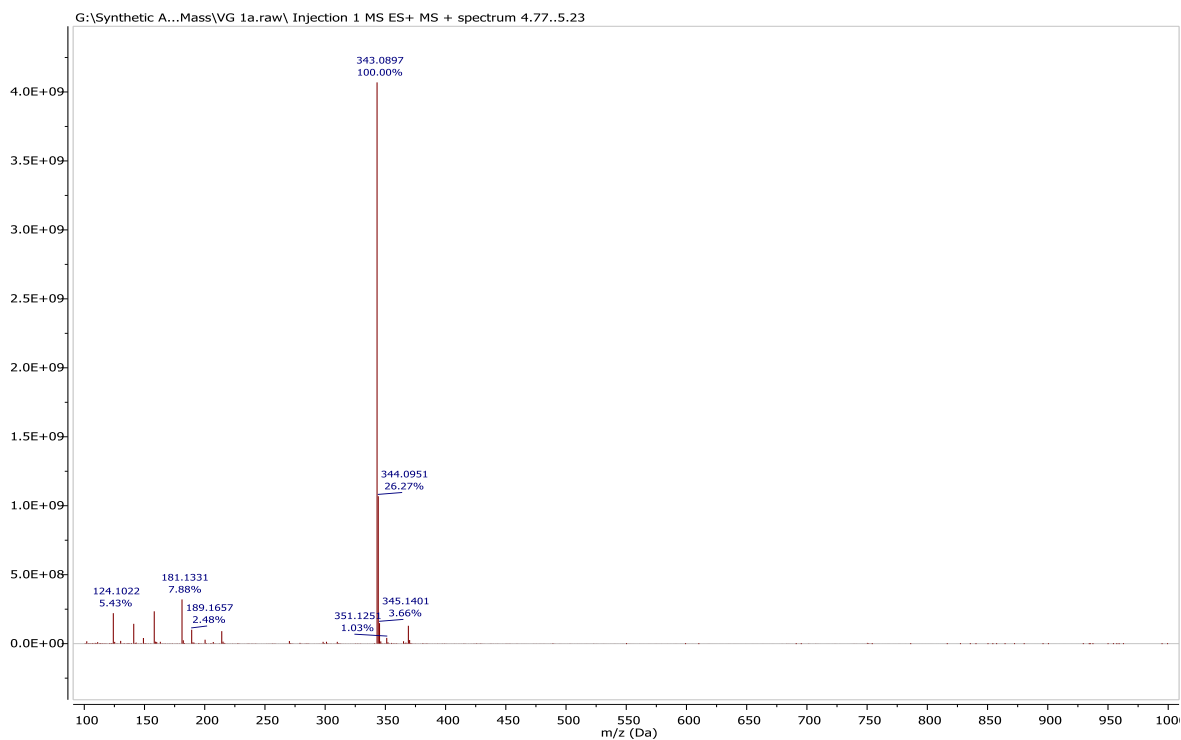
**Figure S3. ESIMS spectrum of chalcone (1a).**
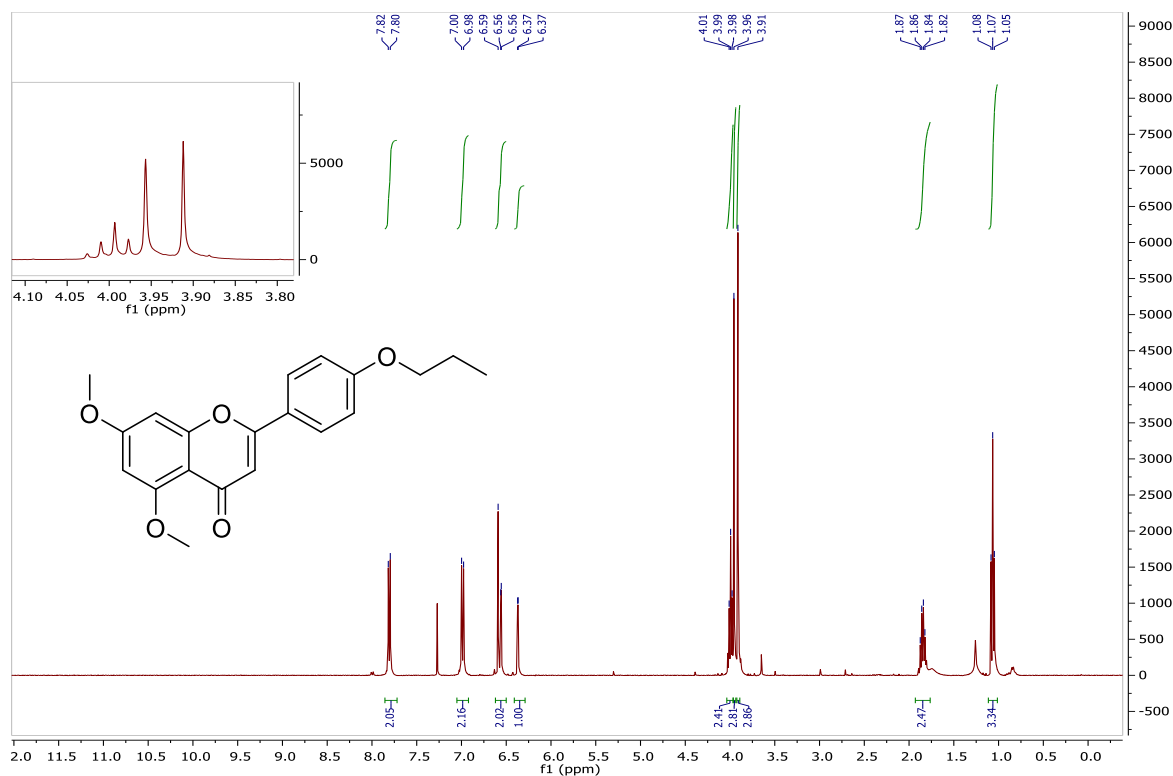
Figure S4. ^{1}H NMR spectrum of flavonoid (1b) in CDCl$_3$, 400 MHz
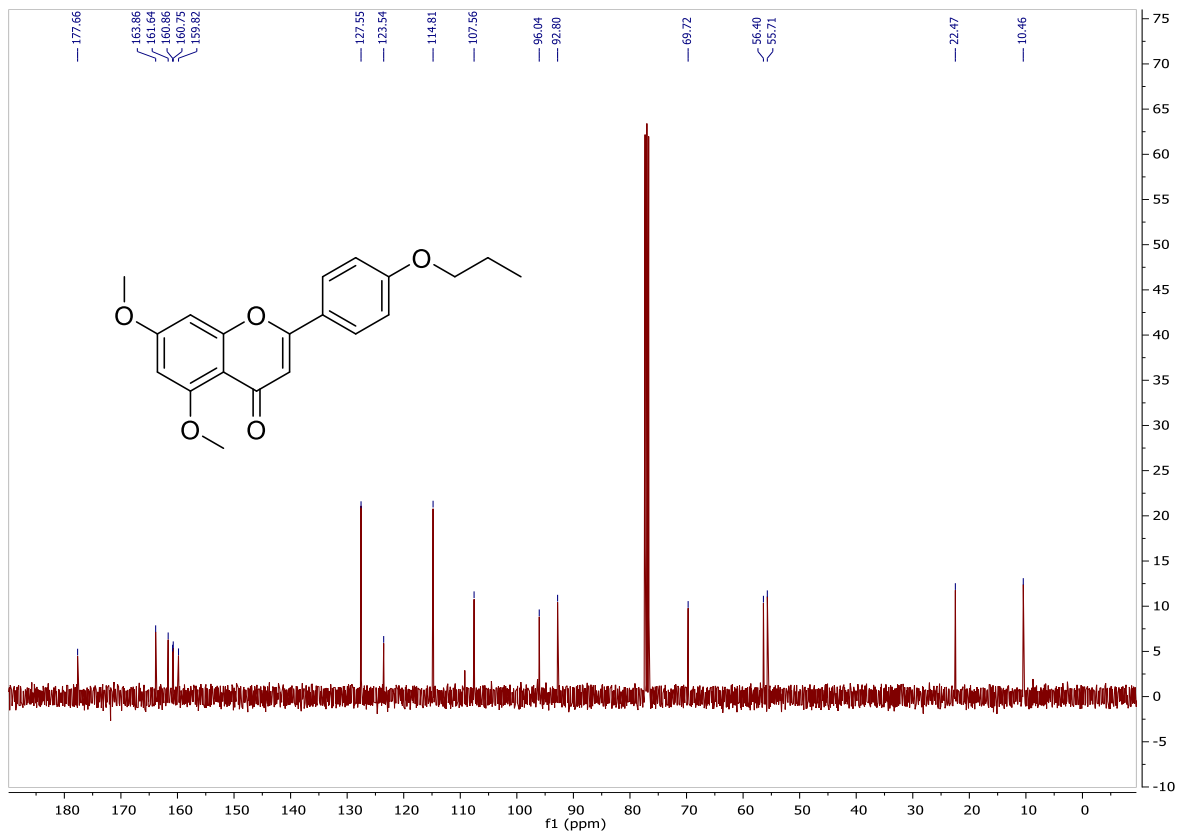
Figure S5. ^{13}C NMR spectrum of flavonoid (1b) in CDCl$_3$, 100 MHz
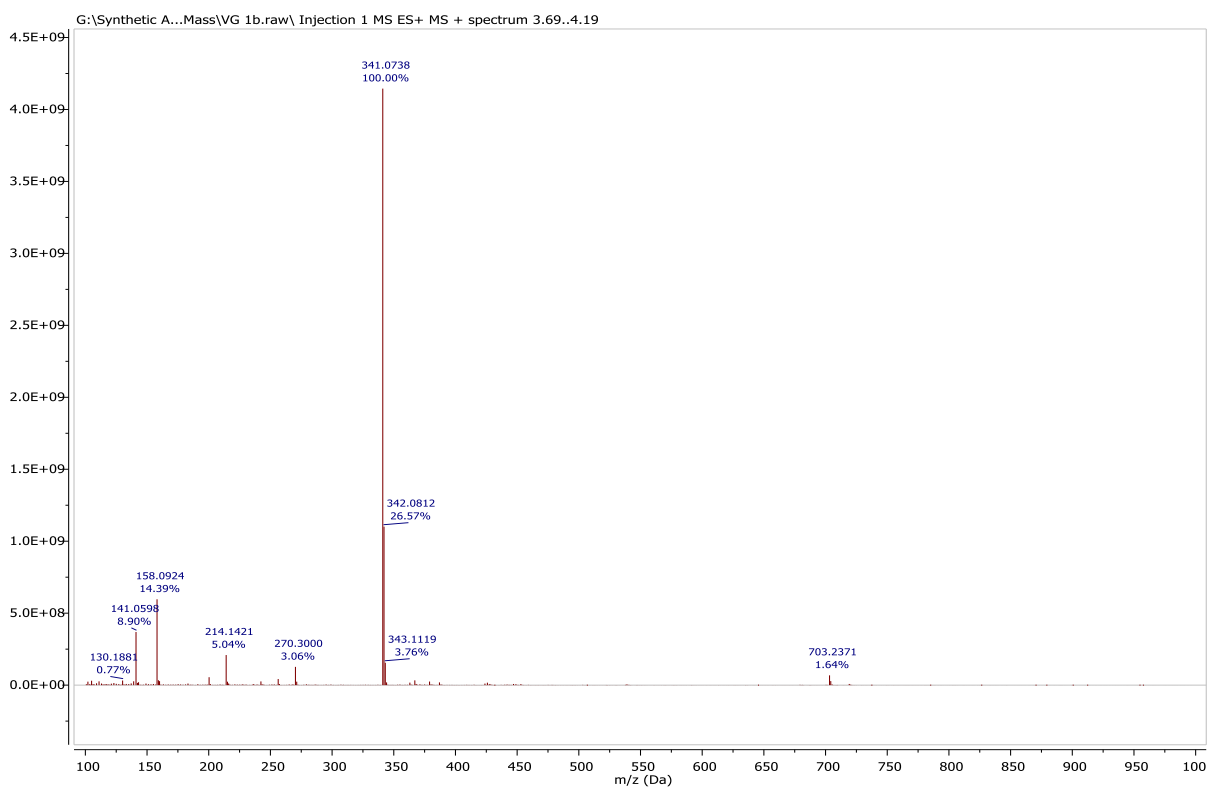
Figure S6. ESIMS spectrum of flavonoid (1b).
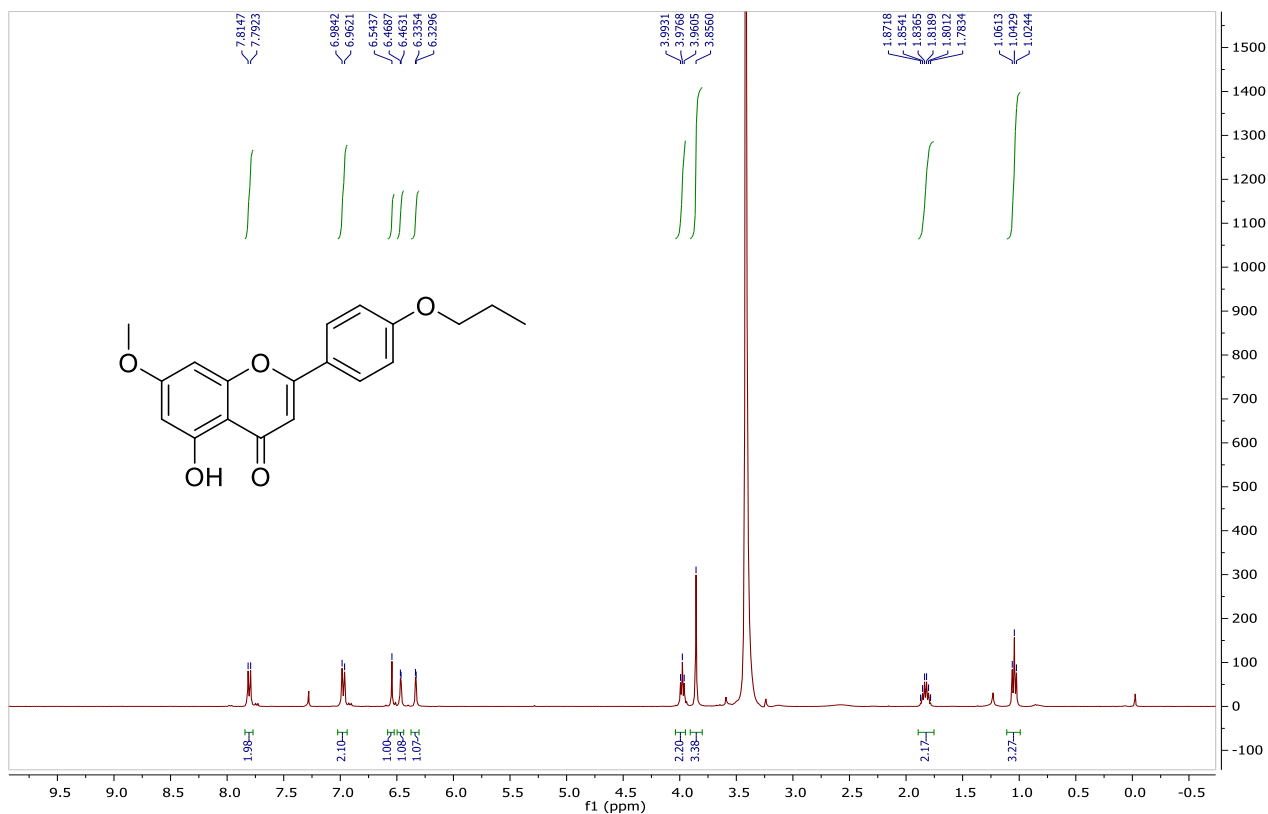
Figure S7. ^{1}H NMR spectrum of flavonoid (1c) in CDCl$_3$, 400 MHz
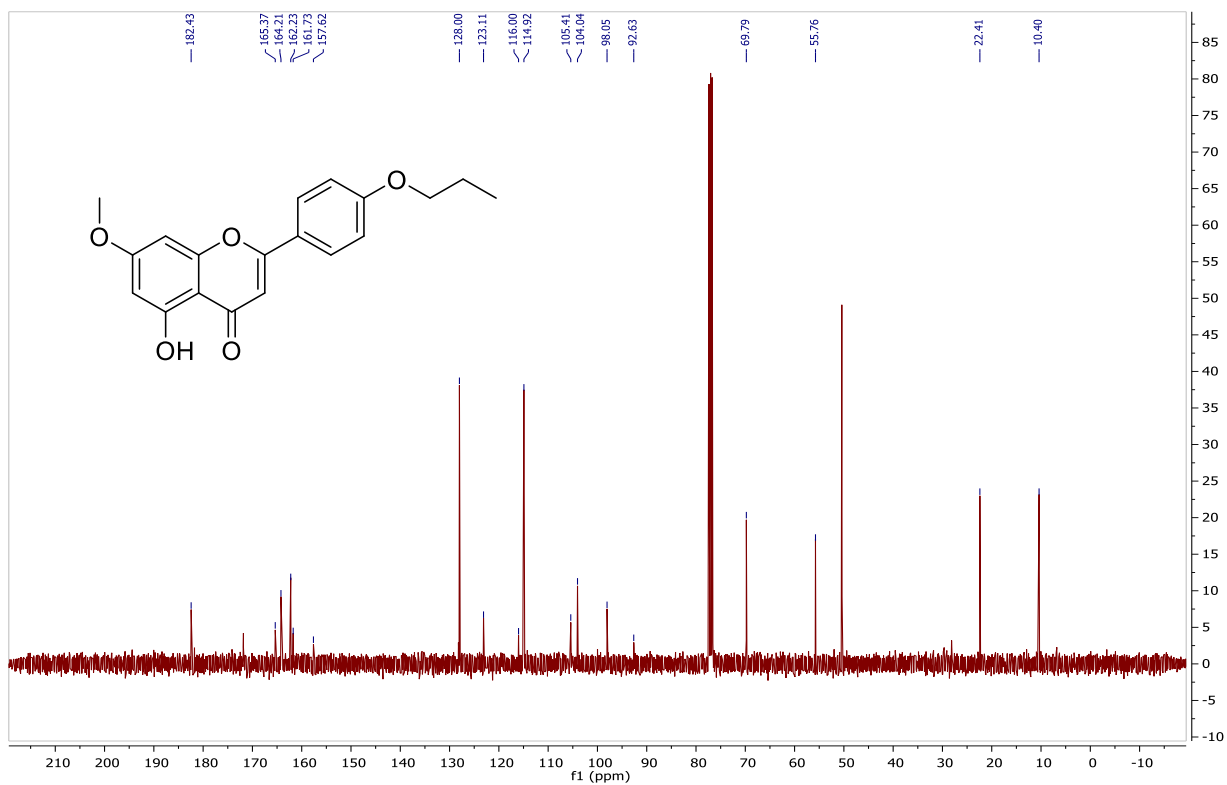
Figure S8. ^{13}C NMR spectrum of flavonoid (1c) in CDCl$_3$, 100 MHz

VG-1c

Formula	Calculated Mass	Target Mass	Double Bond Equivalence	Absolute Error (ppm)	Error (mDa)	Error (ppm)	Fitness
1 C9 H20 N5 O4 S2	327.10295	327.10379	2.5	2.59	0.84	2.59	—
2 C9 H12 N9 O5	327.10342	327.10379	8.5	1.15	0.37	1.15	—
3 C19 H18 O3 S	327.10494	327.10379	11.0	3.53	-1.15	-3.53	—
4 C17 H16 N3 O2 S	327.10360	327.10379	11.5	0.59	0.19	0.59	—
5 C16 H14 N6 O S	327.10226	327.10379	12.0	4.70	1.53	4.70	—
6 C12 H26 N2 S4	327.10516	327.10379	1.0	4.20	-1.37	-4.20	—
7 C11 H22 N2 O5 S2	327.10429	327.10379	2.0	1.53	-0.50	-1.53	—
8 C11 H14 N6 O6	327.10476	327.10379	8.0	2.97	-0.97	-2.97	—
9 C10 H18 N2 O10	327.10342	327.10379	3.0	1.13	0.37	1.13	—
10 C10 H16 N9 S2	327.10428	327.10379	7.5	1.52	-0.49	-1.52	—

Figure S9. ESIMS of flavonoid (1c).

	RT	Area	% Area	Height
1	2.025	44612	1.11	2653
2	5.135	58004	1.45	3804
3	8.592	3898897	97.44	123939
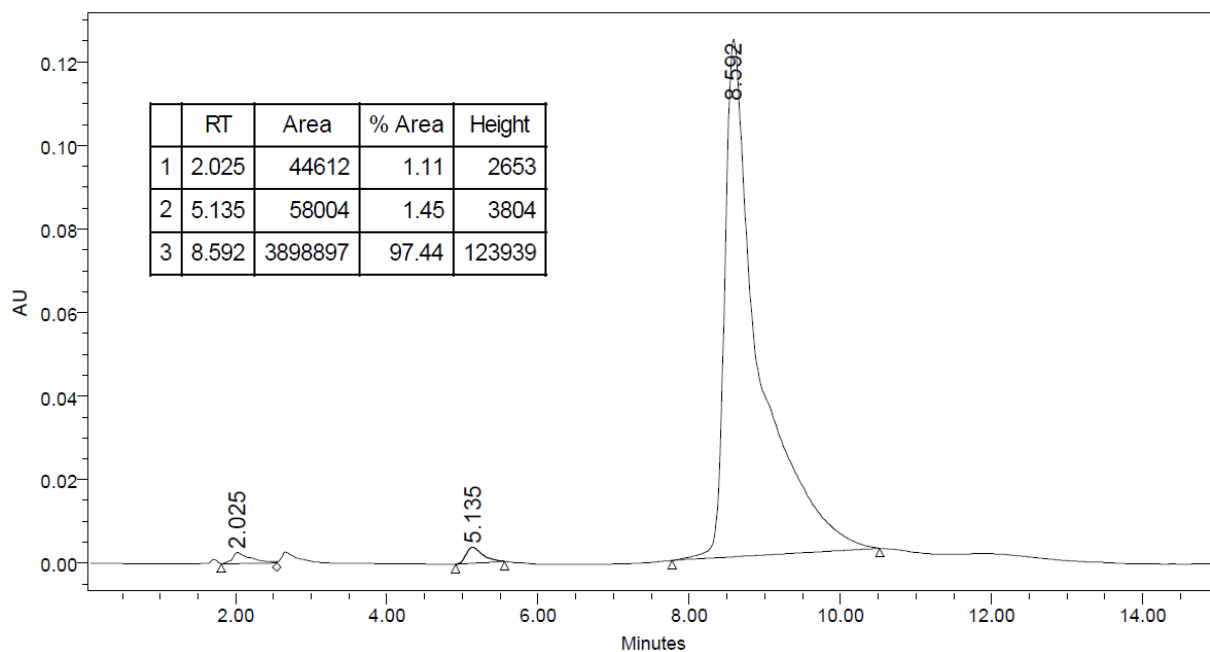
Figure S10. HPLC analysis of flavonoid (1c).
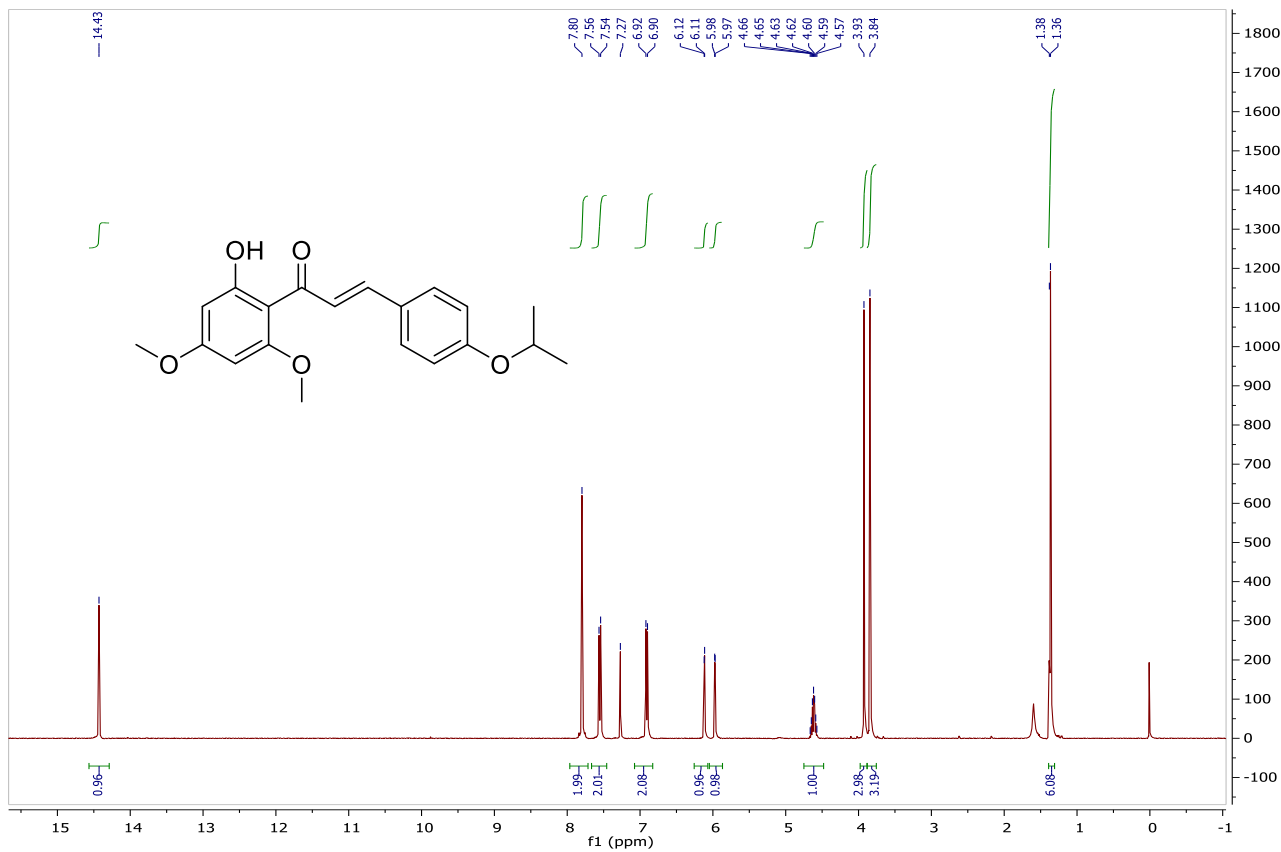
Figure S11. ^{1}H NMR spectrum of chalcone (2a) in CDCl$_3$, 400 MHz
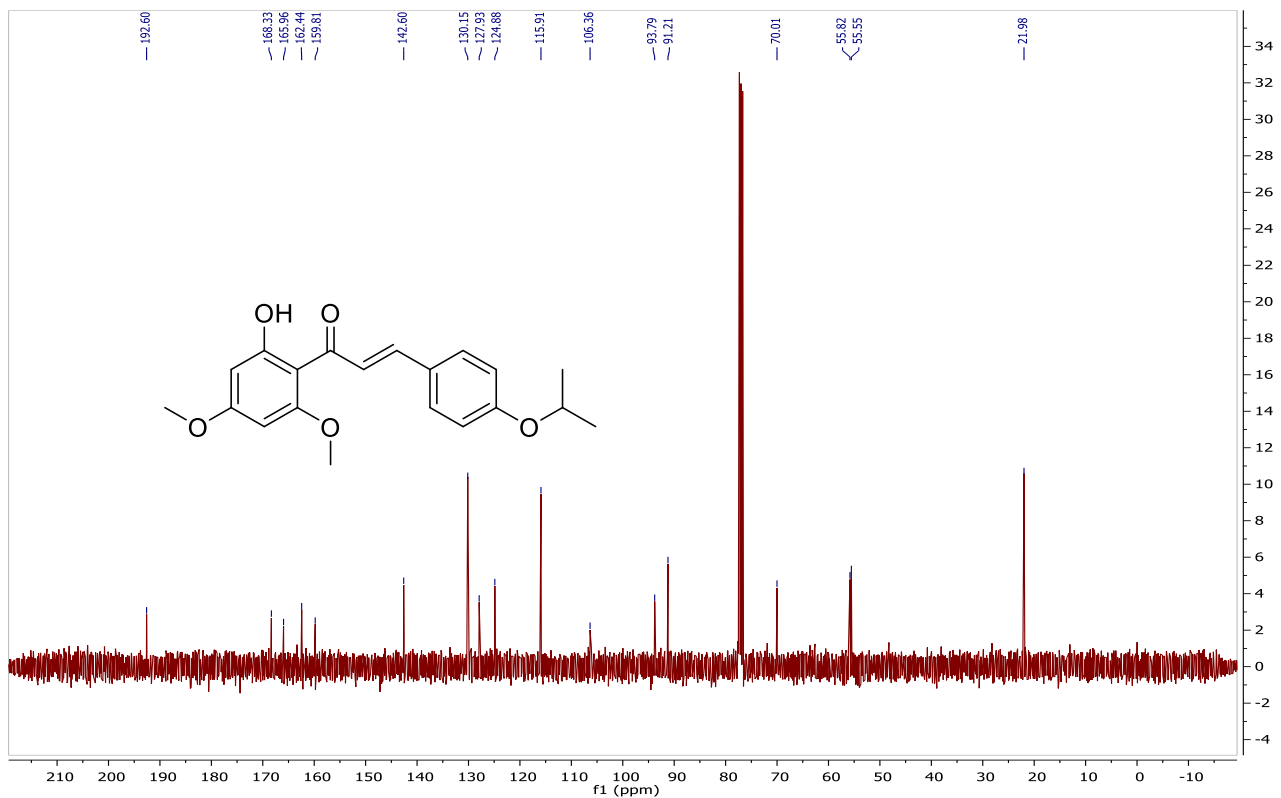
Figure S12. ^{13}C NMR spectrum of chalcone (2a) in CDCl$_3$, 100 MHz
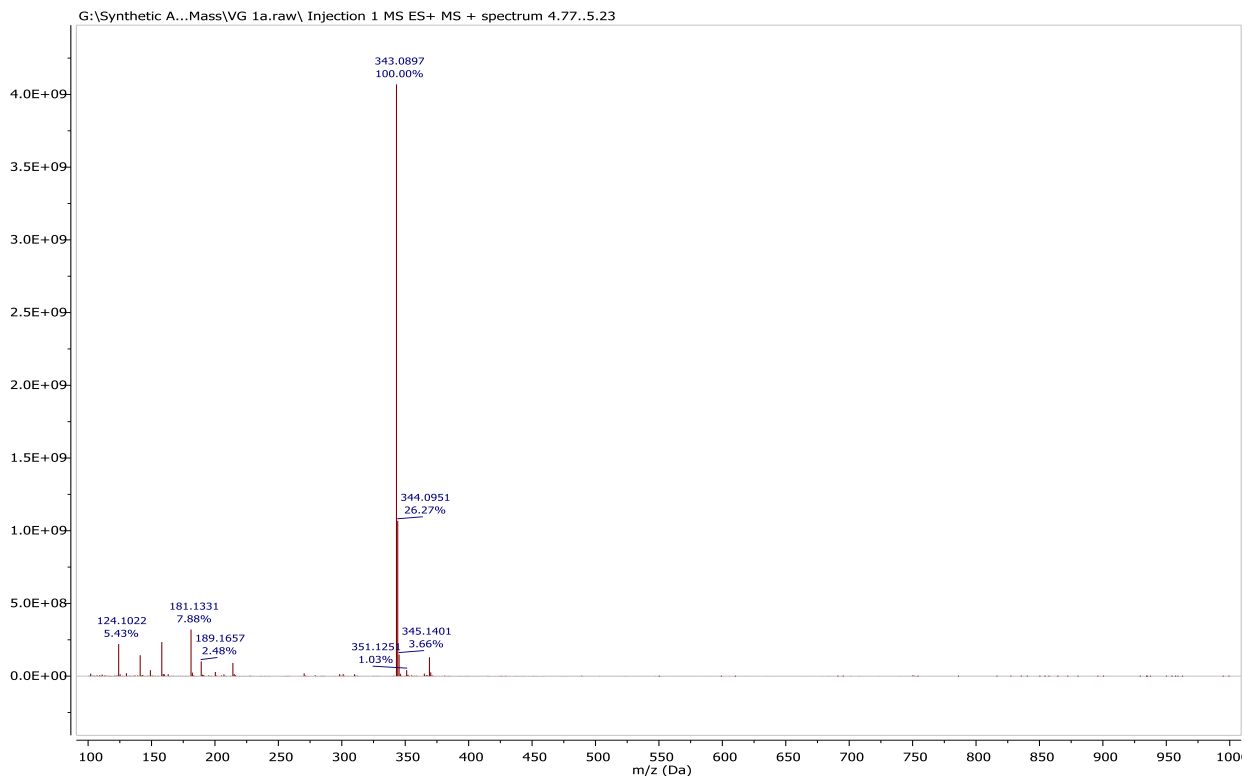
Figure S13. ESIMS spectrum of chalcone (2a).
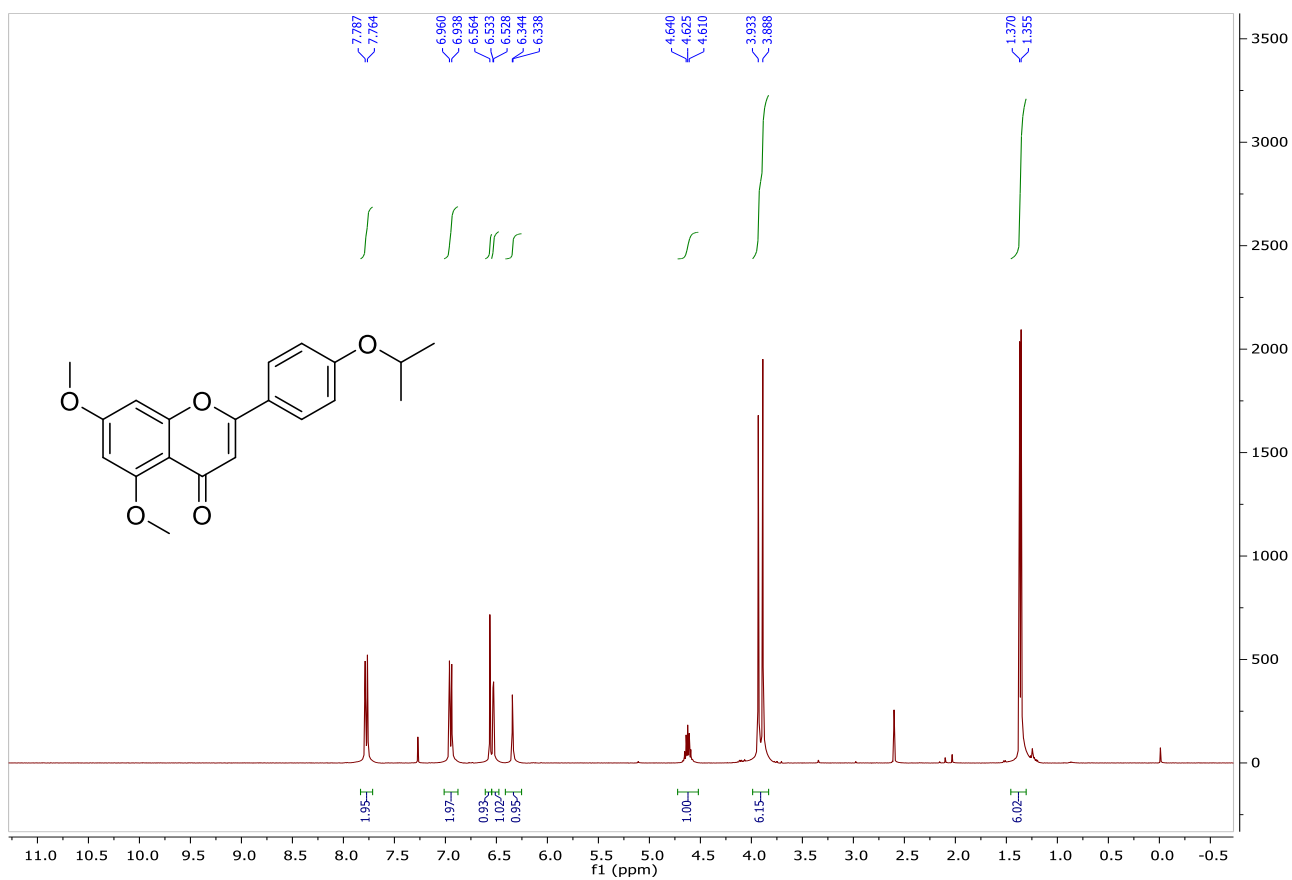
**Figure S14. ^{1}H NMR spectrum of flavonoid (2b) in CDCl$_3$, 400 MHz**
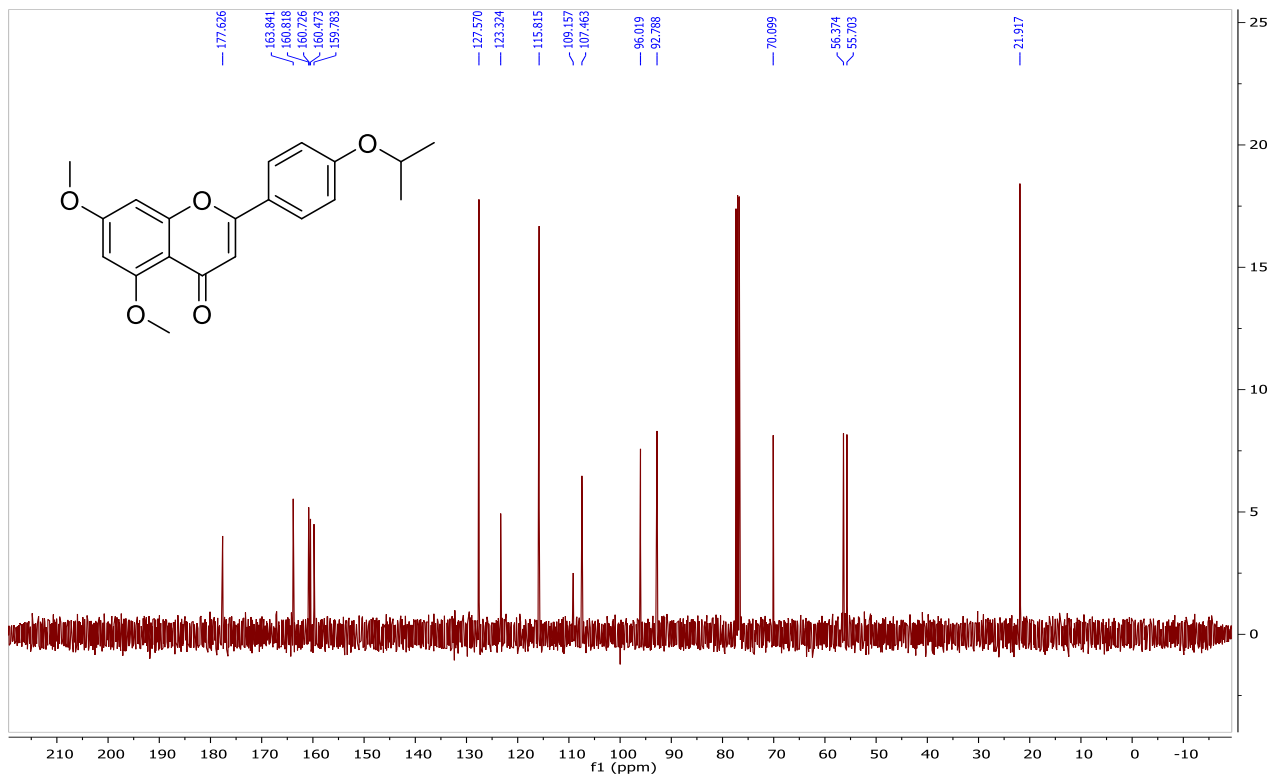
Figure S15. ^{13}C NMR spectrum of flavonoid (2b) in CDCl$_3$, 100 MHz
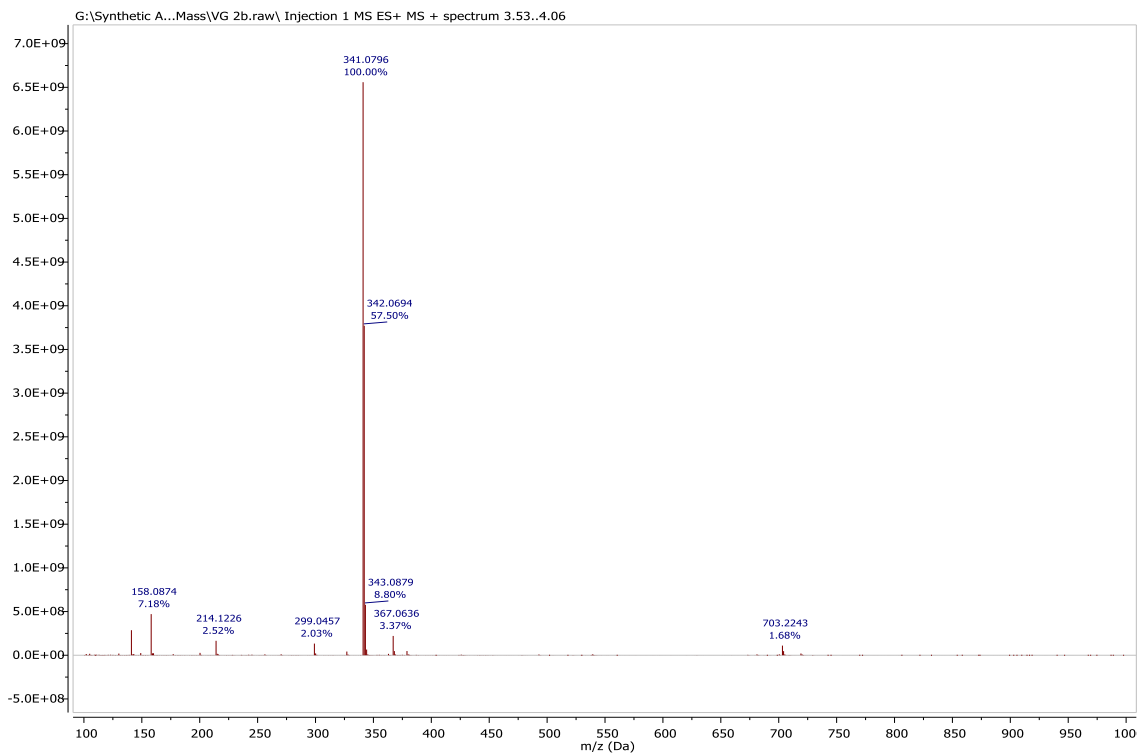

**Figure S16.** ESIMS spectrum of flavonoid (2b).
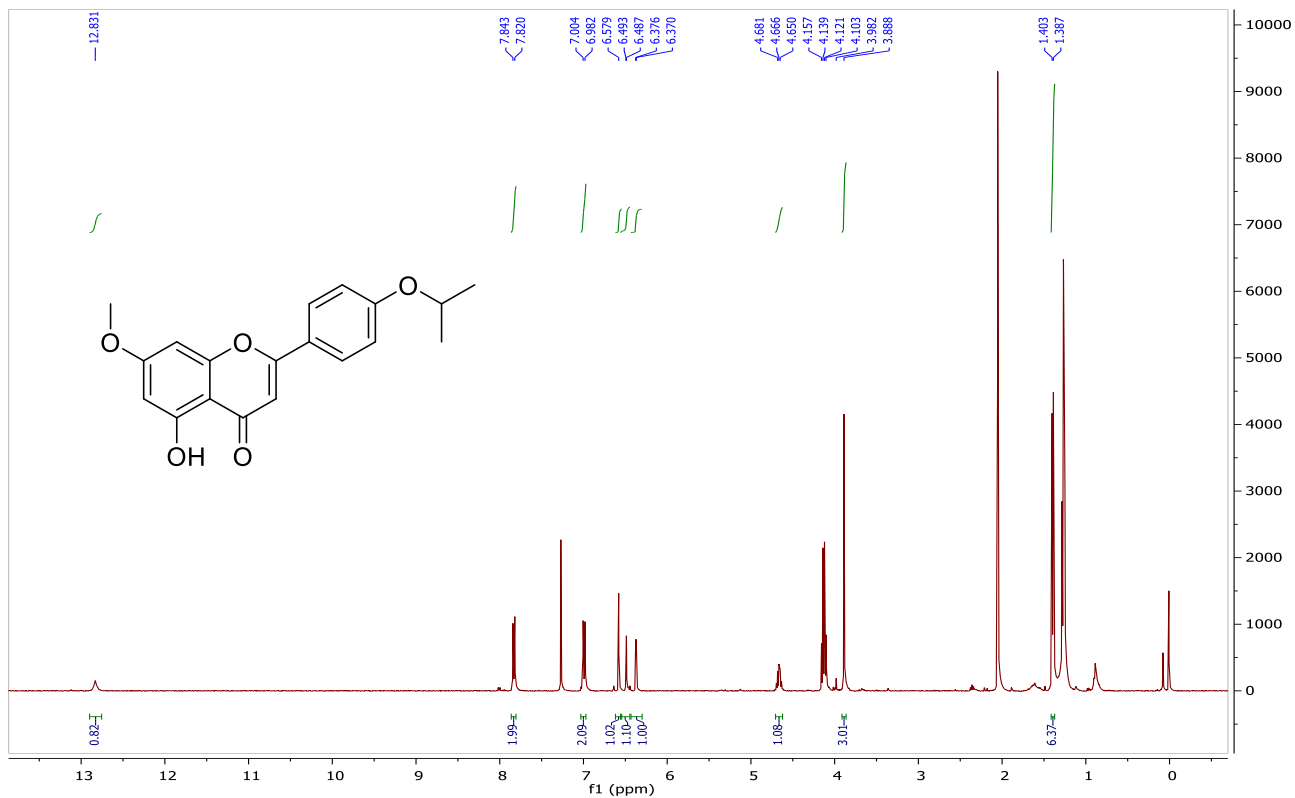
Figure S17. ^{1}H NMR spectrum of flavonoid (2c) in CDCl$_3$, 400 MHz
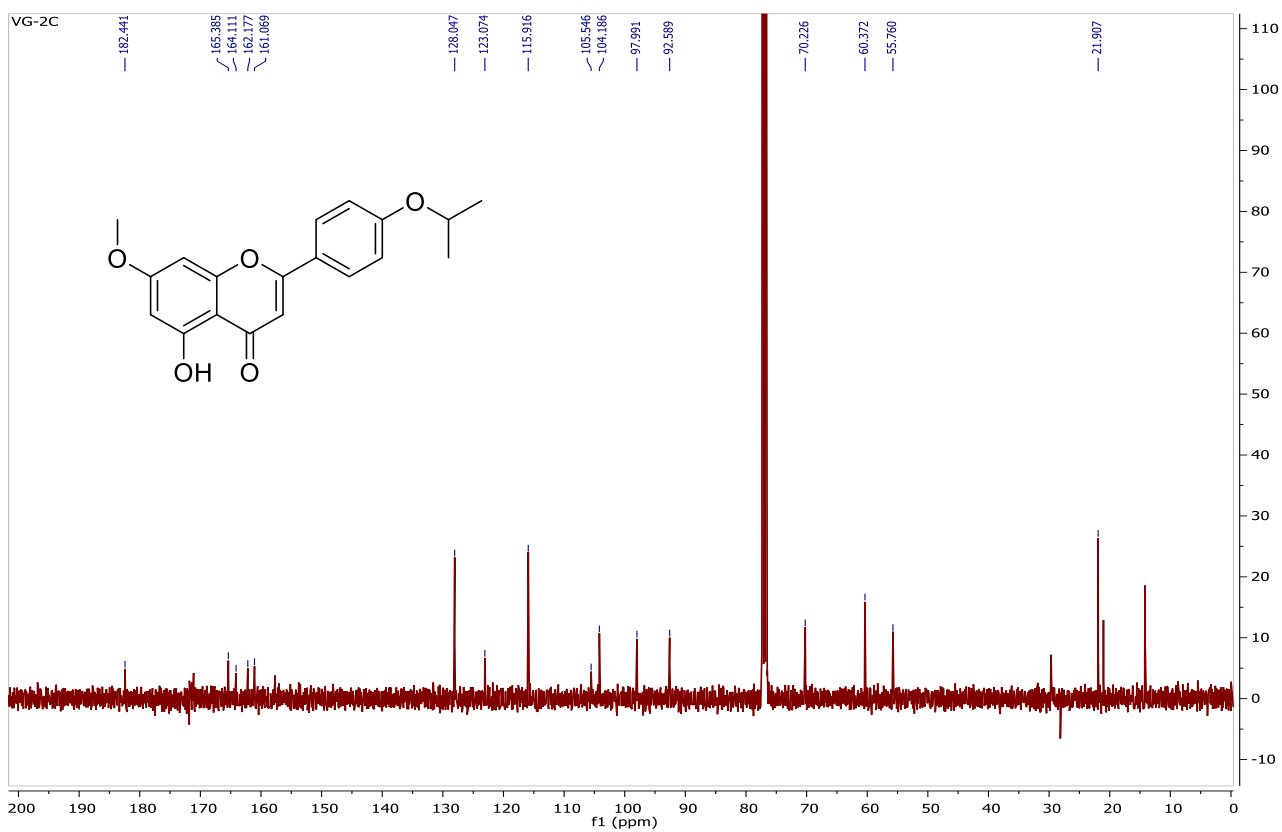
**Figure S18. ^{13}C NMR spectrum of flavonoid (2c) in CDCl$_3$, 100 MHz**
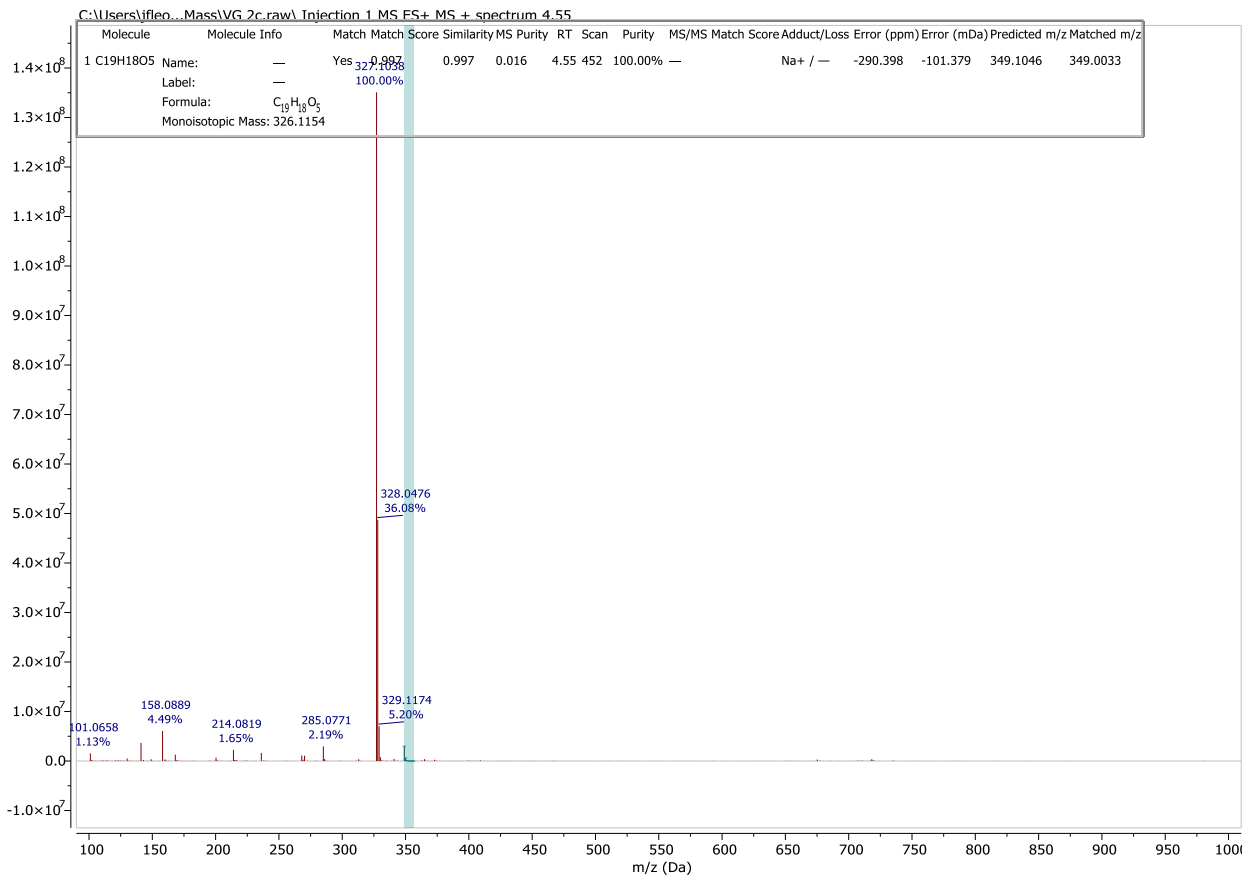
Figure S19. ESIMS spectrum of flavonoid (2c).
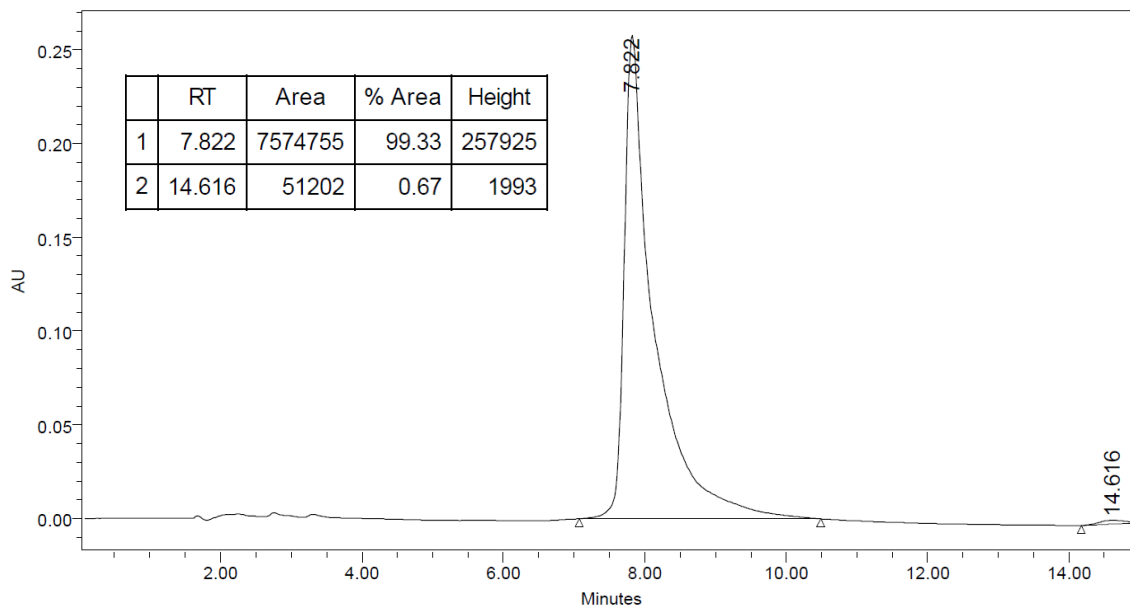

Figure S20. HPLC analysis of flavonoid (2c).
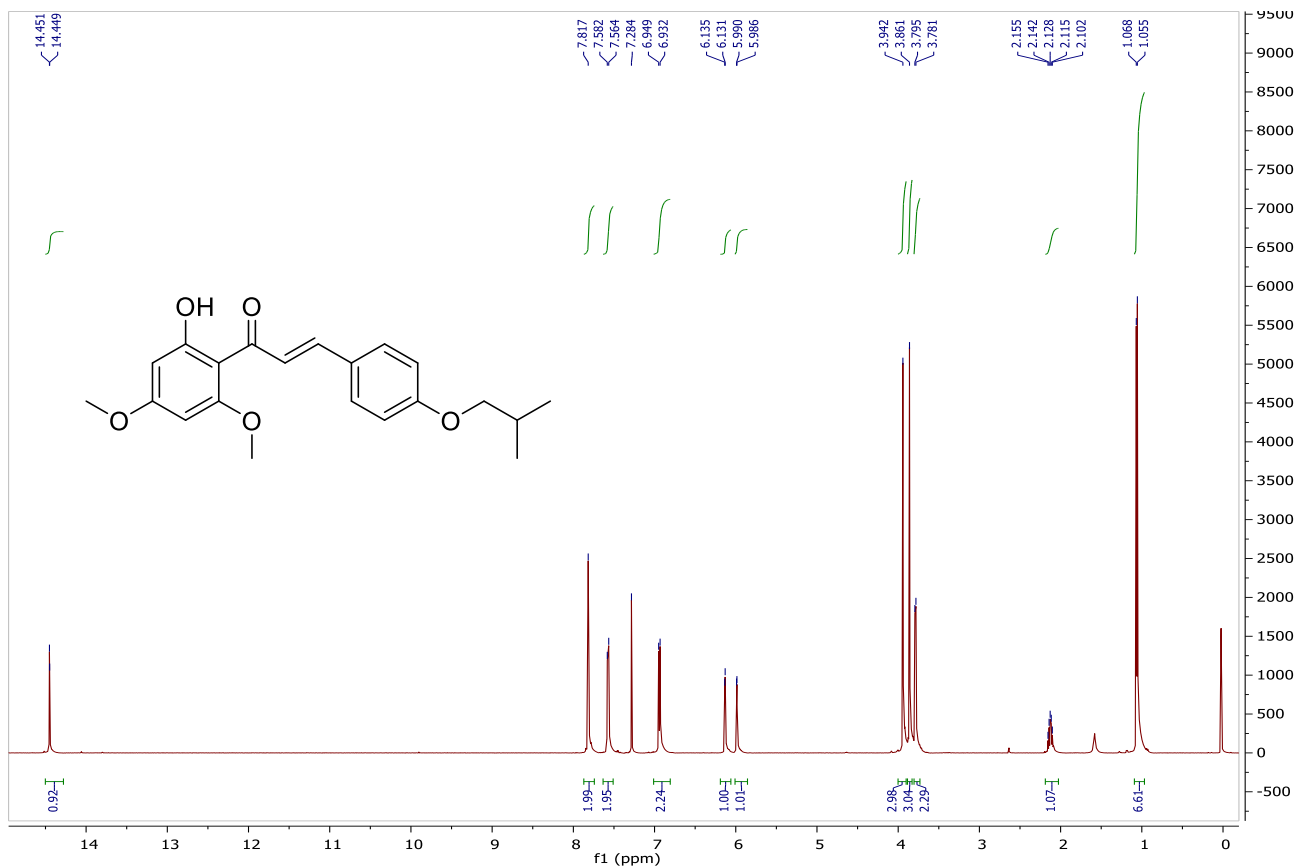
Figure S21. ^{1}H NMR spectrum chalcone (3a) in CDCl$_3$, 500 MHz
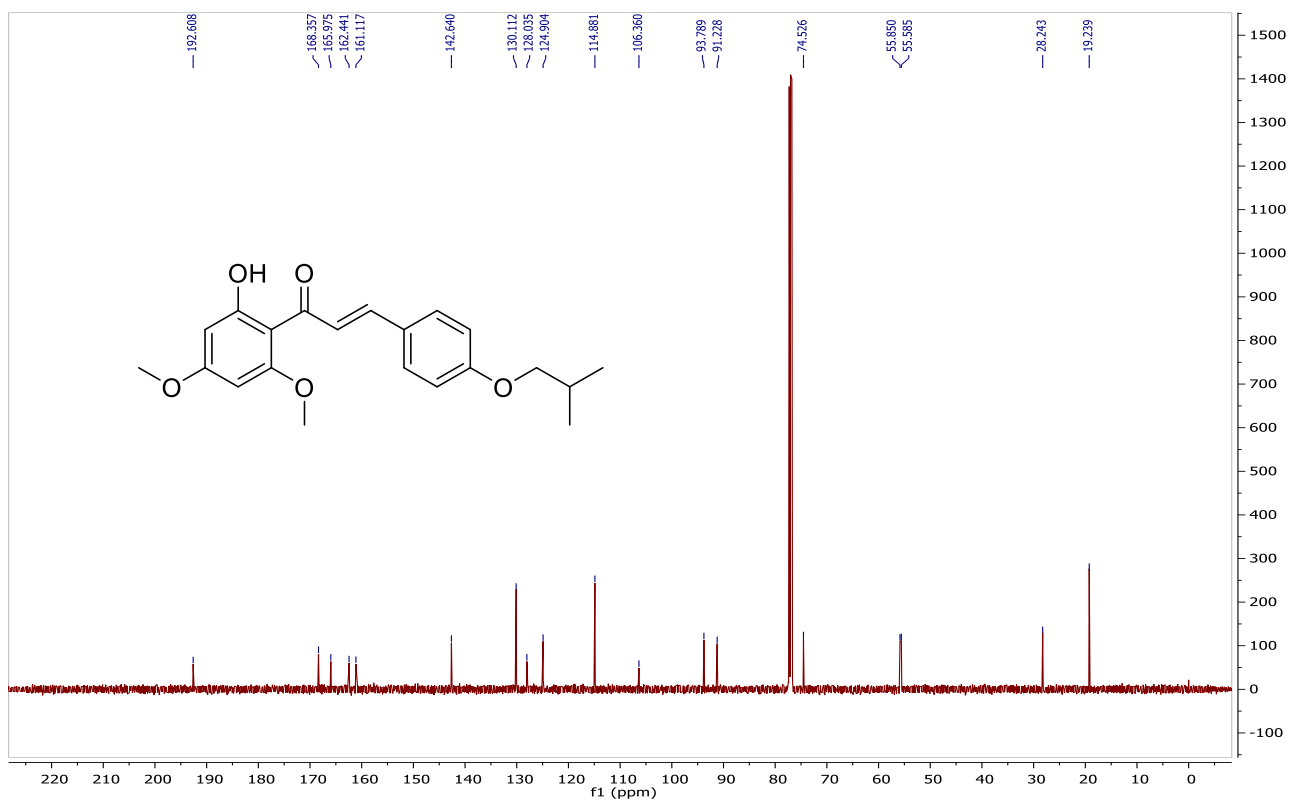
Figure S22. ^{13}C NMR spectrum of chalcone (3a) in CDCl$_3$, 125 MHz
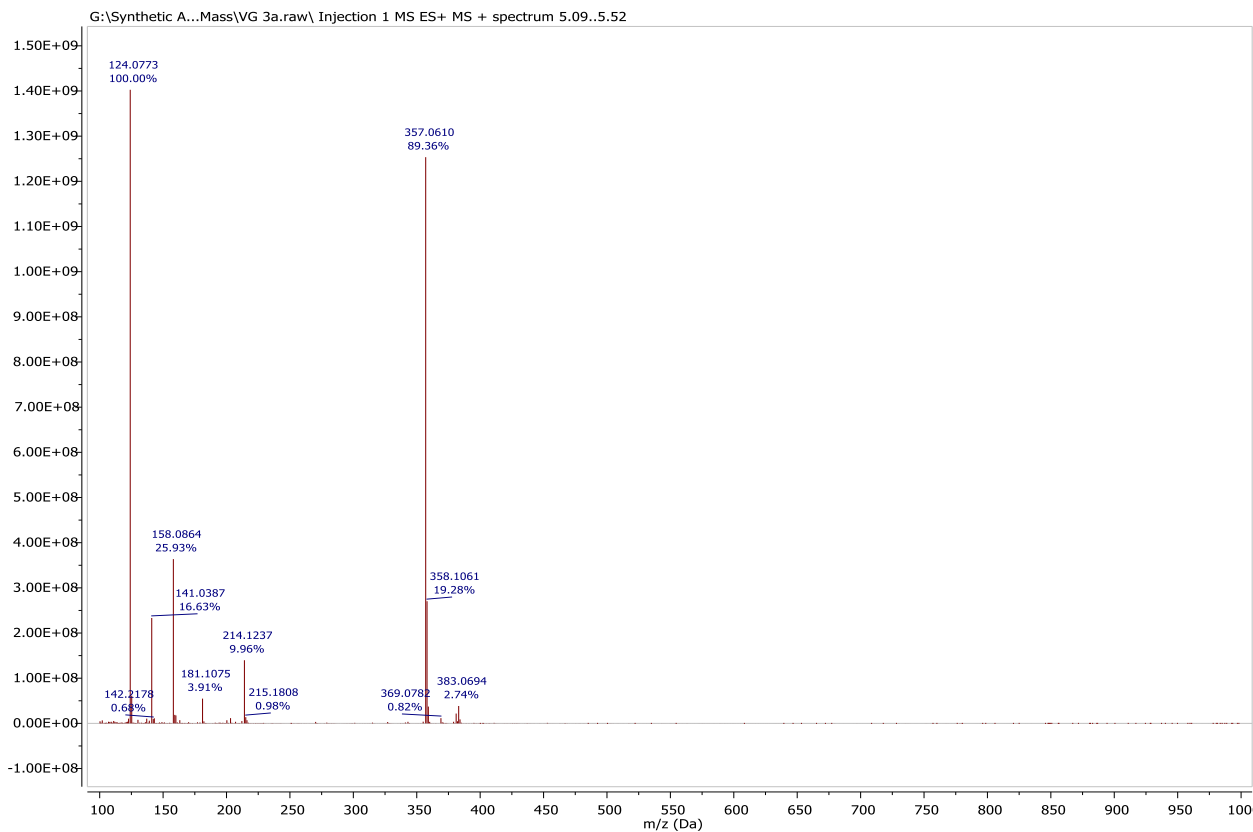
Figure S23. ESIMS spectrum of chalcone (3a).
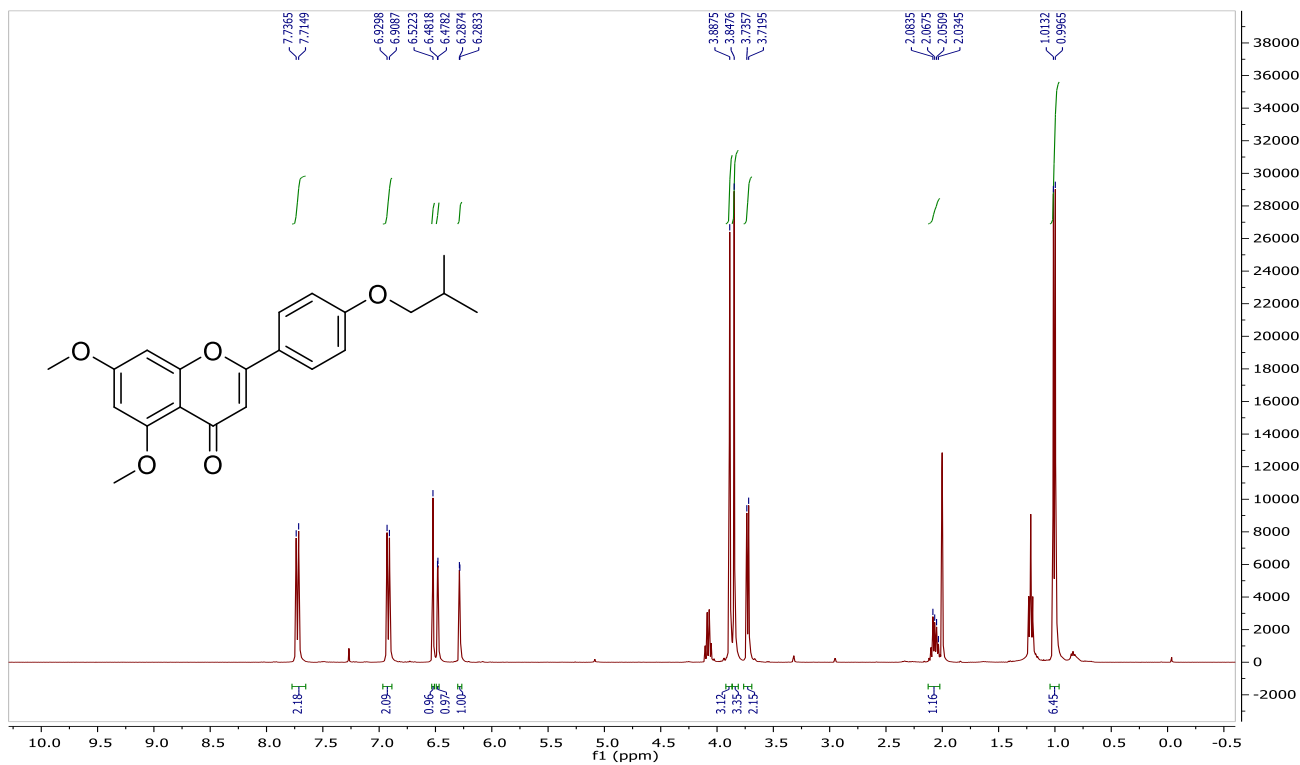
Figure S24. ^{1}H NMR spectrum of flavonoid (3b) in CDCl$_3$, 400 MHz
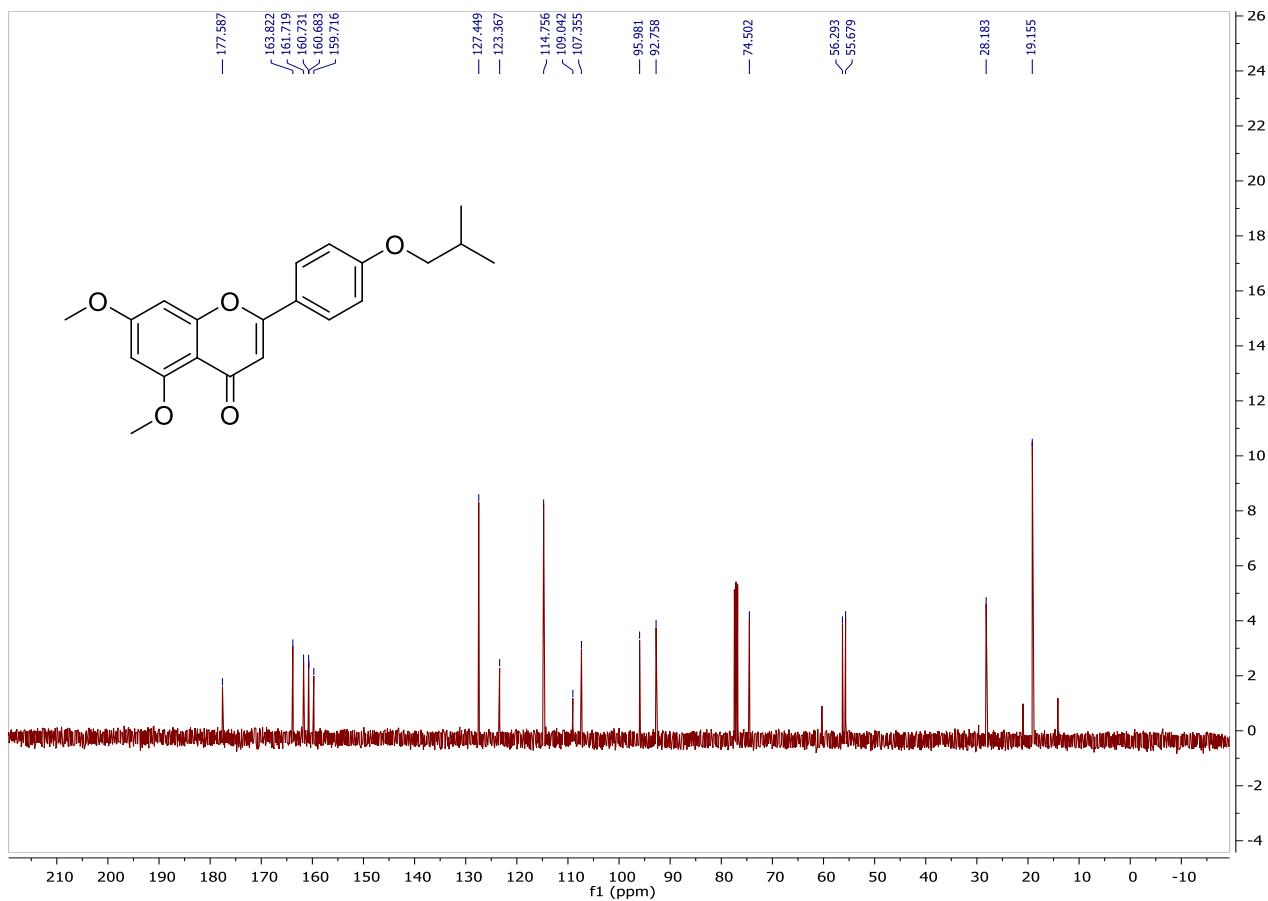
Figure S25. ^{13}C NMR spectrum of flavonoid (3b) in CDCl$_3$, 100 MHz
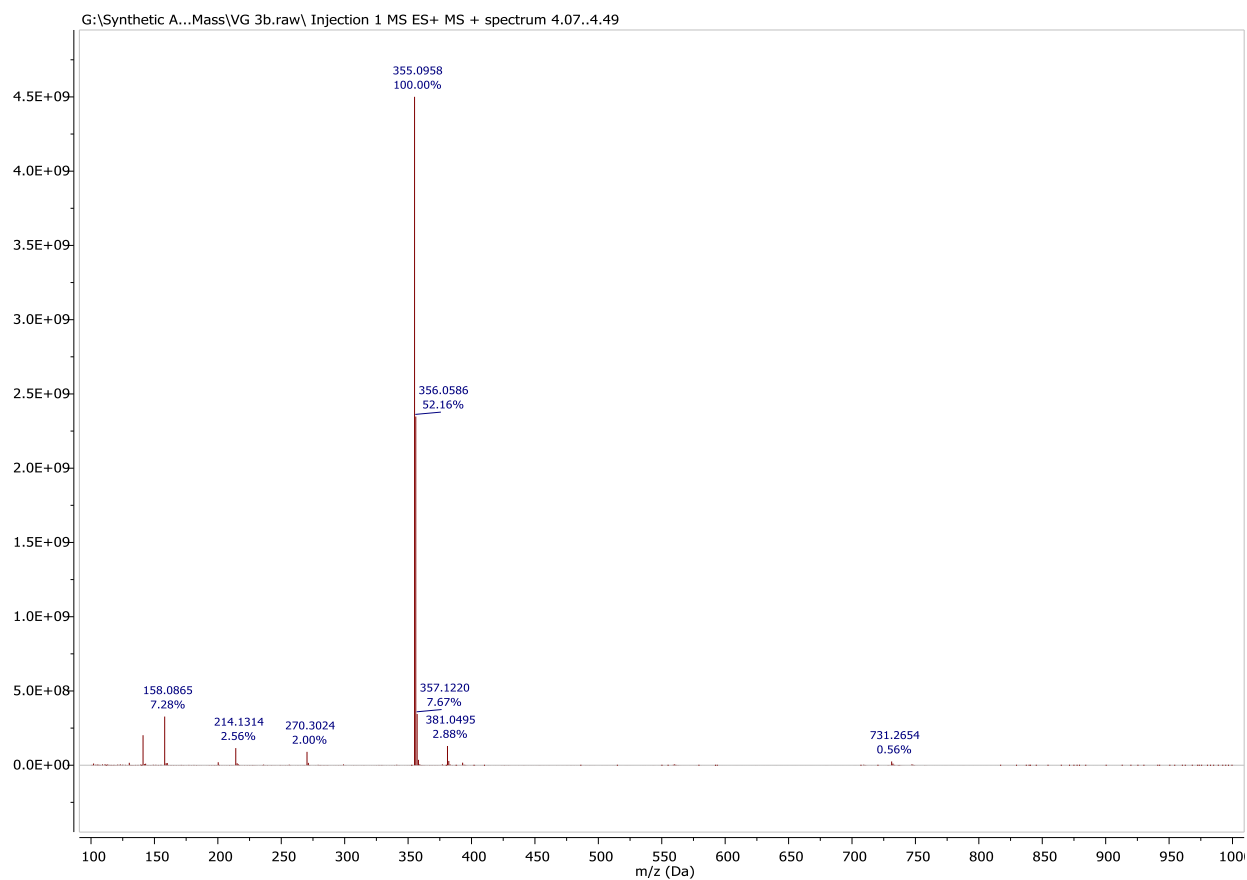
**Figure S26. ESIMS spectrum of flavonoid (3b).**

S15
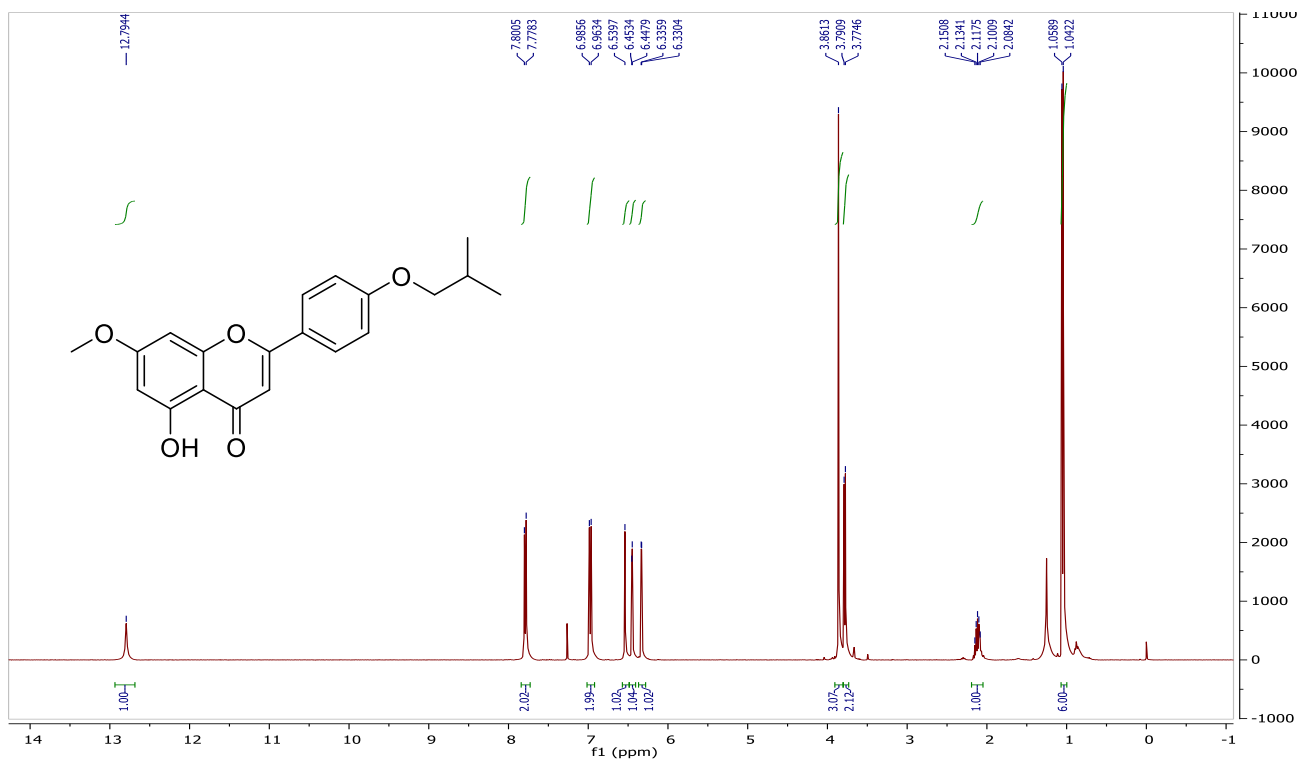
Figure S27. ^{1}H NMR spectrum of flavonoid (3c) in CDCl$_3$, 400 MHz
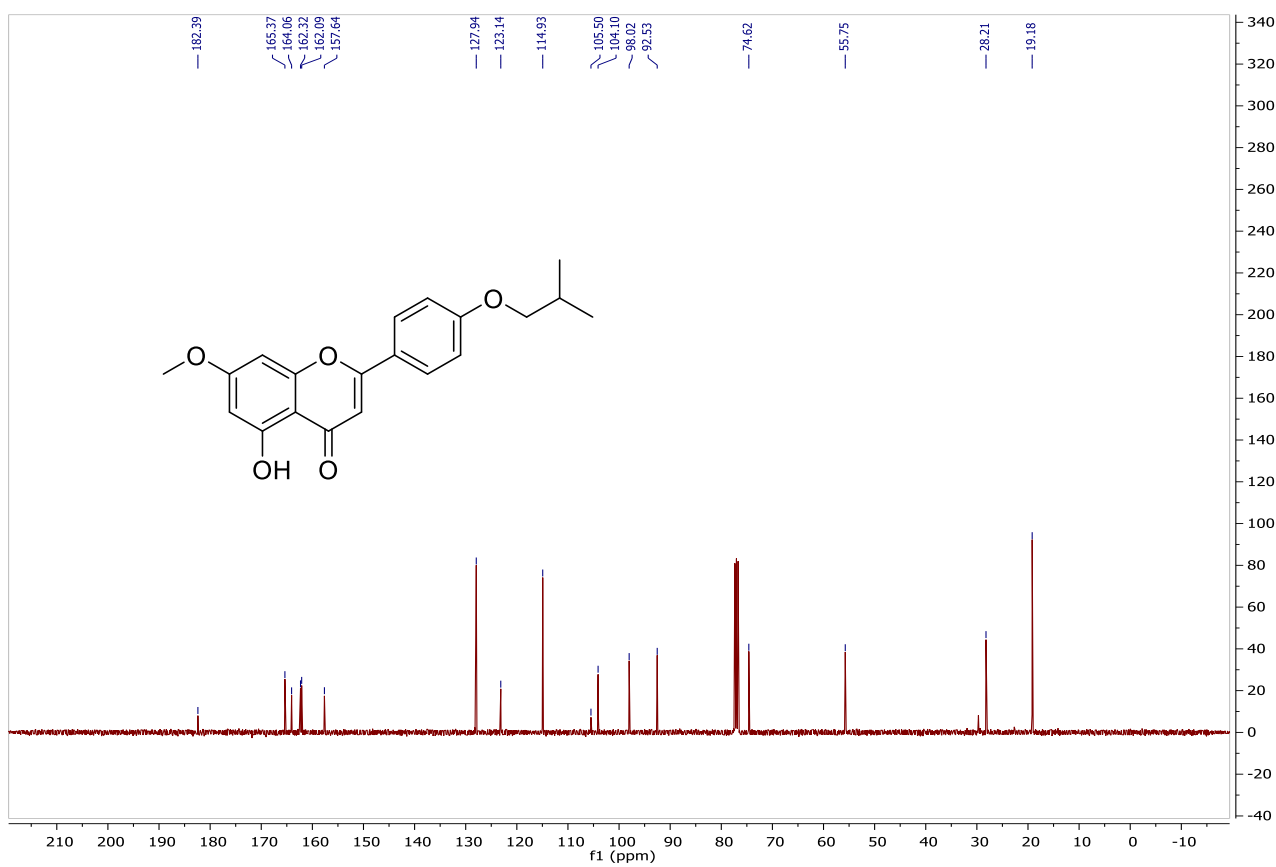
Figure S28. ^{13}C NMR spectrum of flavonoid (3c) in CDCl$_3$, 100 MHz
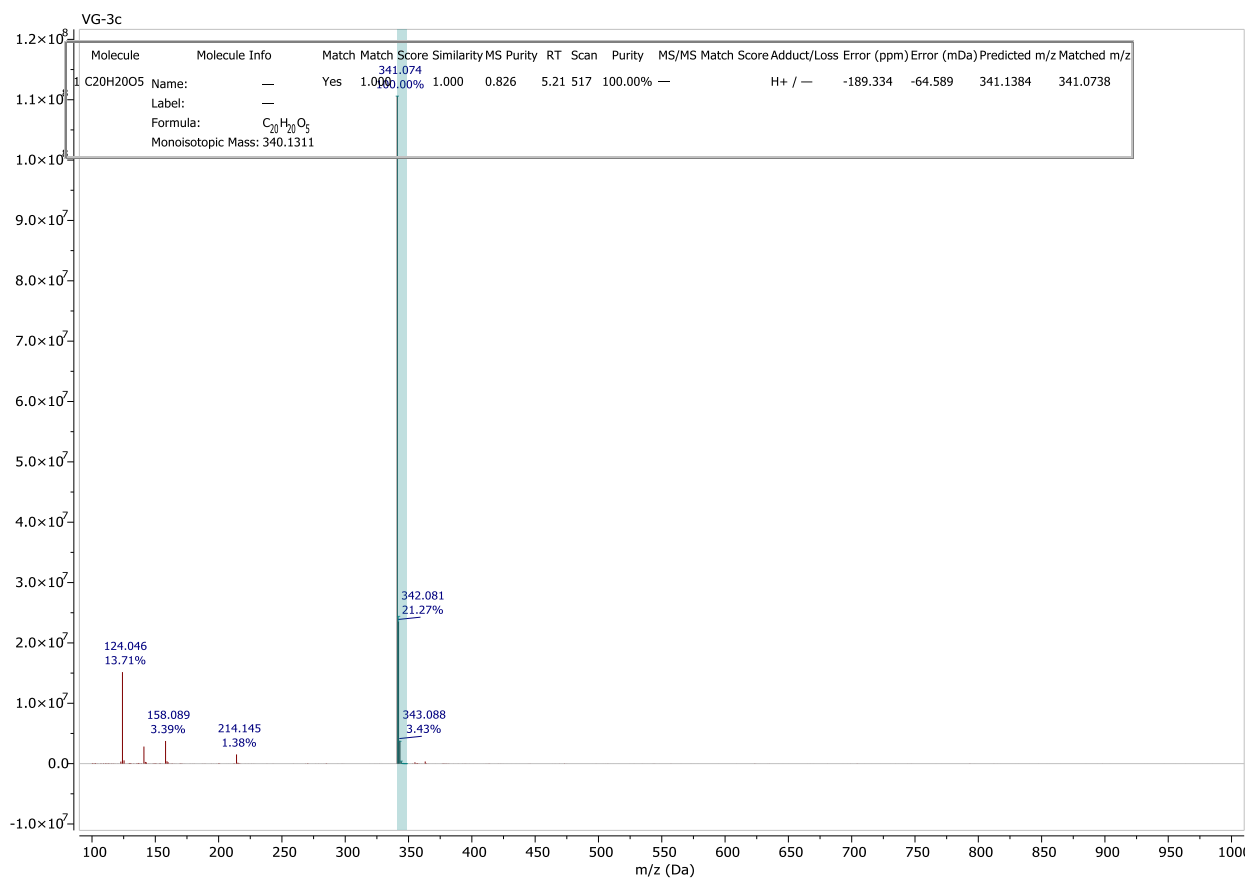
Figure S29. ESIMS spectrum of flavonoid (3c).
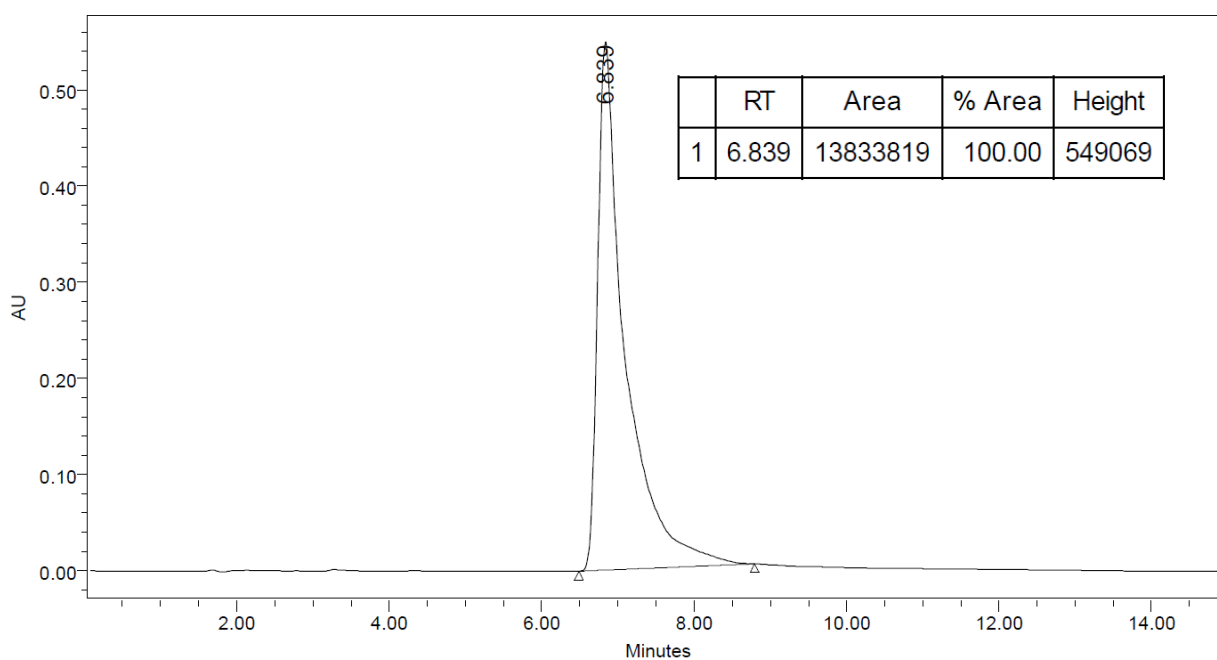
Figure S30. HPLC analysis of flavonoid (3c).
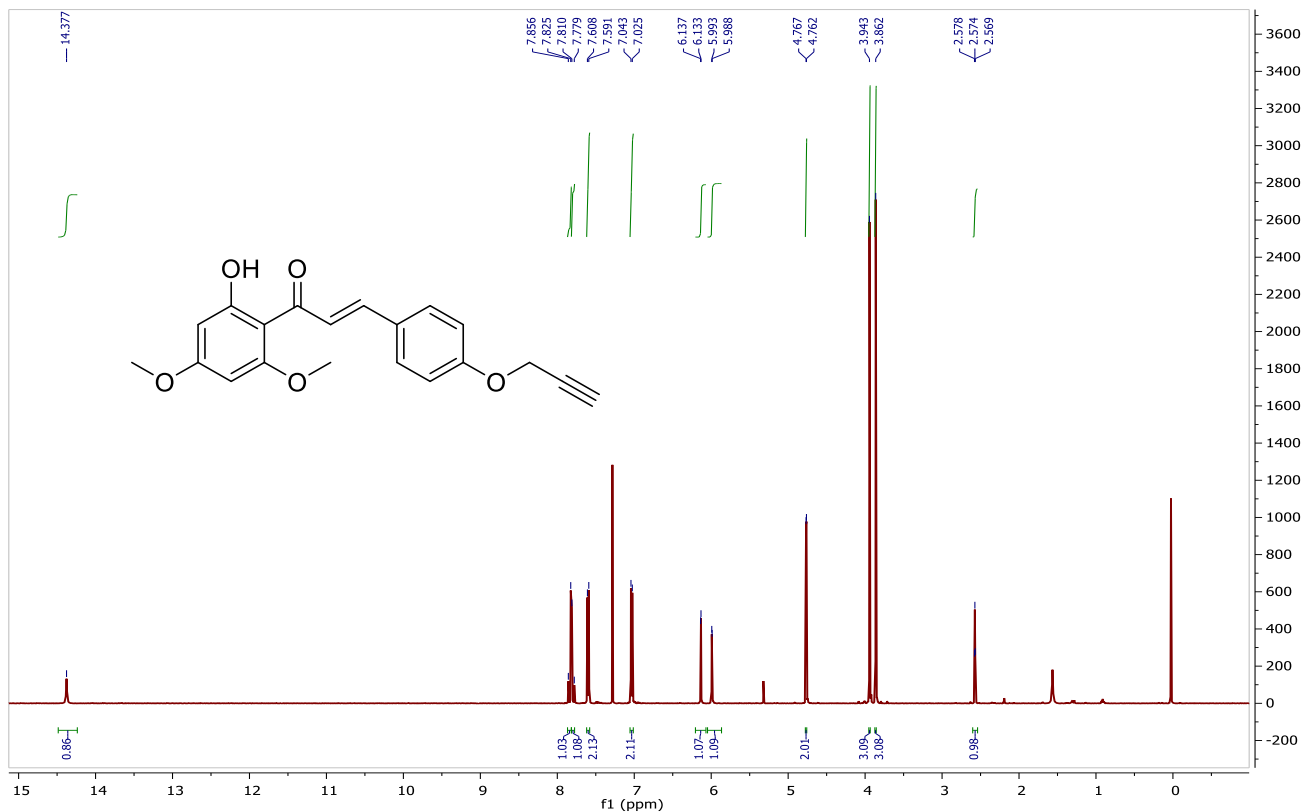
Figure S31. ^{1}H NMR spectrum of chalcone (4a) in CDCl$_3$, 500 MHz
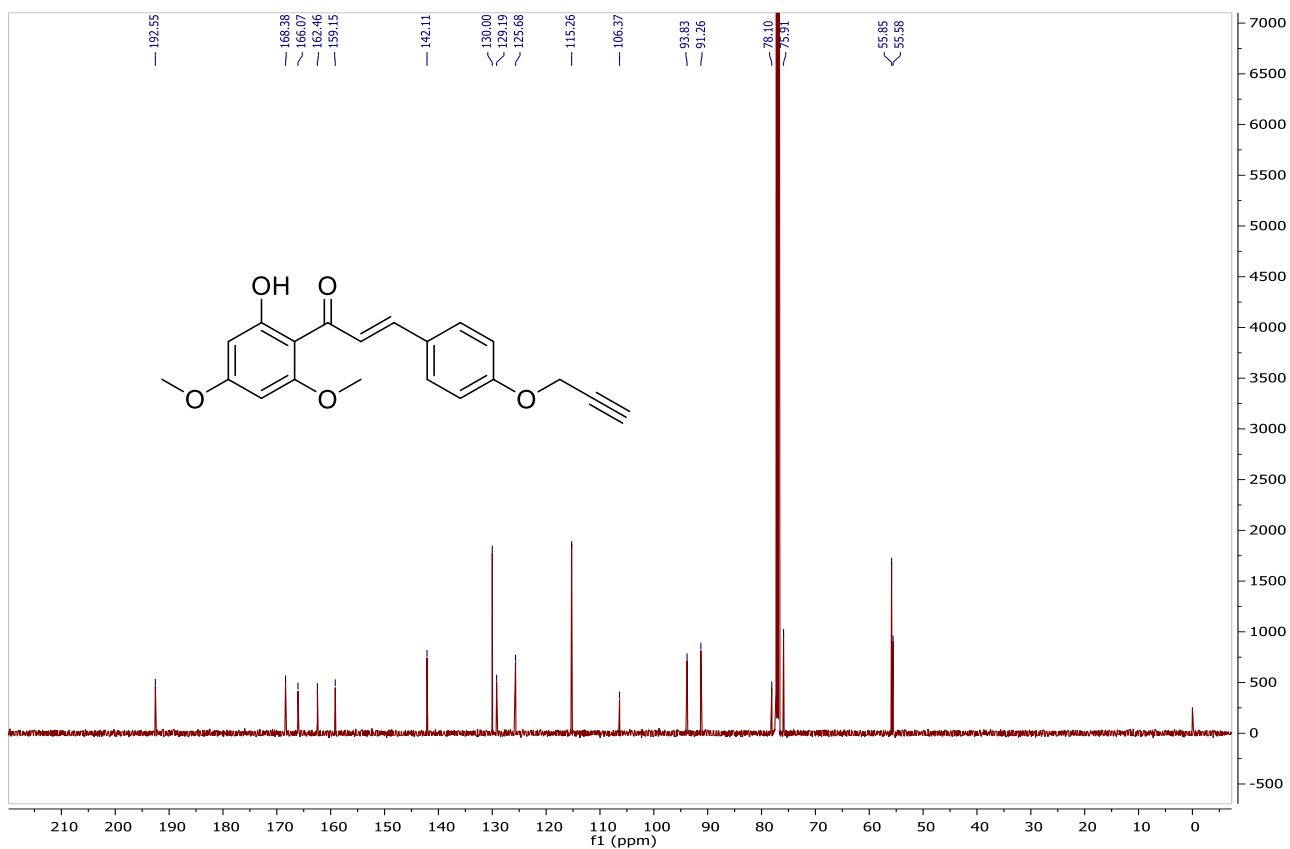
Figure S32. ^{13}C NMR spectrum of chalcone (4a) in CDCl$_3$, 125 MHz
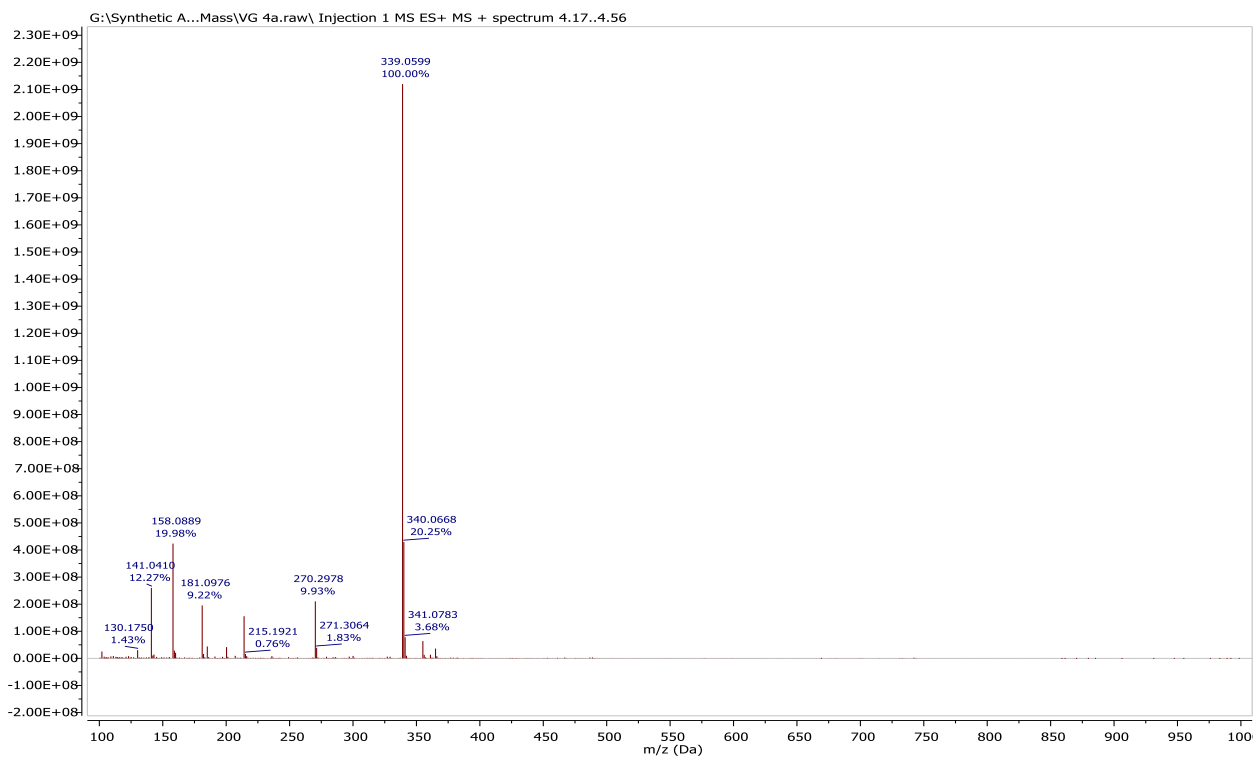
Figure S33. ESIMS spectrum of chalcone (4a).
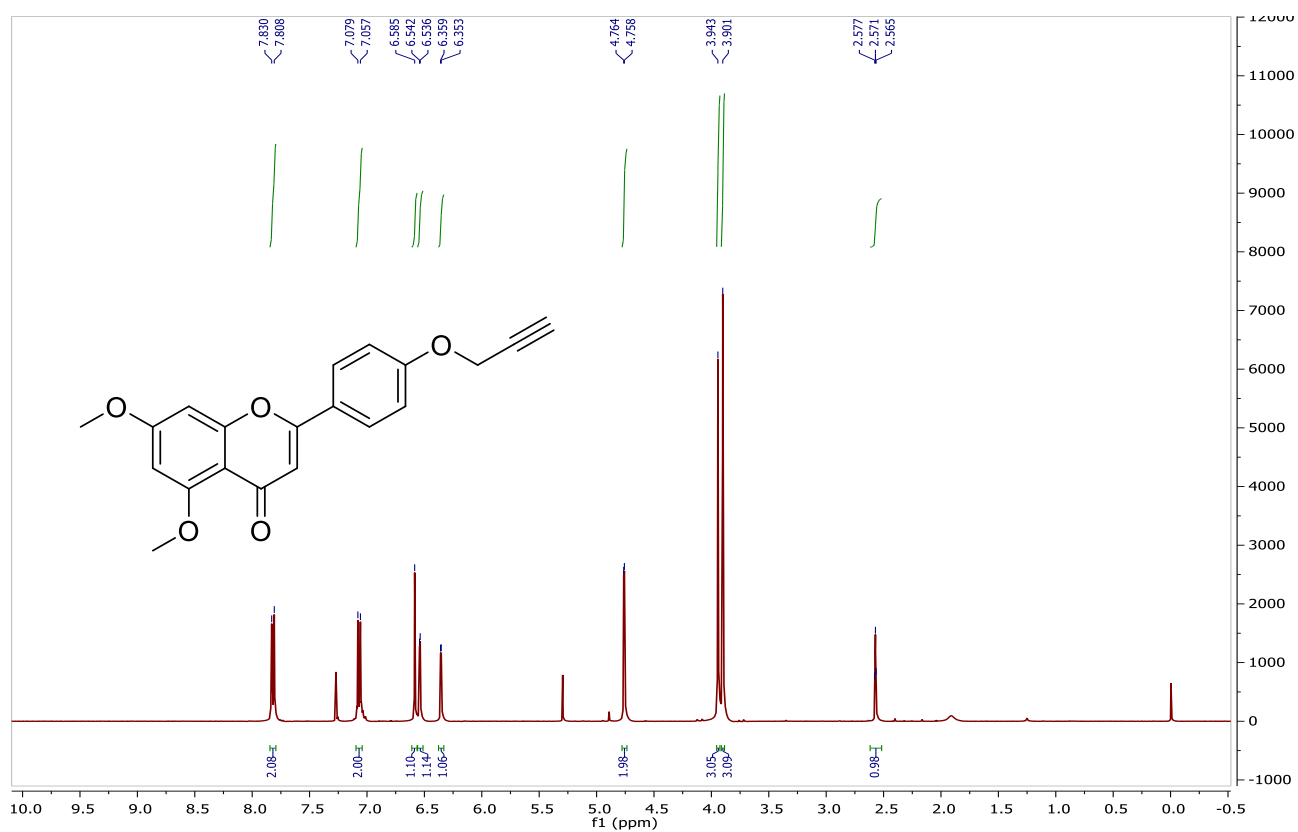

Figure S34. ^{1}H NMR spectrum of flavonoid (4b) in CDCl$_3$, 400 MHz

S19
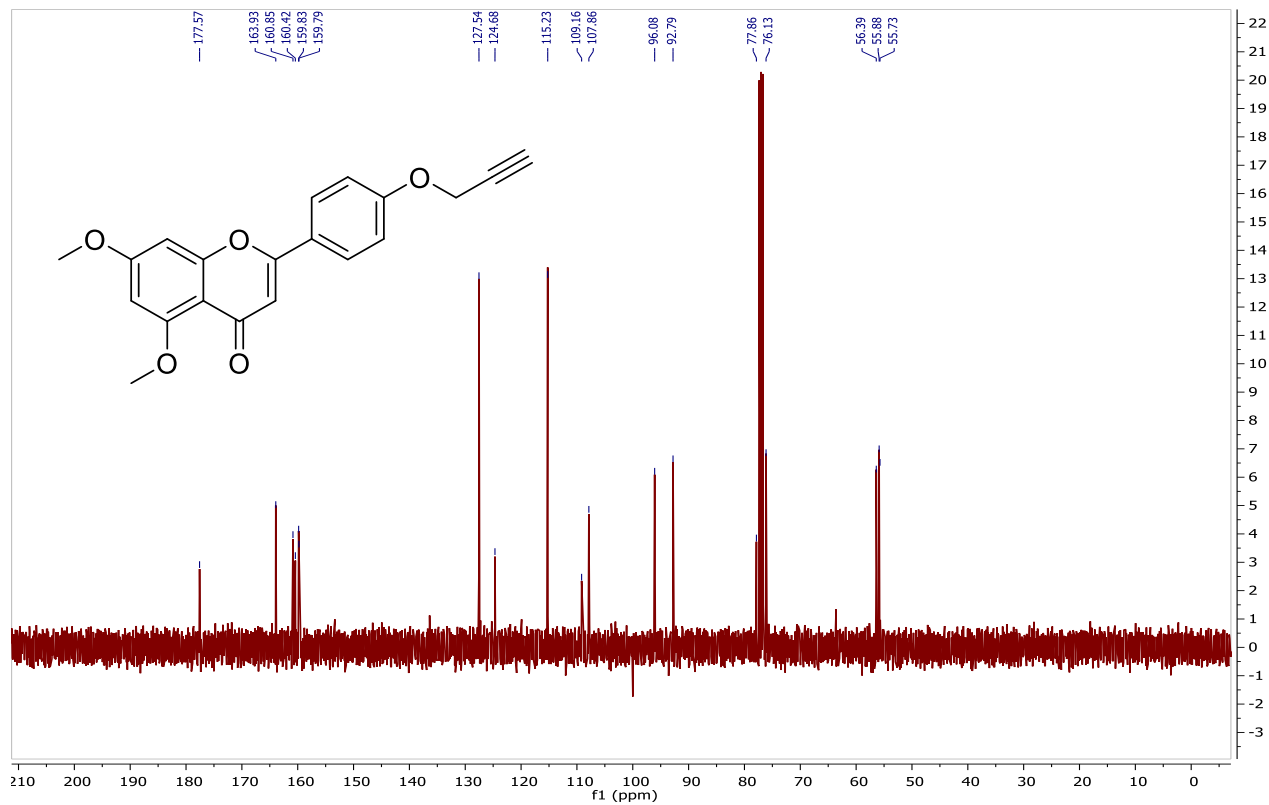
Figure S35. ^{13}C NMR spectrum of flavonoid (4b) in CDCl$_3$, 100 MHz
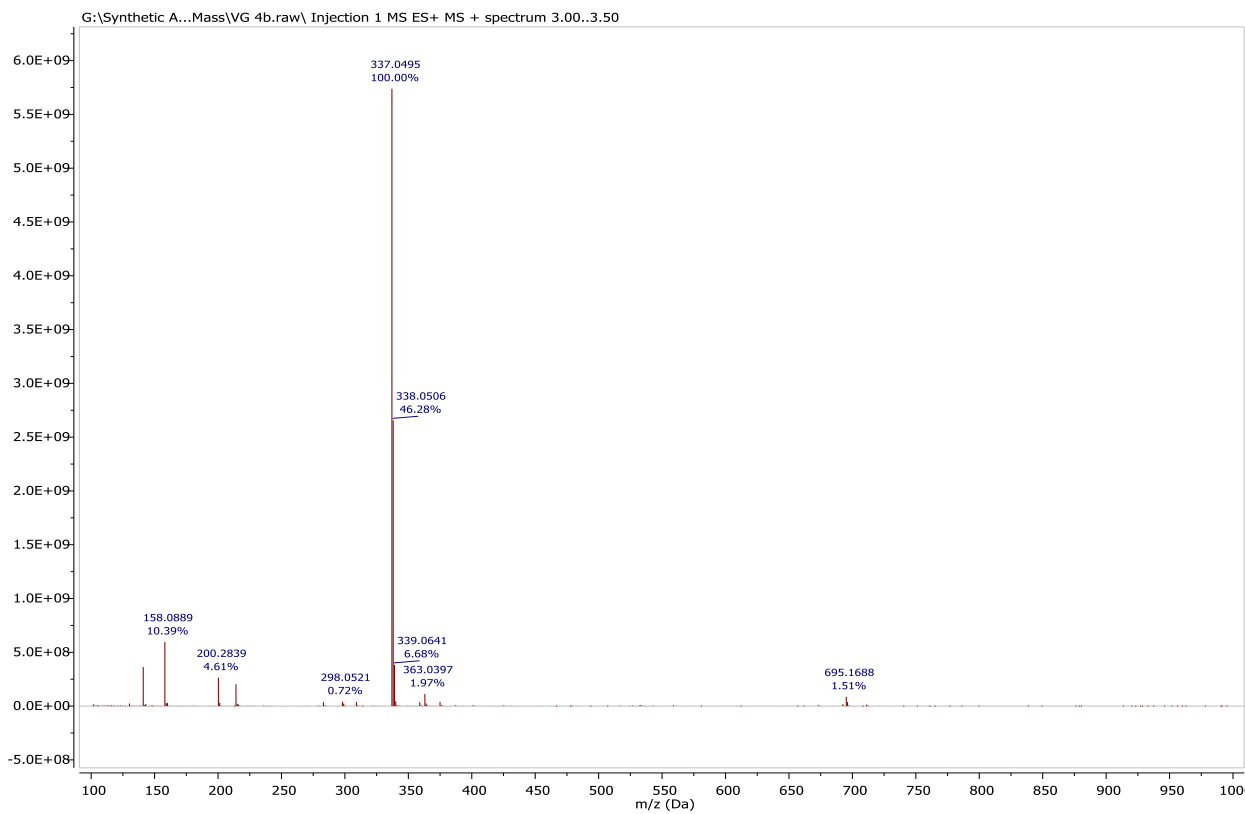
Figure S36. ESIMS spectrum of flavonoid (4b).

S20
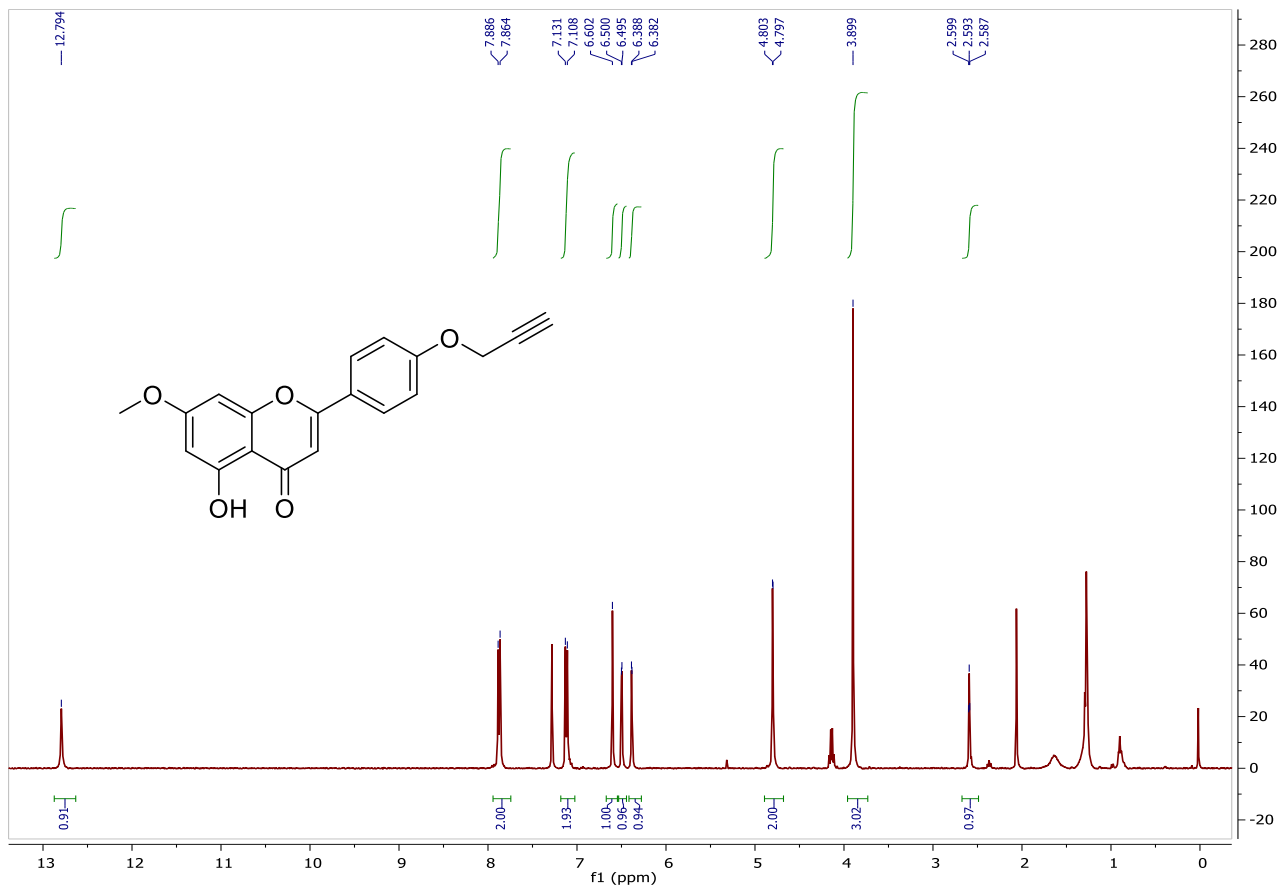
Figure S37. ^{1}H NMR spectrum of flavonoid (4c) in CDCl$_3$, 400 MHz
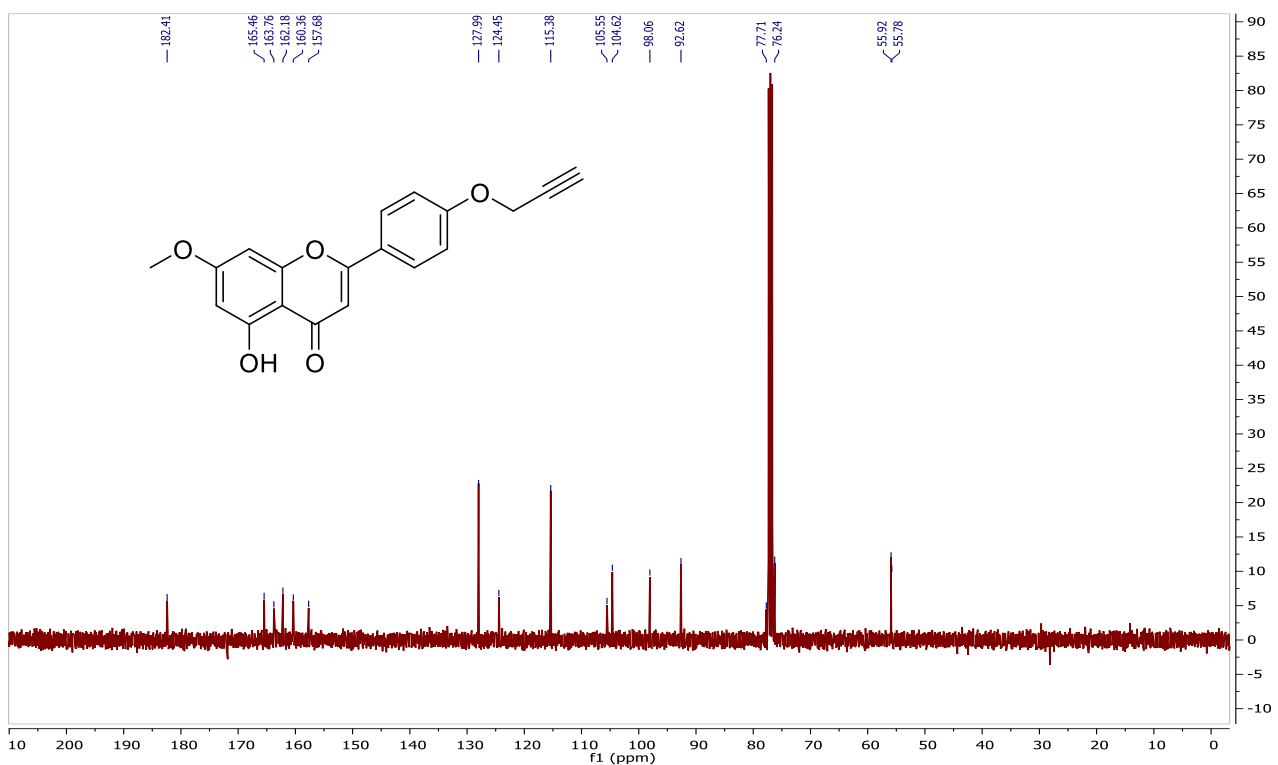
**Figure S38.** ^{13}C NMR spectrum of flavonoid (4c) in CDCl$_3$, 100 MHz
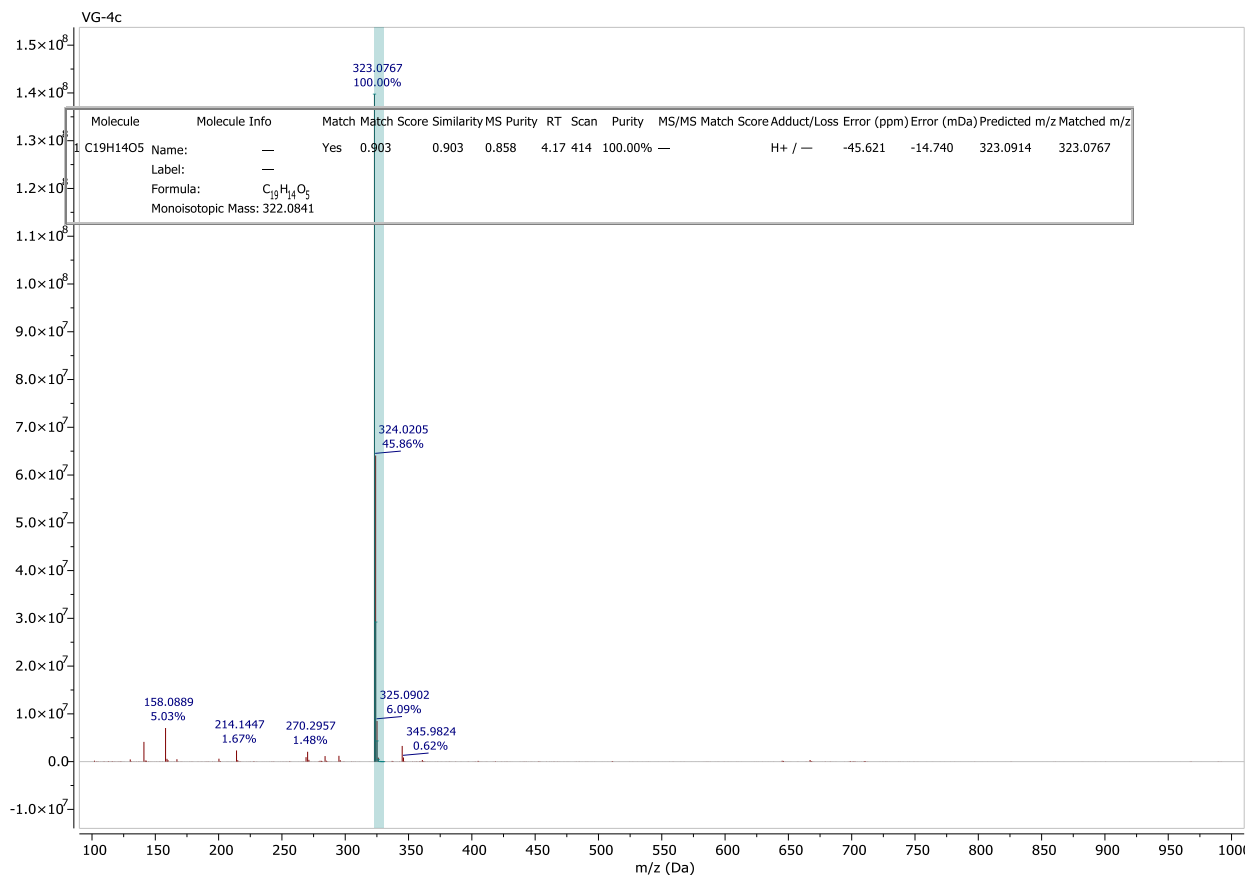
Figure S39. ESIMS spectrum of flavonoid (4c).
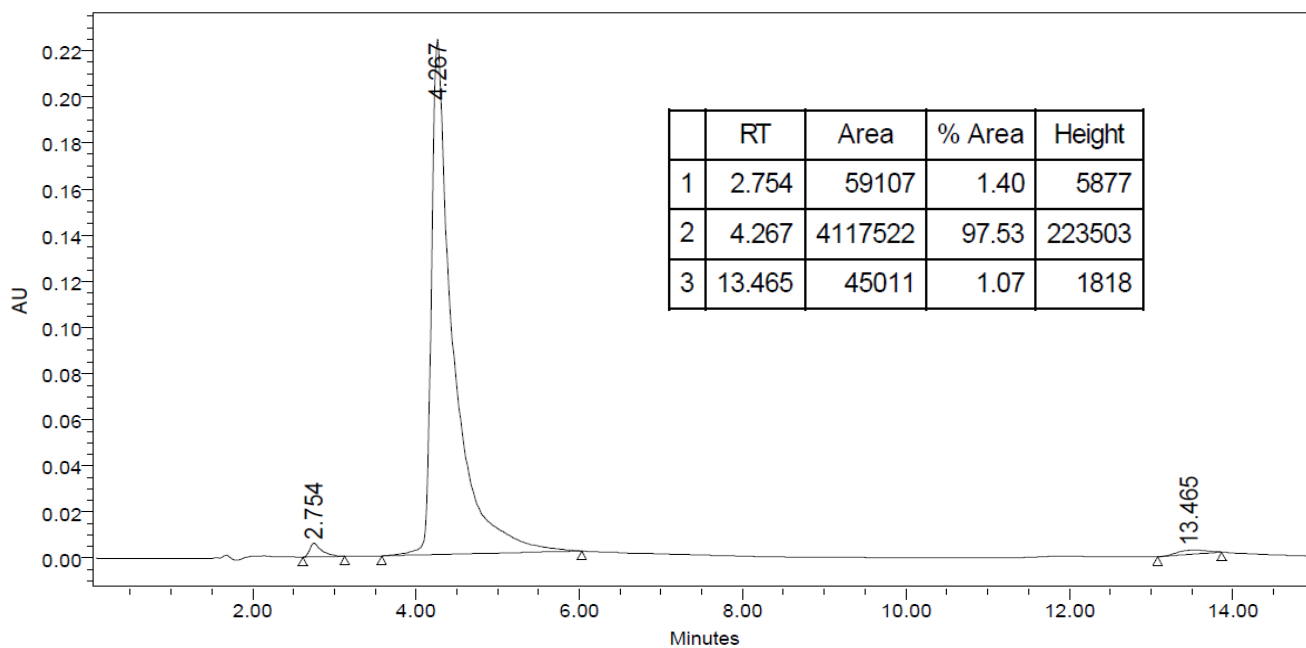

Figure S40. HPLC analysis of flavonoid (4c).
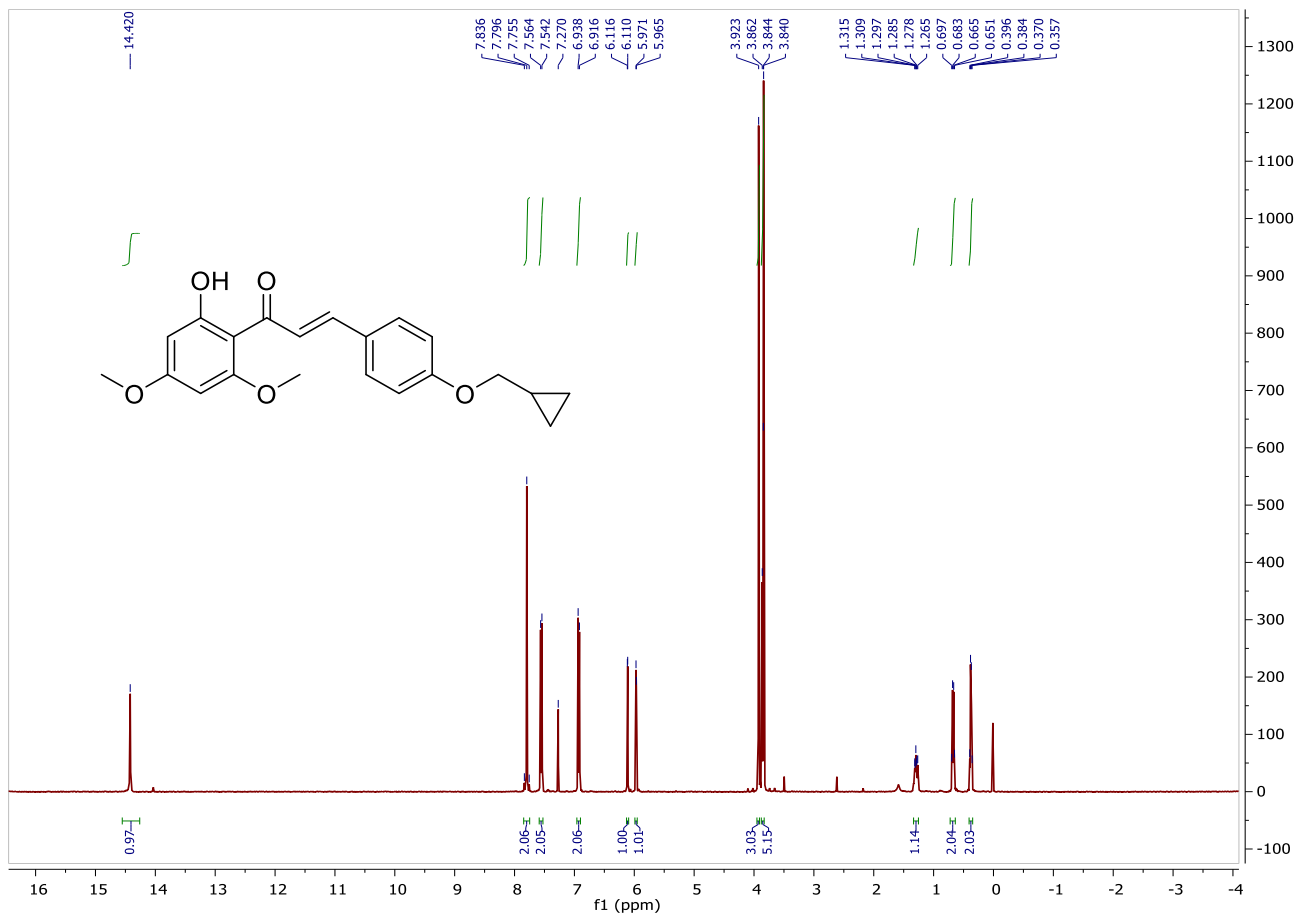
Figure S41. ^{1}H NMR spectrum of chalcone (5a) in CDCl$_3$, 400 MHz
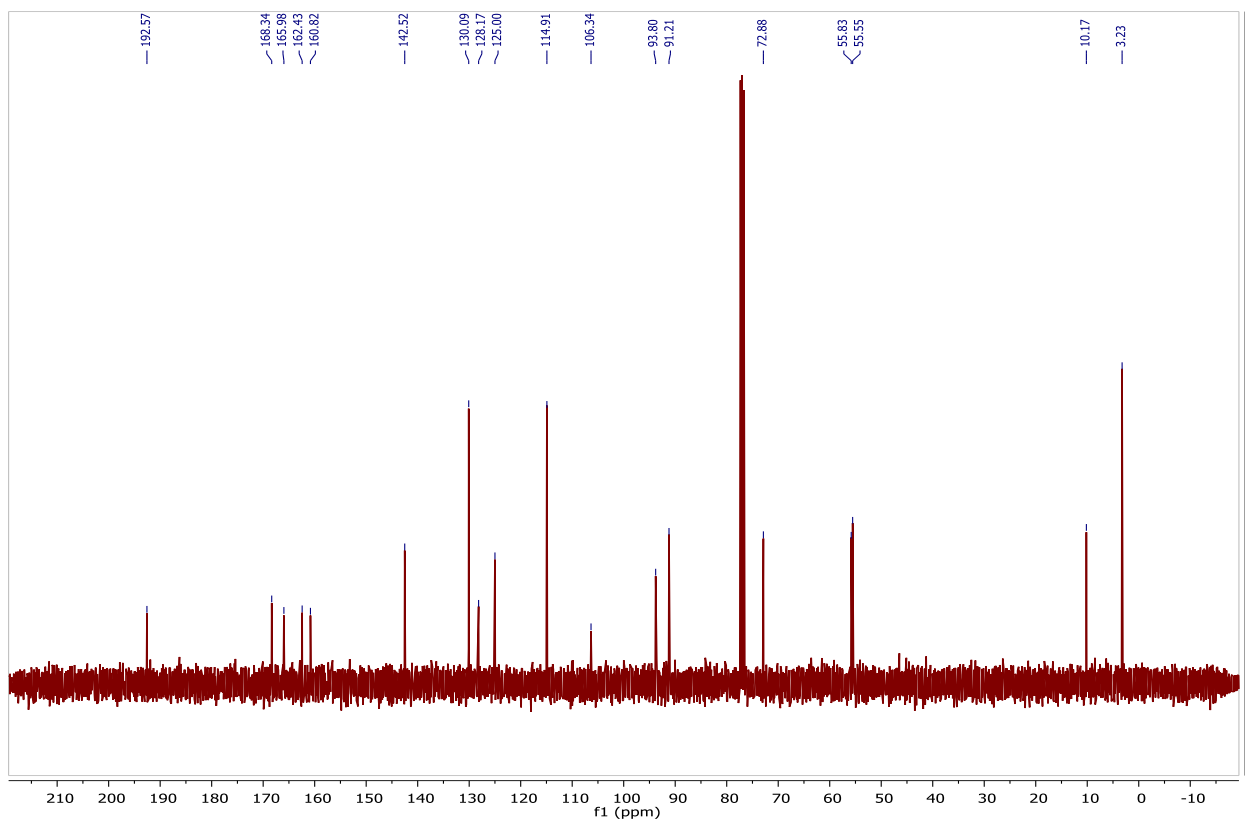
**Figure S42.** ^{13}C NMR spectrum of chalcone (5a) in CDCl$_3$, 100 MHz
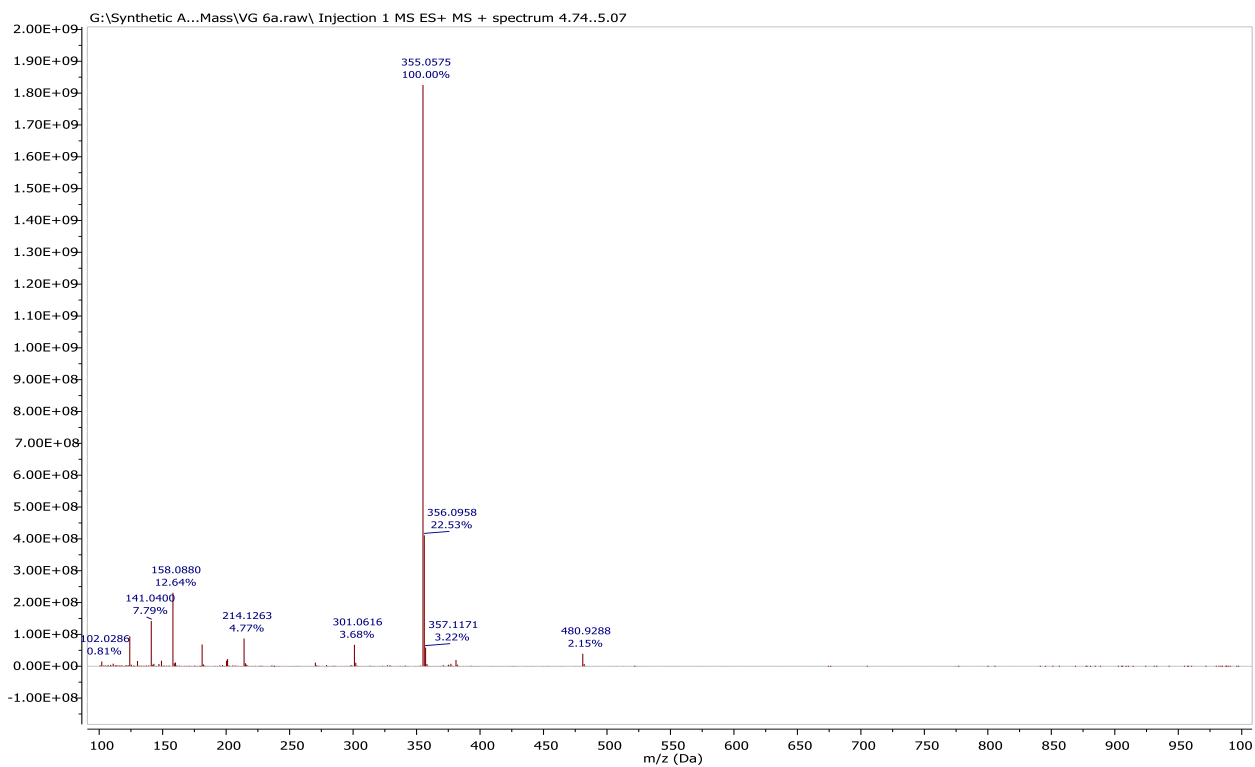
Figure S43. ESIMS spectrum of flavonoid (5a).
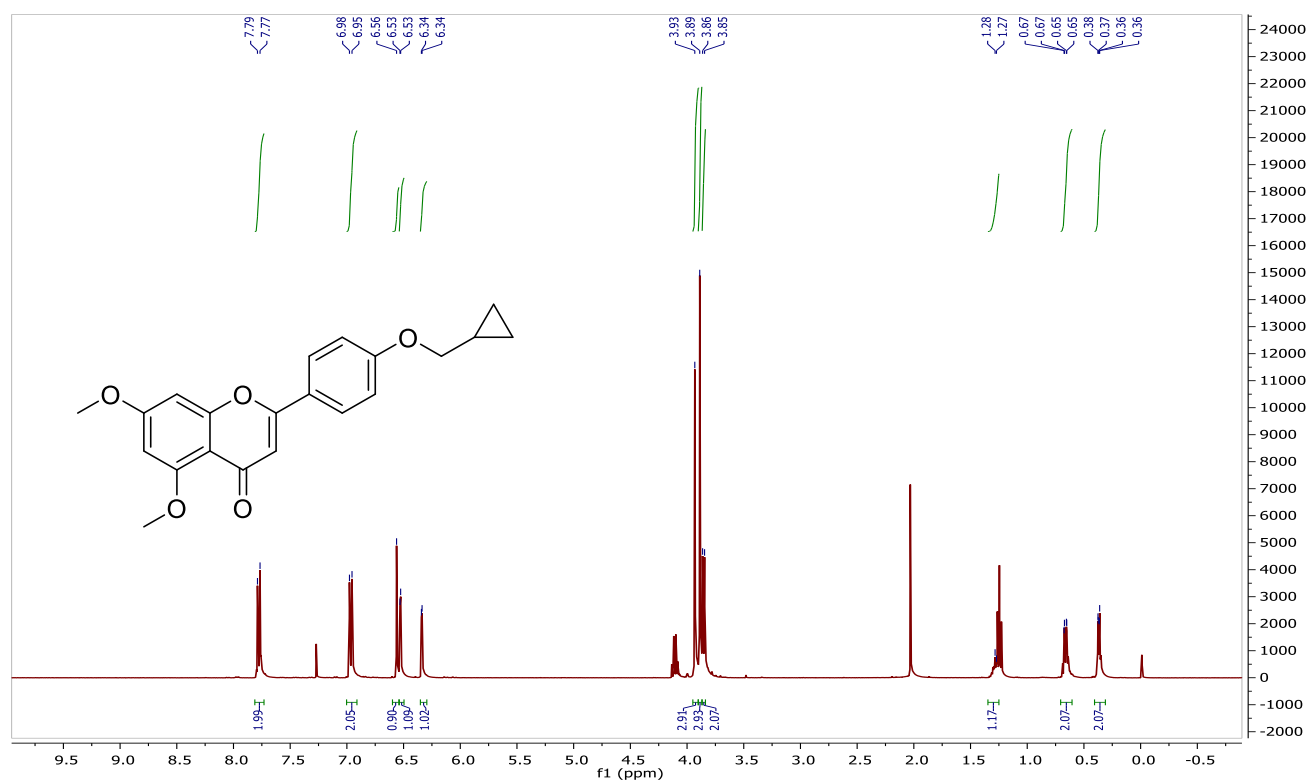
Figure S44. ^{1}H NMR spectrum of flavonoid (5b) in CDCl$_3$, 400 MHz
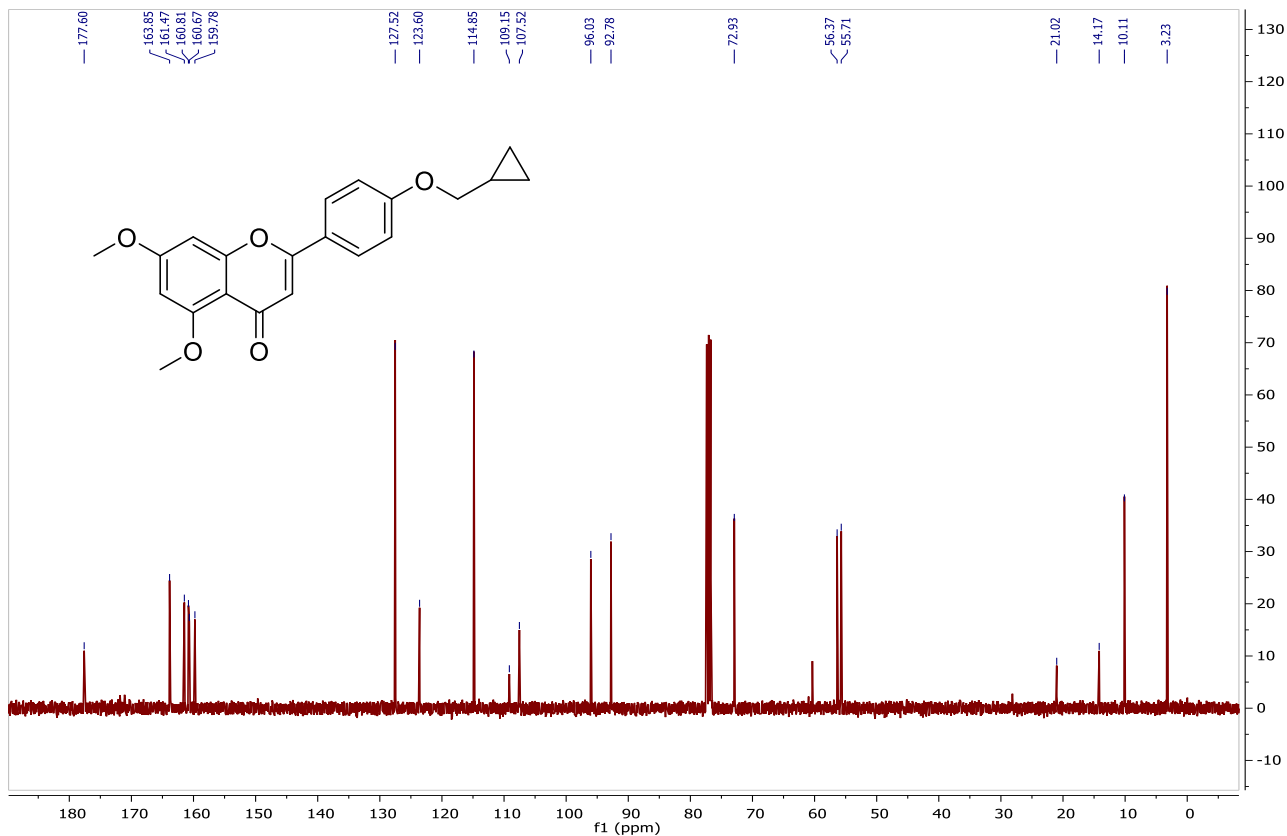
Figure S45. ^{13}C NMR spectrum of flavonoid (5b) in CDCl$_3$, 100 MHz
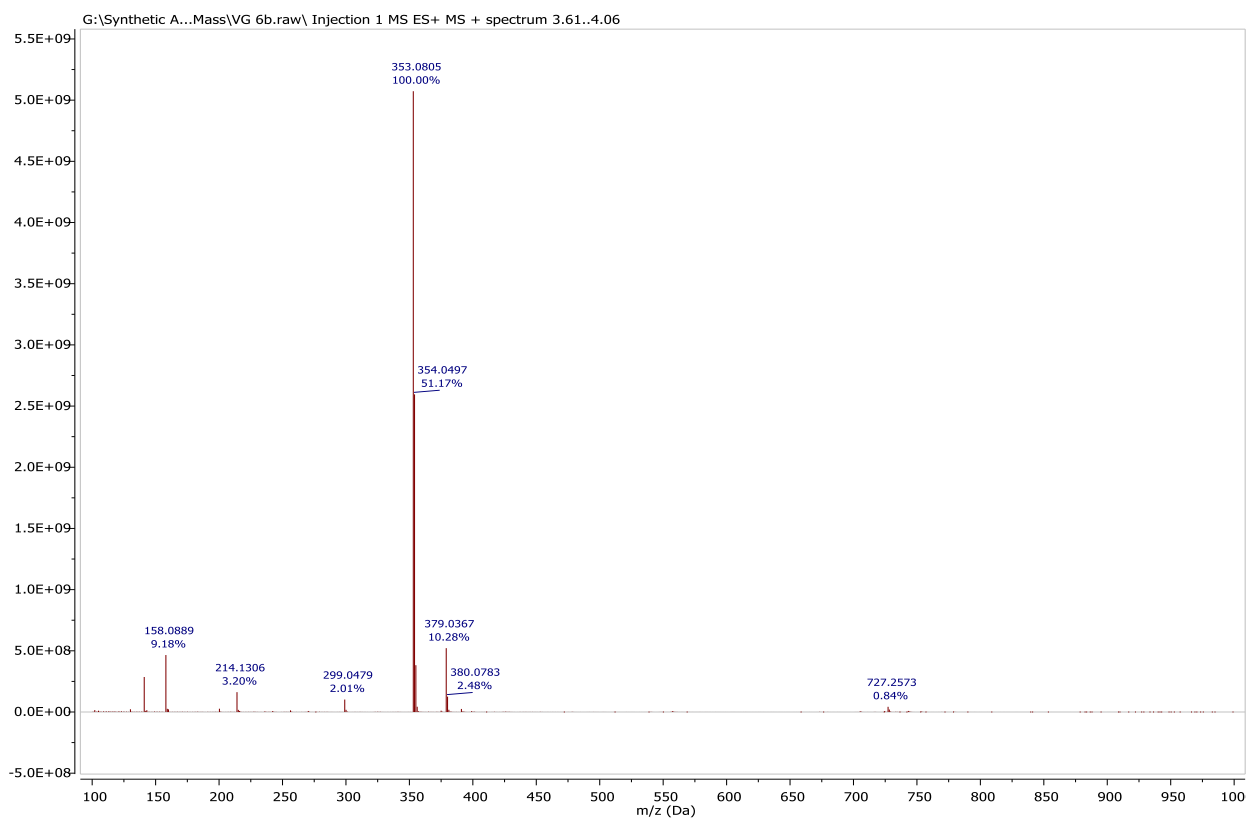
Figure S46. ESIMS spectrum of flavonoid (5b).
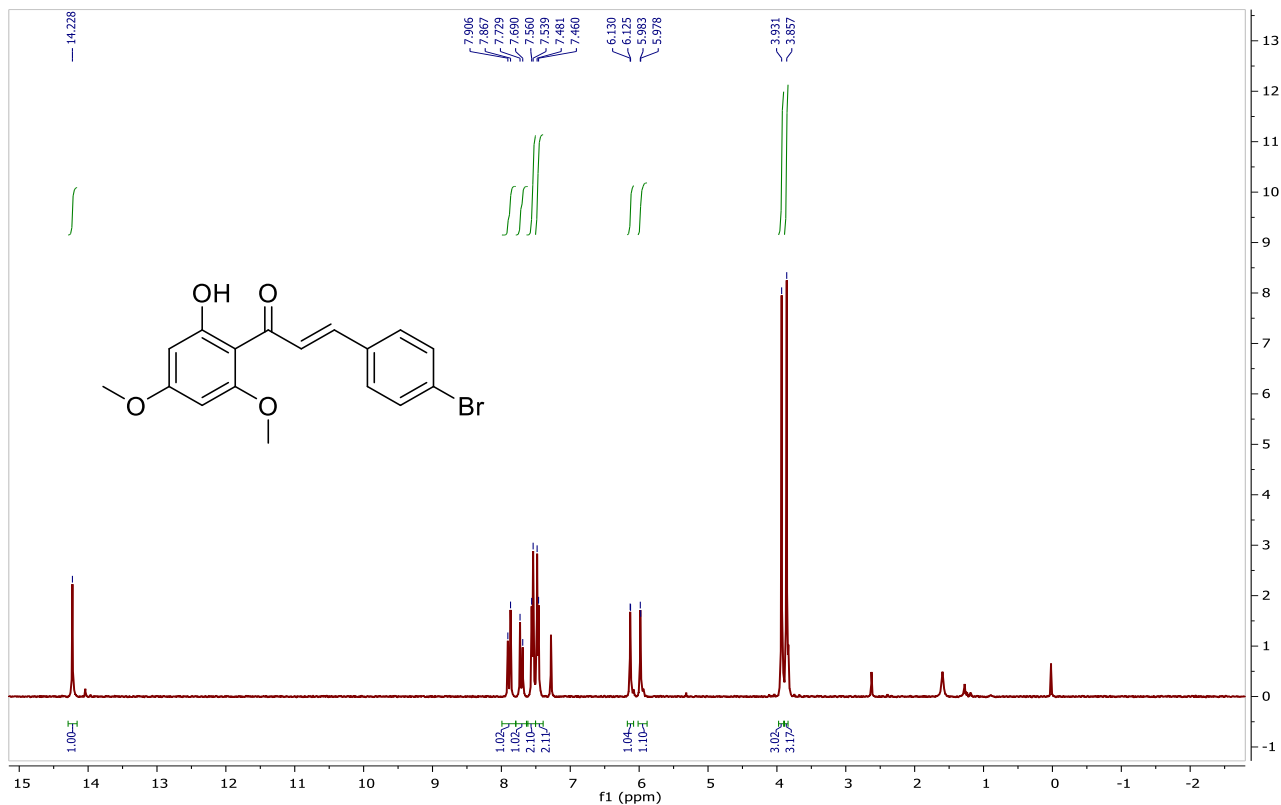
Figure S47. ^{1}H NMR spectrum of chalcone (6a) in CDCl$_3$, 400 MHz
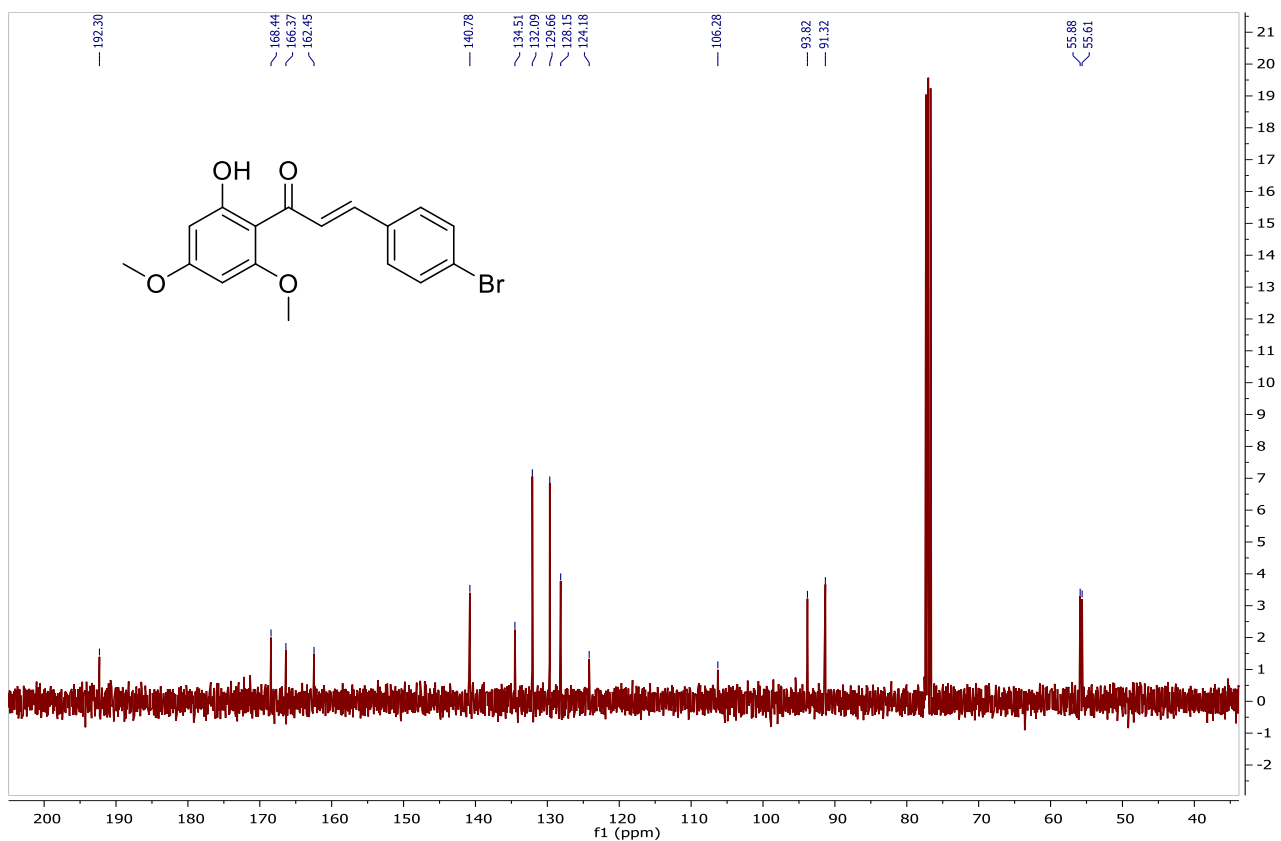
Figure S48. ^{13}C NMR spectrum of chalcone (6a) in CDCl$_3$, 100 MHz
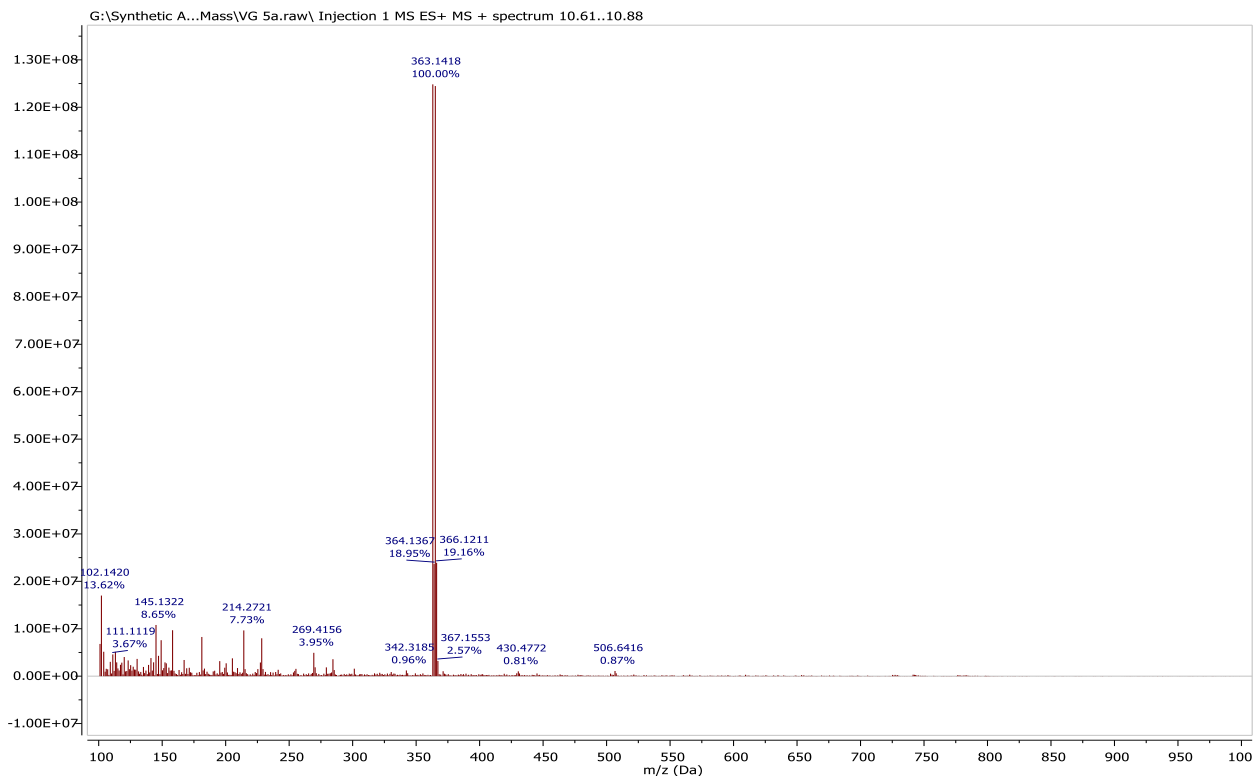
Figure S49. ESIMS spectrum of chalcone (6a).
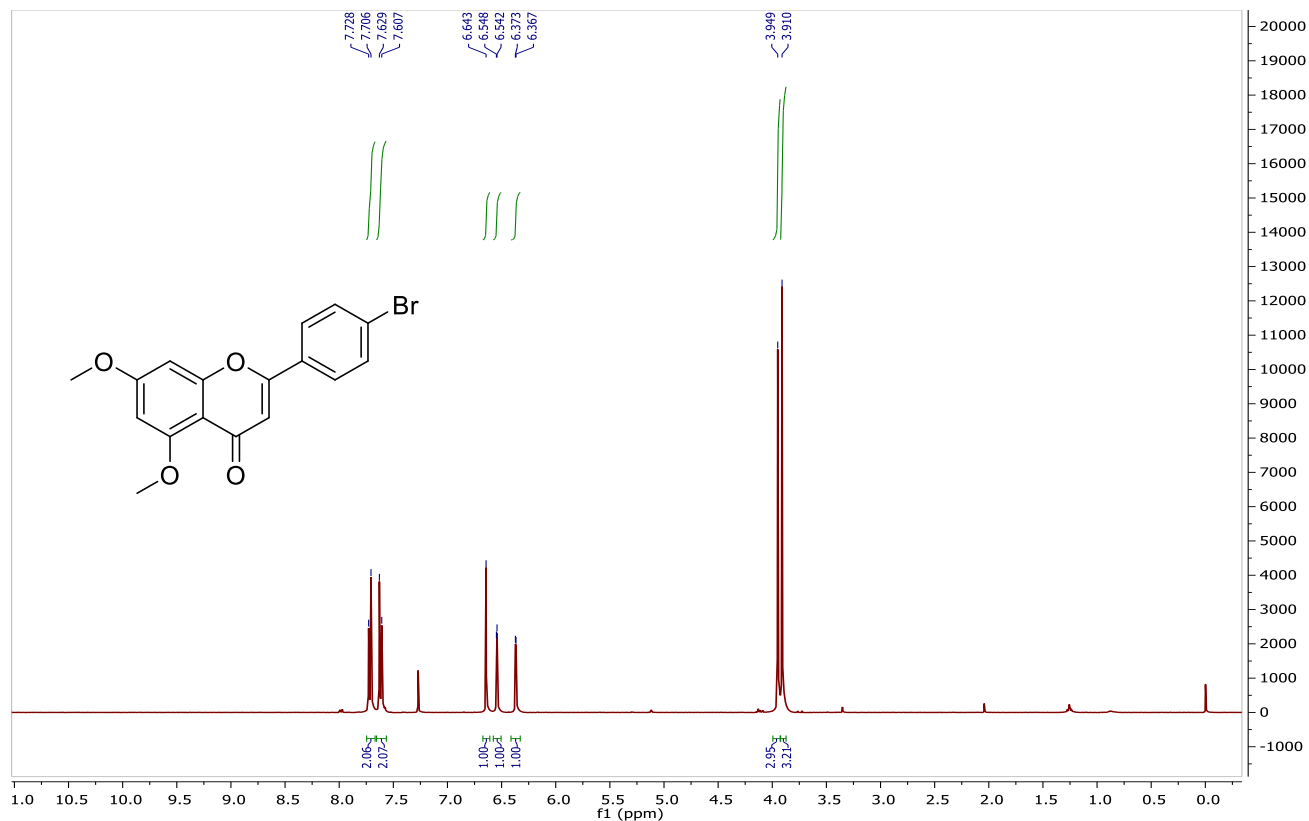
Figure S50. ¹H NMR spectrum of flavonoid (6b) in CDCl₃, 400 MHz
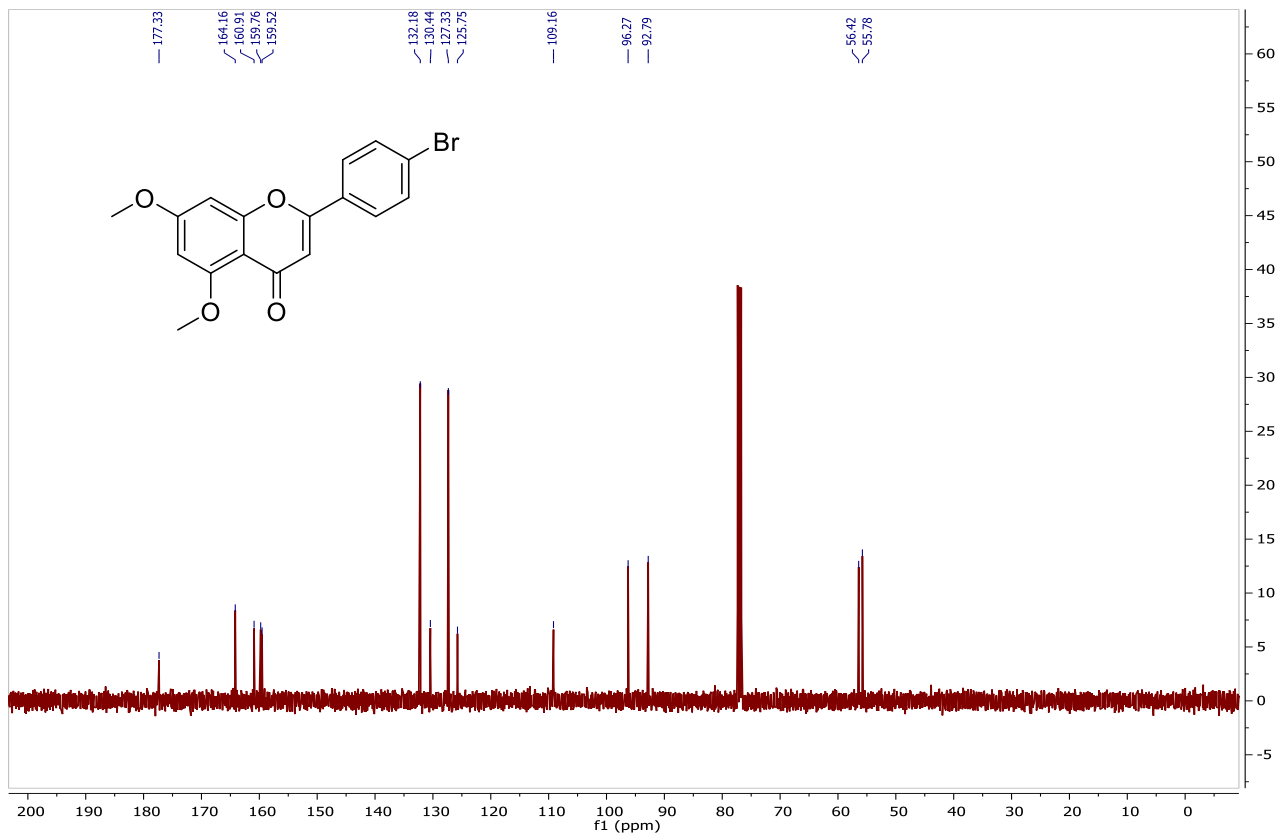
**Figure S51. ¹³C NMR spectrum of flavonoid (6b) in CDCl₃, 100 MHz**
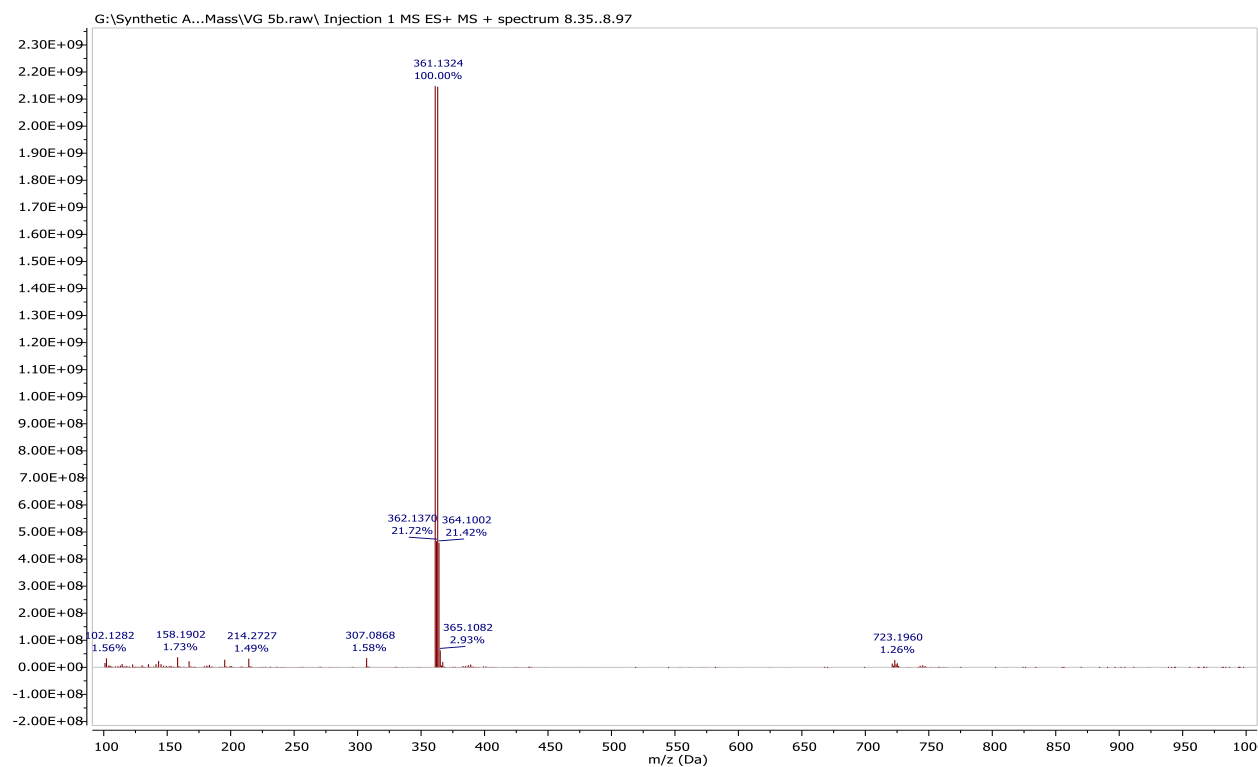
**Figure S52. ESIMS spectrum of flavonoid (6b).**
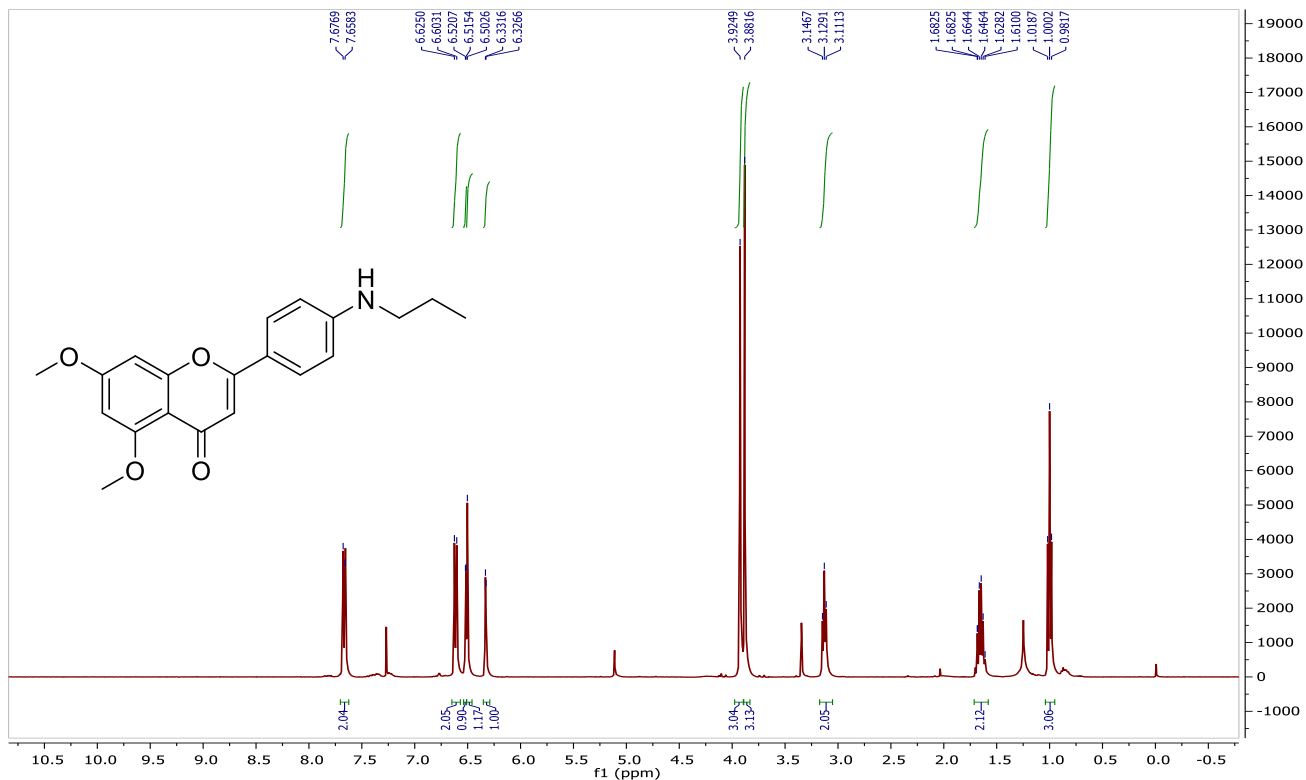
**Figure S53.** ^{1}H NMR spectrum of flavonoid (6c) in CDCl$_3$, 500 MHz
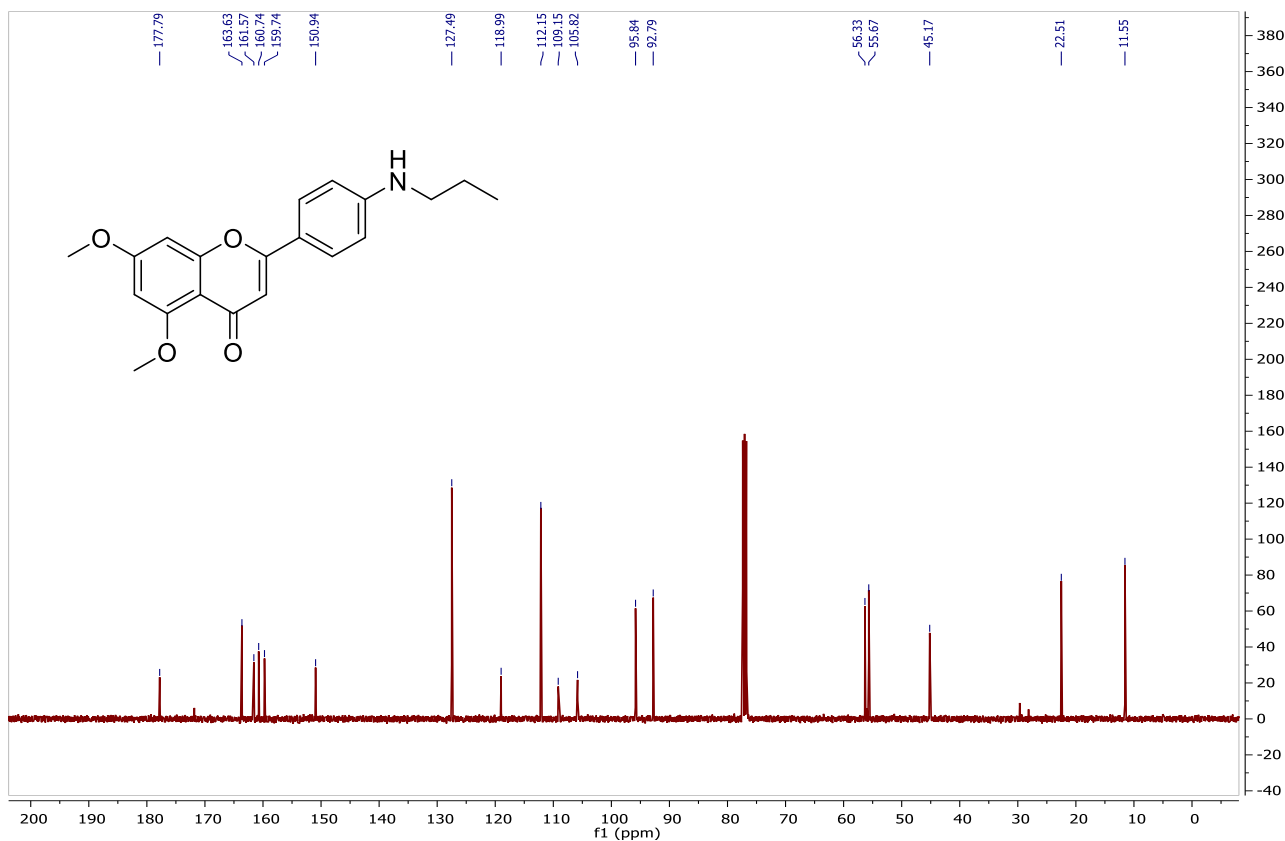
Figure S54. ^{13}C NMR spectrum of flavonoid (6c) in CDCl$_3$, 125 MHz
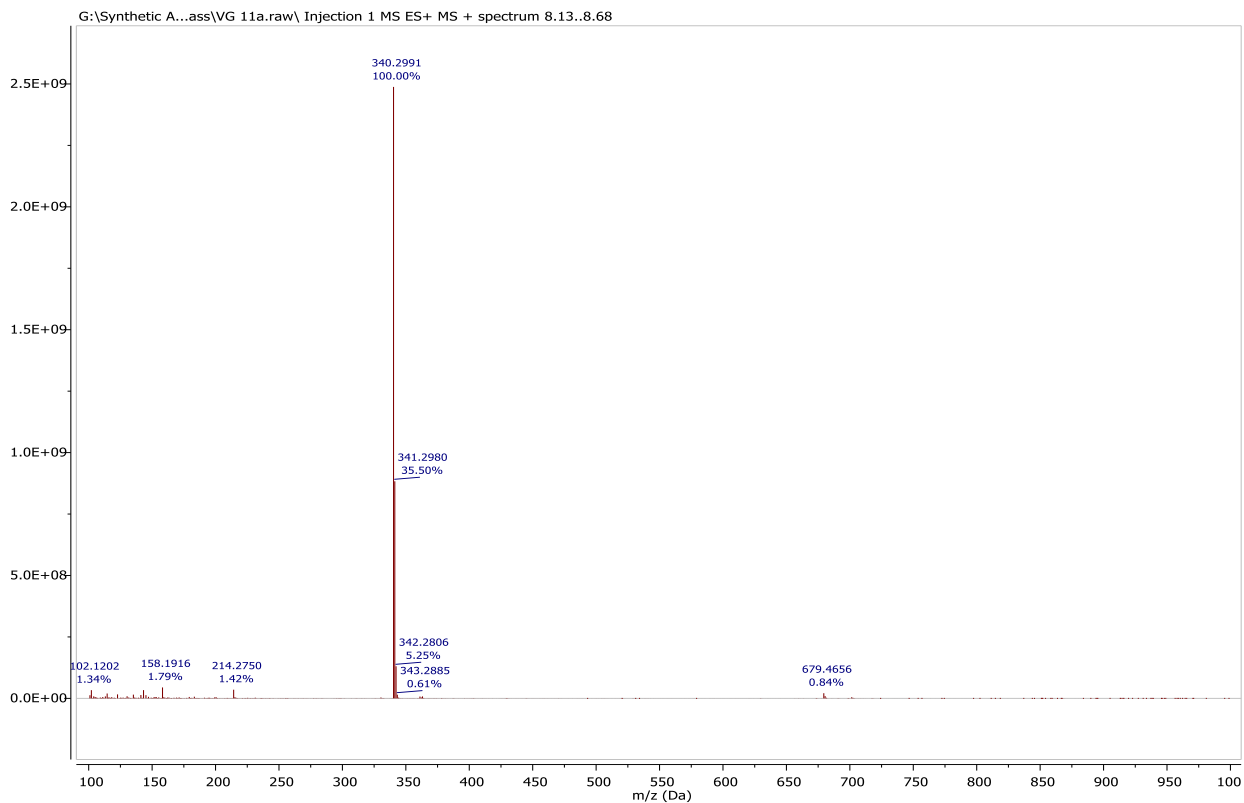
Figure S55. ESIMS spectrum of flavonoid (6c).
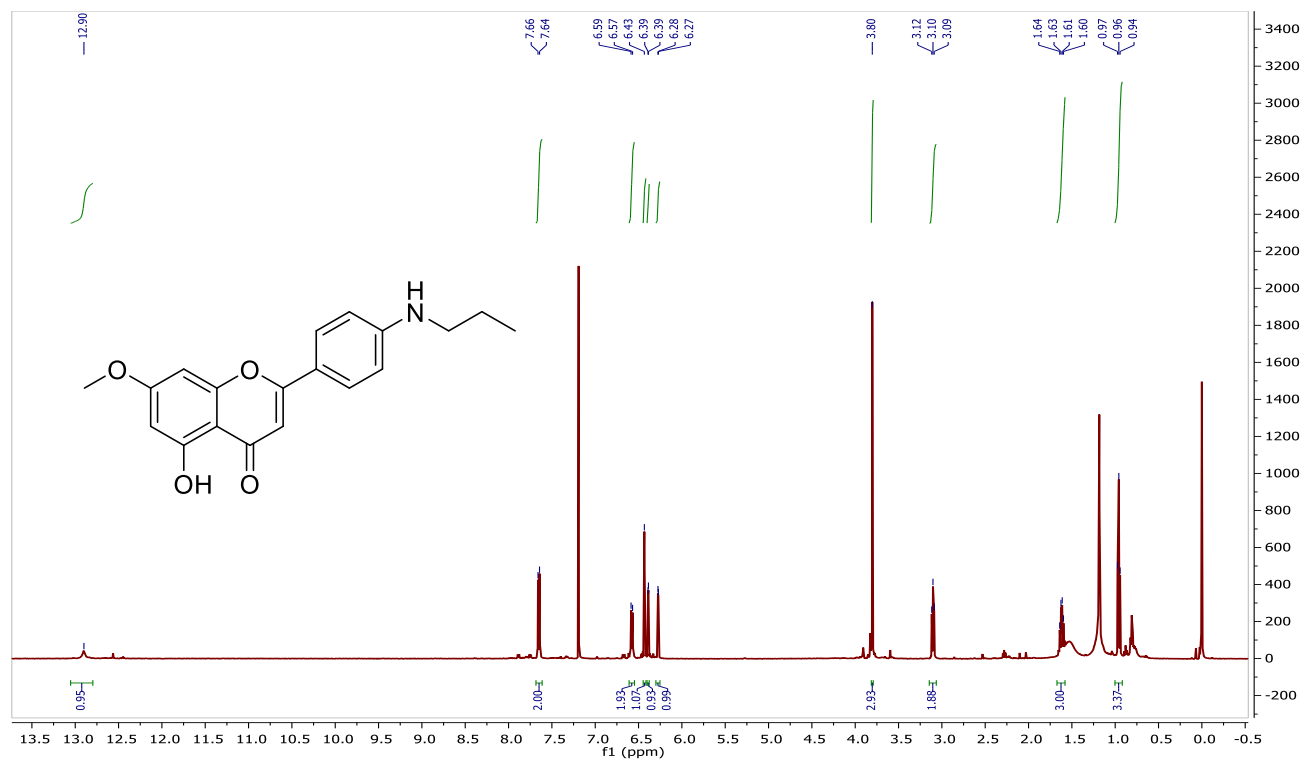
Figure S56. ^{1}H NMR spectrum of flavonoid (6d) in CDCl₃, 500 MHz

S30
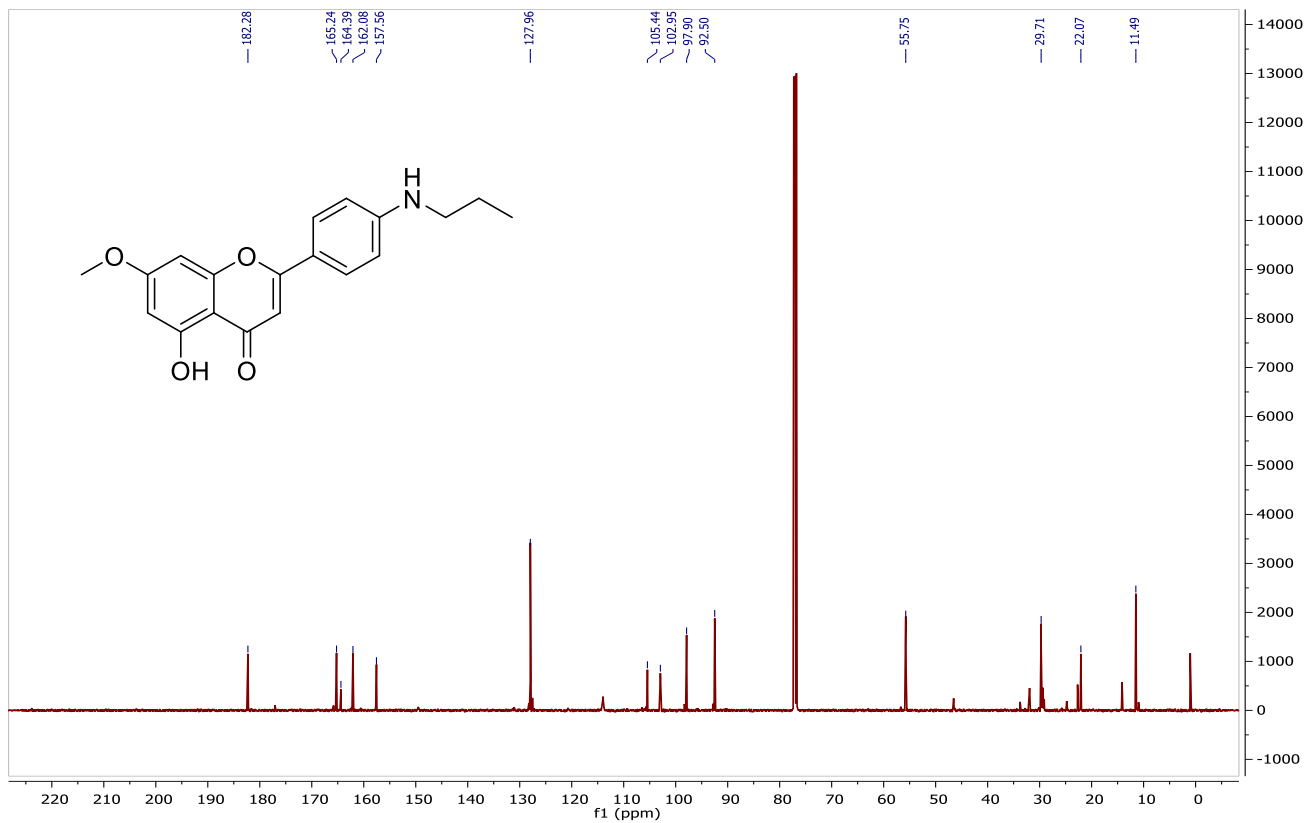
Figure S57. ^{13}C NMR spectrum of flavonoid (6d) in CDCl$_3$, 125 MHz
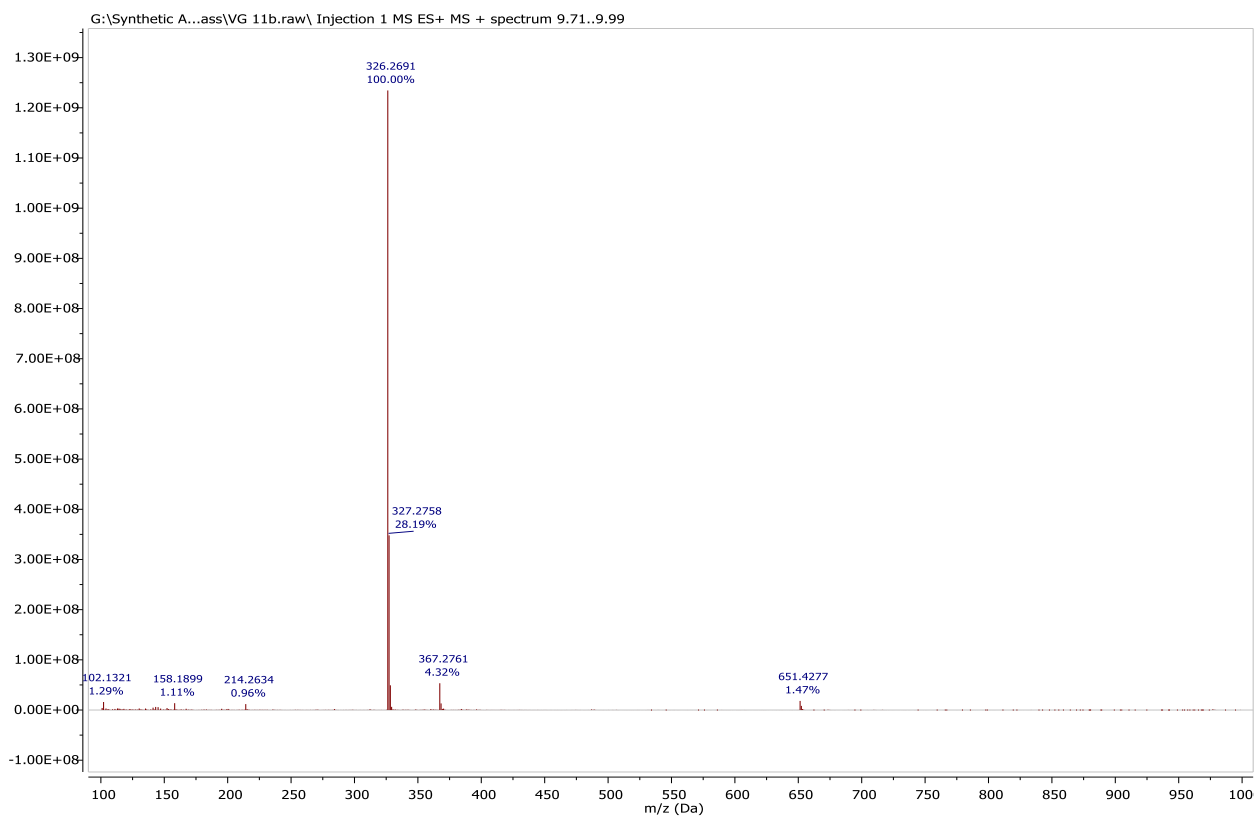
Figure S58. ESIMS spectrum of flavonoid (6d).
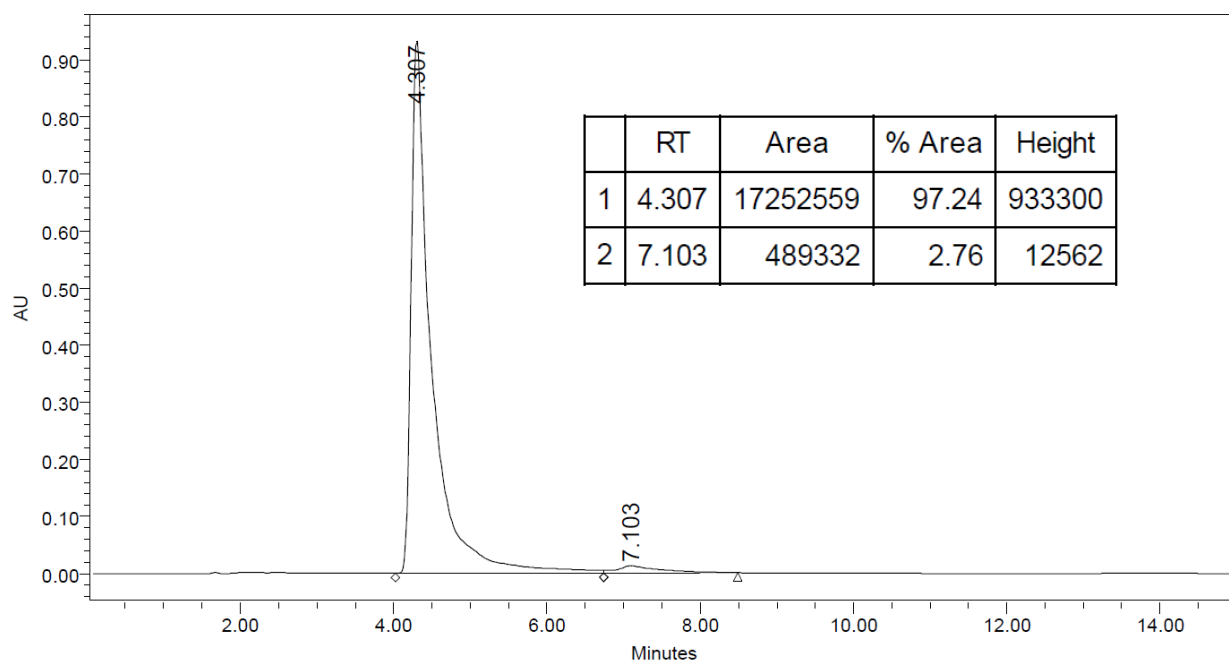
Figure S59. HPLC analysis of flavonoid (6d).
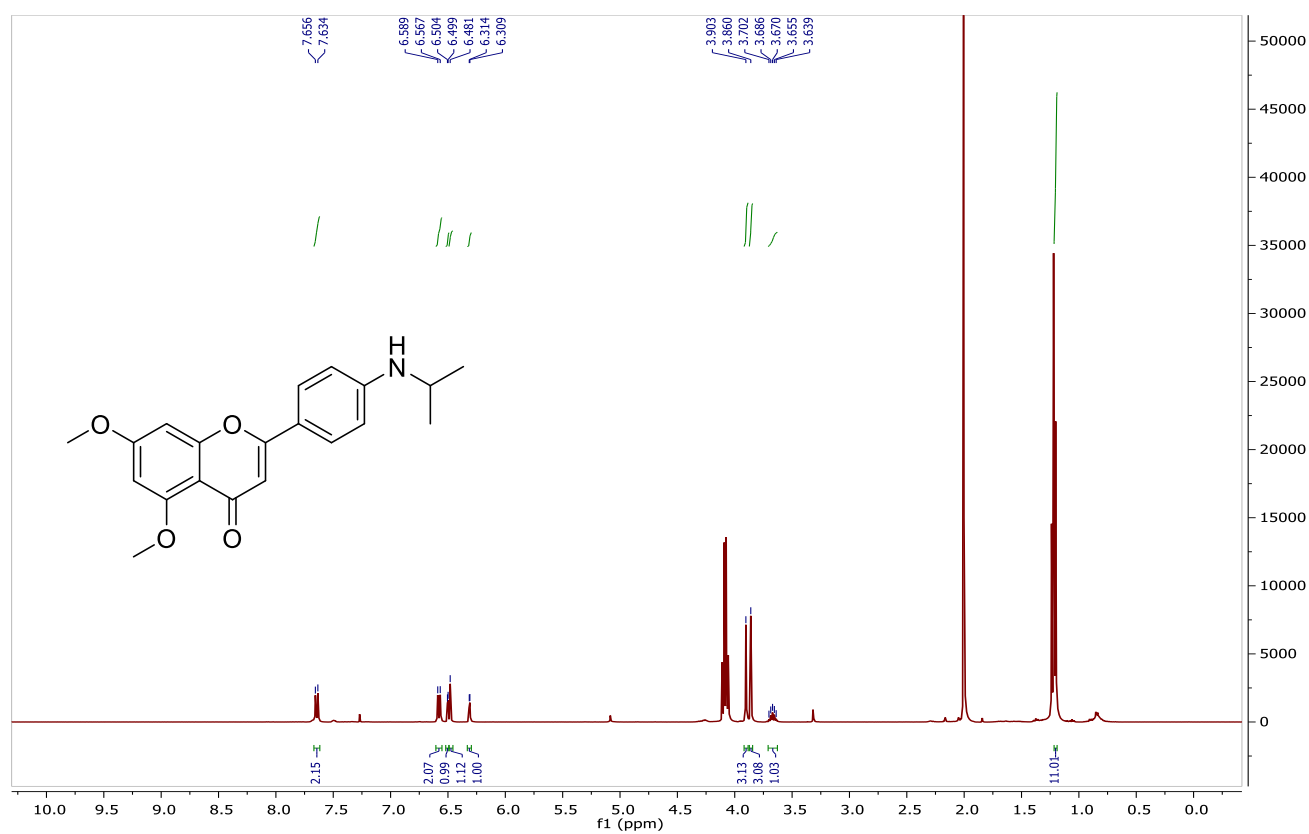
Figure S60. ^{1}H NMR spectrum of flavonoid (7c) in CDCl$_3$, 400 MHz
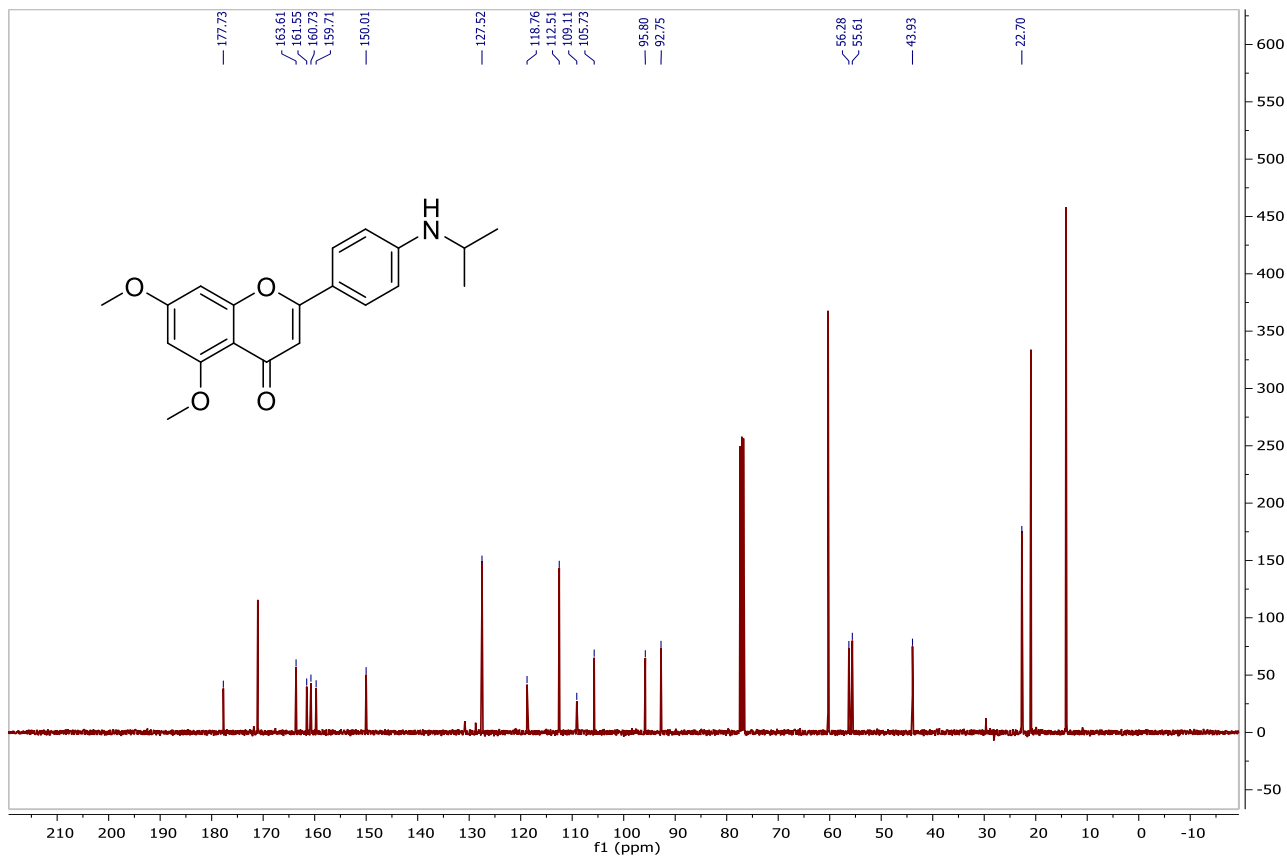
Figure S61. ^{13}C NMR spectrum of flavonoid (7c) in CDCl$_3$, 100 MHz
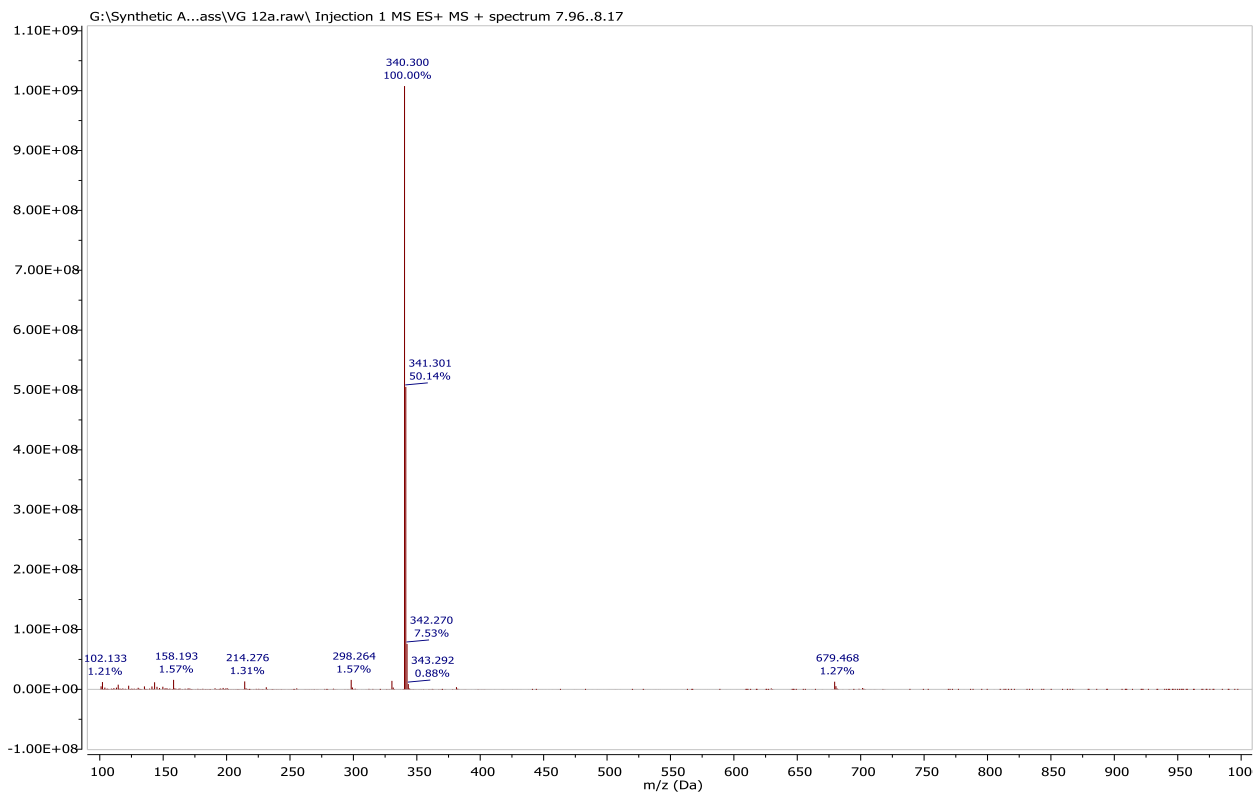
Figure S62. ESIMS spectrum of flavonoid (7c).
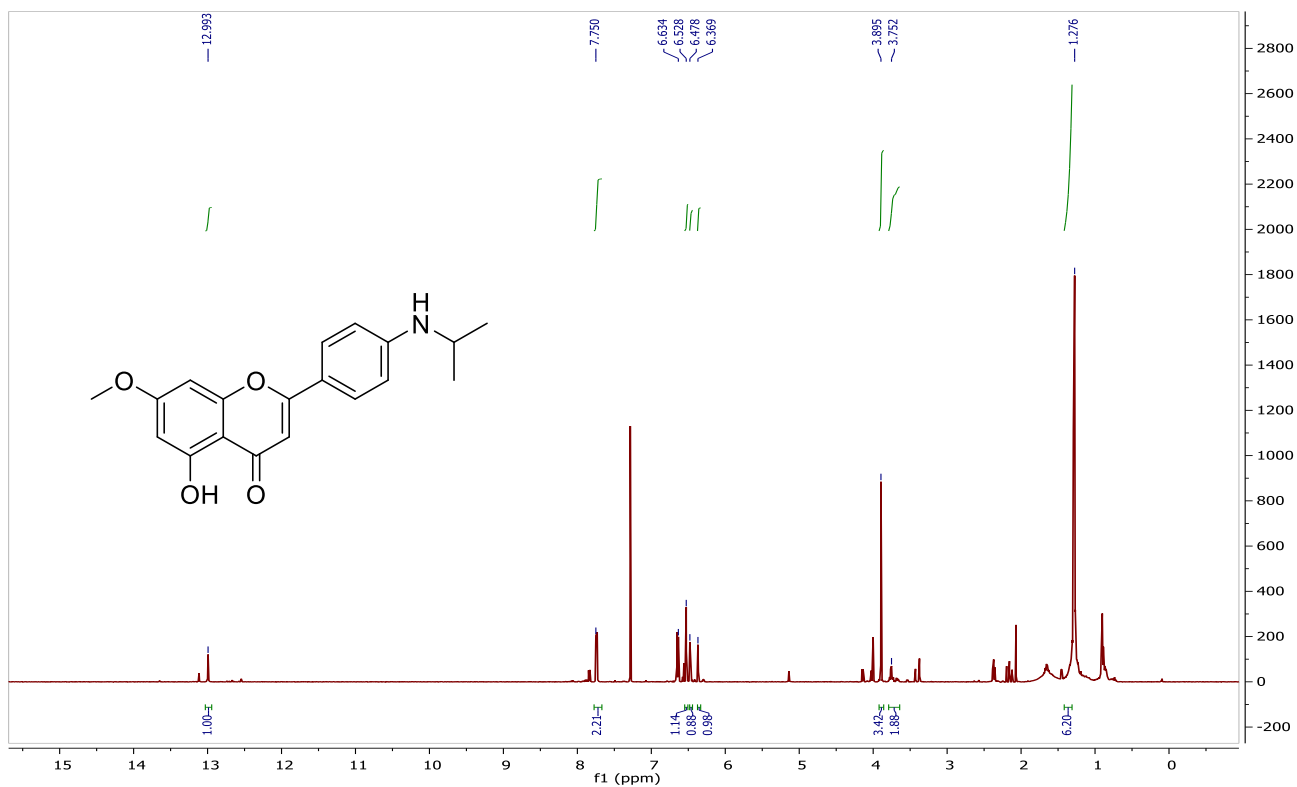
Figure S63. ^{1}H NMR spectrum of flavonoid (7d) in CDCl$_3$, 500 MHz
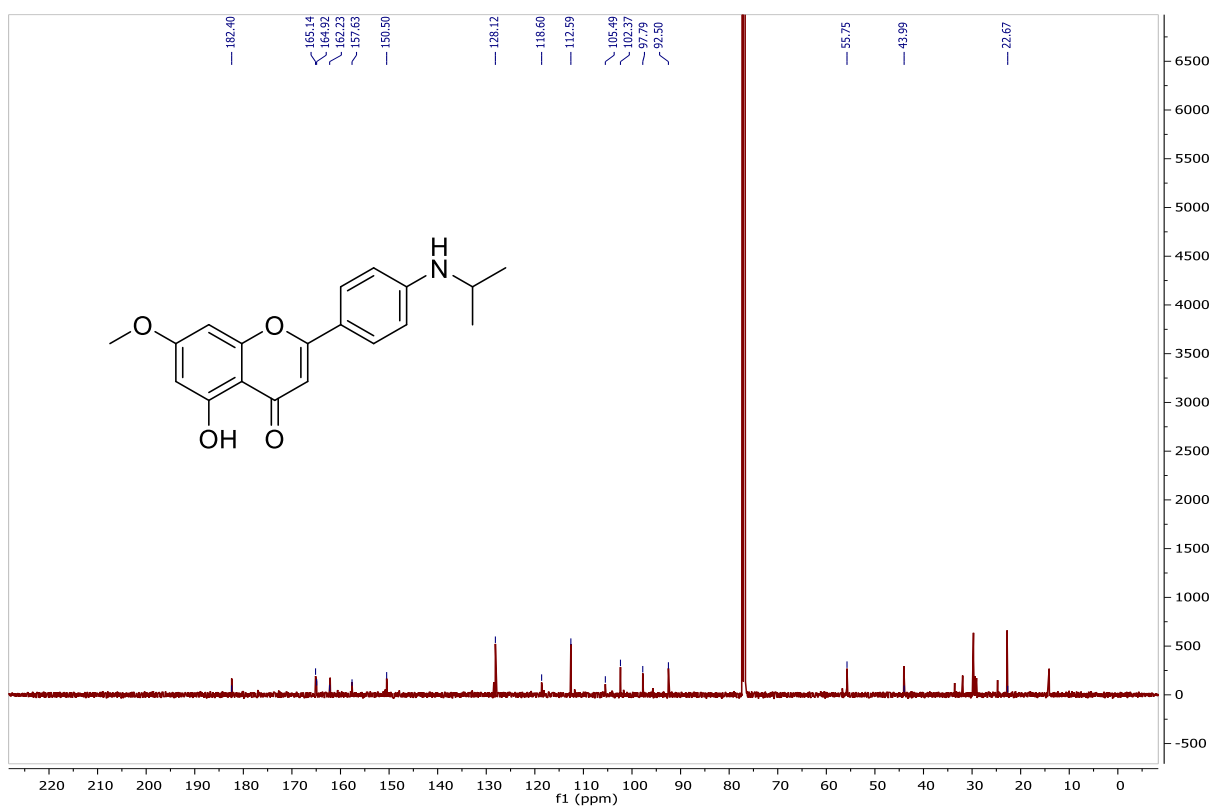
Figure S64. ^{1}H NMR spectrum of flavonoid (7d) in CDCl$_3$, 125 MHz
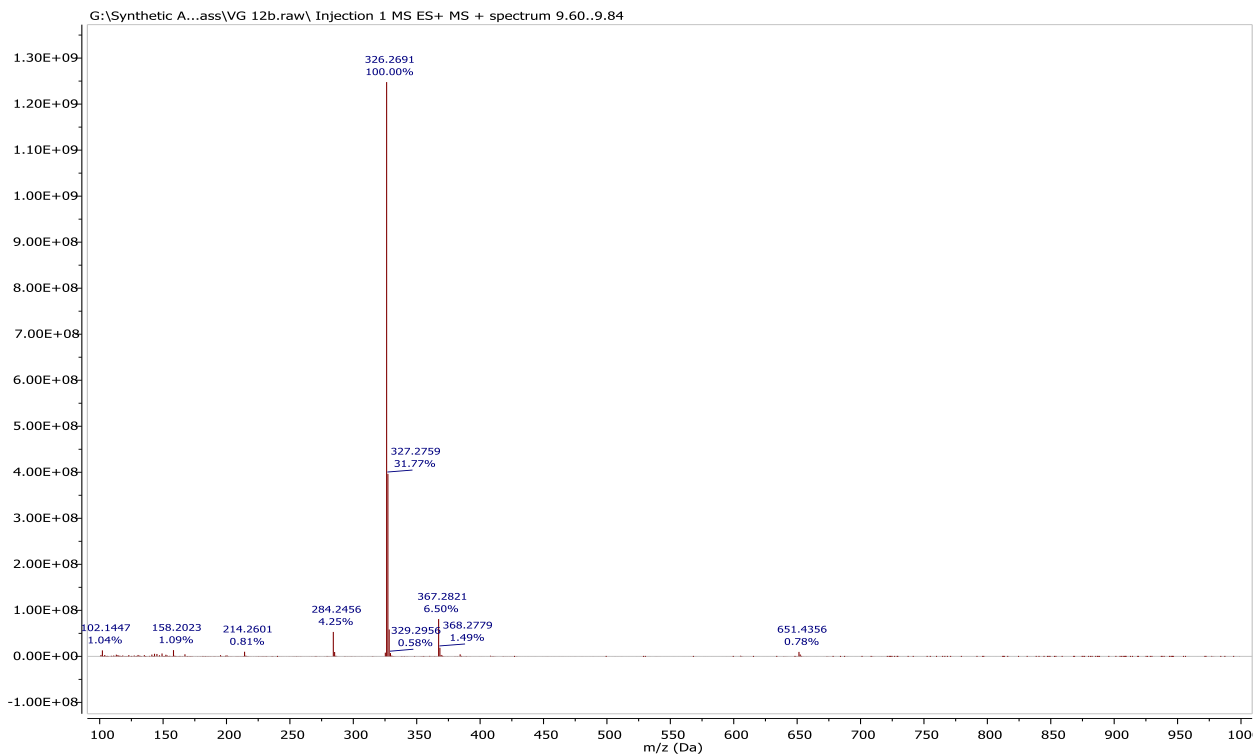
Figure S65. ESIMS spectrum of flavonoid (7d).

	RT	Area	% Area	Height
1	2.243	93465	1.04	8591
2	4.474	8915956	98.96	501399
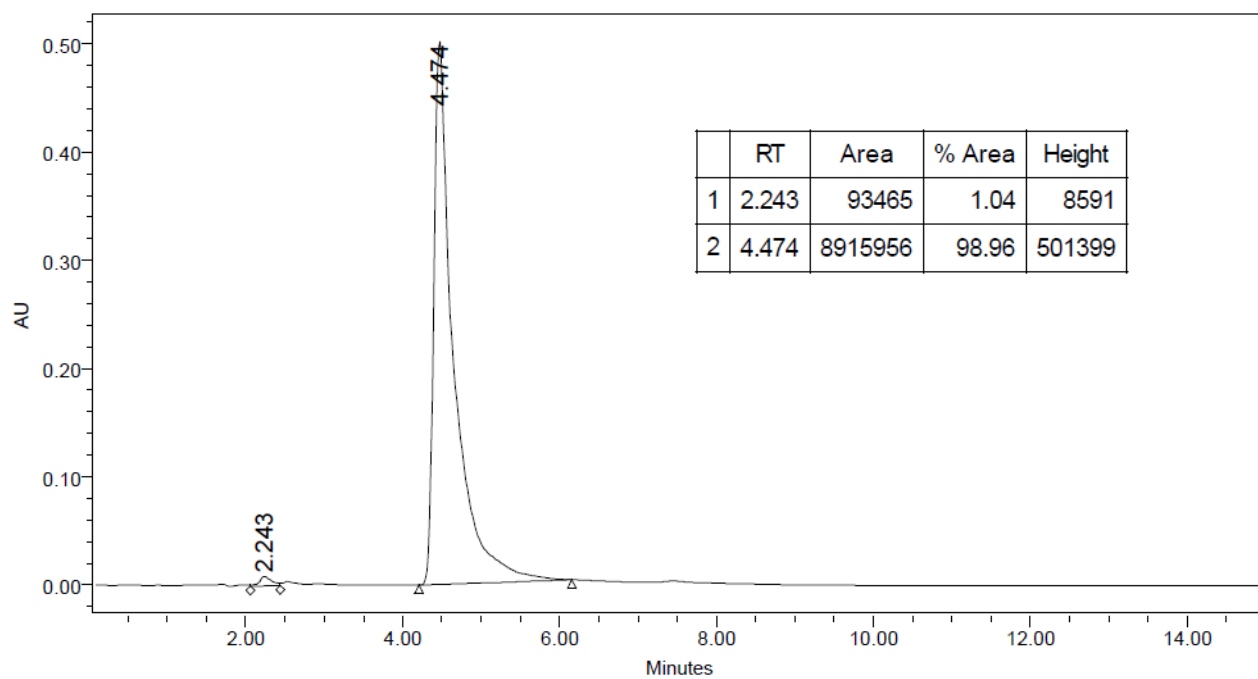
Figure S66. HPLC analysis of flavonoid (7d).
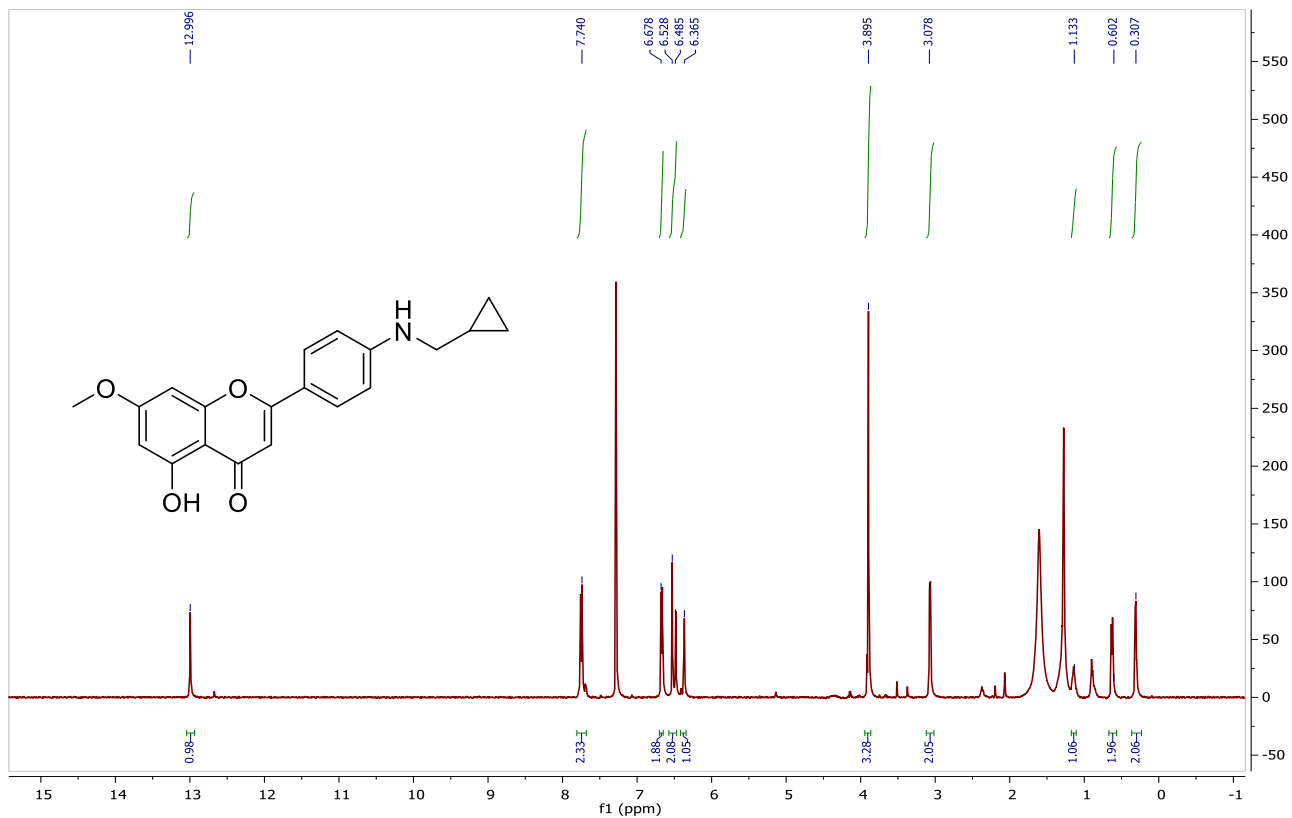
Figure S67. ^{1}H NMR spectrum of flavonoid (8d) in CDCl$_3$, 500 MHz
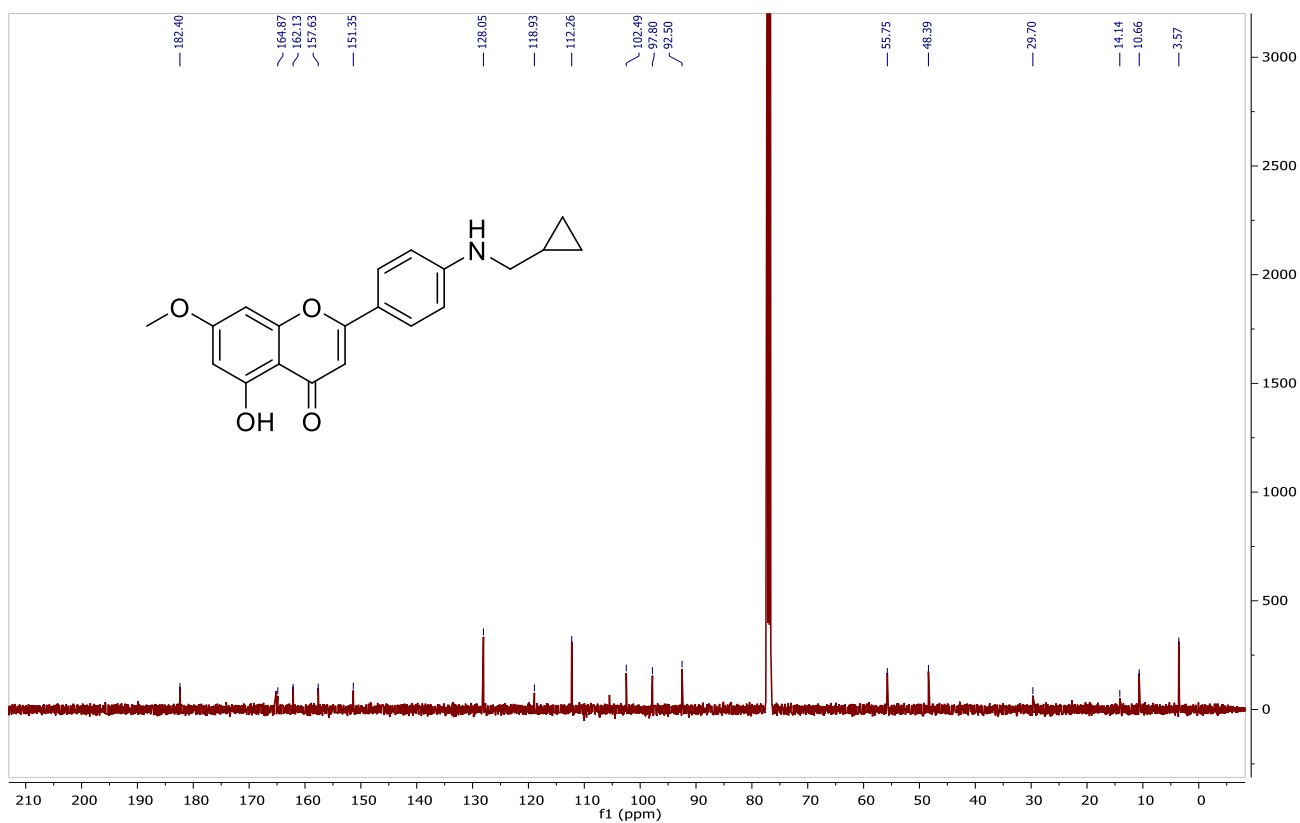
Figure S68. ^{1}H NMR spectrum of flavonoid (8d) in CDCl$_3$, 125 MHz
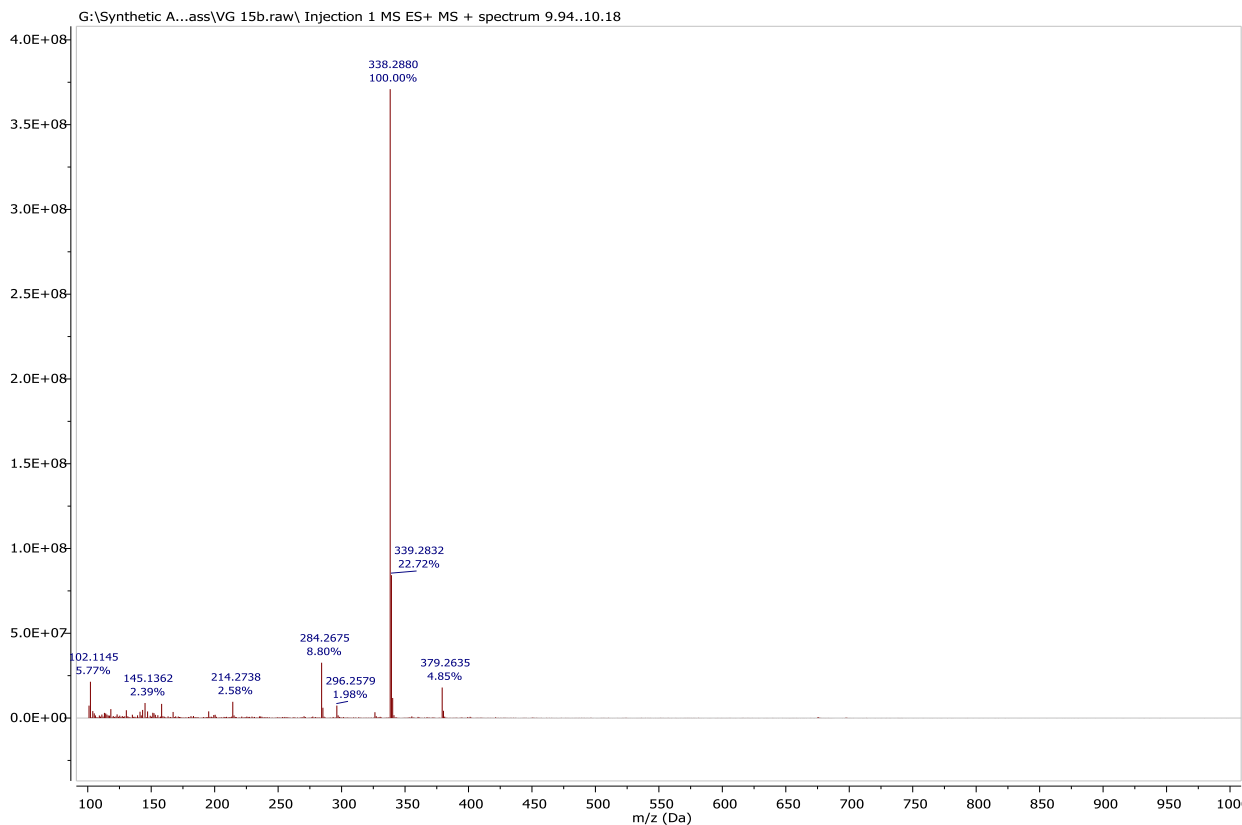
**Figure S69. ESIMS spectrum of flavonoid (8d)**

	RT	Area	% Area	Height
1	2.041	19203	2.59	1078
2	5.048	722712	97.41	38387
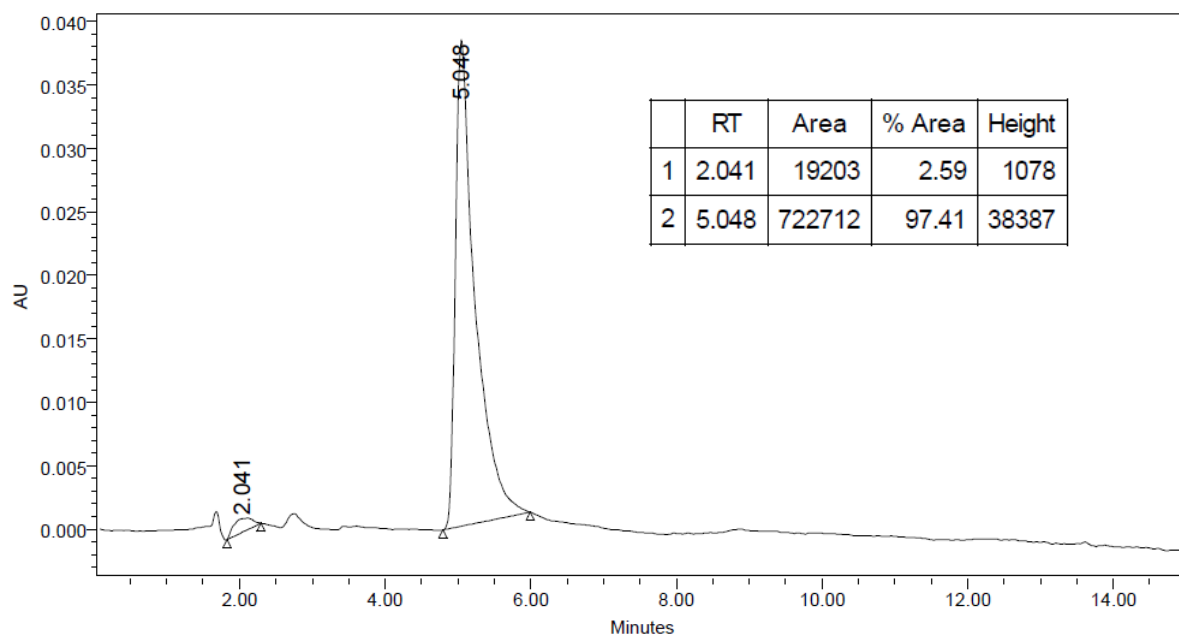
Figure S70. HPLC analysis of flavonoid (8d).

S37

Computational Interactions of Acacetin and MAO-A and MAO-B

To understand the binding behavior of acacetin in MAO-A and MAO-B binding sites, a long molecular dynamics (MD) simulation study (200 ns) was conducted. The interaction profile and the average changes in the heavy atom displacement of acacetin (Figure S71) were monitored over the course of the MD simulations time with respect to the original frame using the following equation:

$$RMSD_x = \sqrt{\frac{1}{N}\sum_{i=1}^{N}\left(r'_i(t_x) - r_i(t_{ref})\right)^2}$$

Frame x is recorded at time t_x; $RMSD_x$ is the root mean square deviation of selected atoms in frame x; N is the number of atoms; t_{ref} is the reference time; r_i' is the position of the selected atom (i) after aligning on the reference frame.
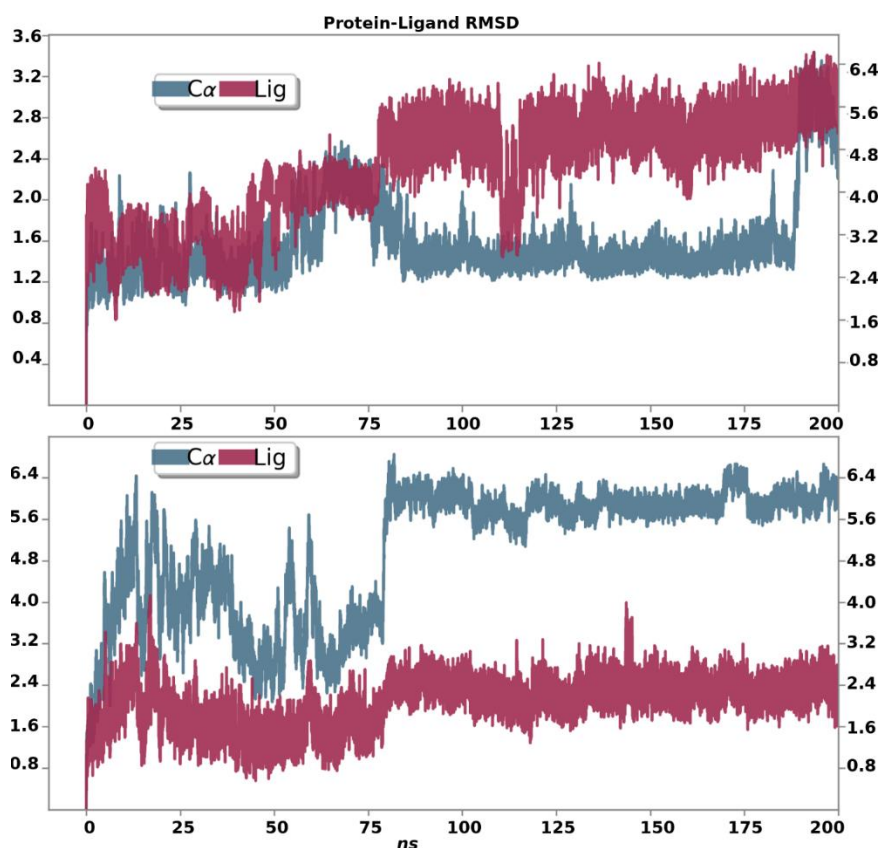
Figure S71. Protein-ligand RMSD. Top: RMSD of MAO-B. Bottom: RMSD of MAO-A.

Acacetin displayed stable binding in MAO-B with an average RMSD of 2.8 Å for the protein backbone and 6.0 Å for the ligand (Figure S71, top), while it has an average RMSD of 6.4 Å for MAO-A backbone and 2.4 Å for the ligand (Figure S71, bottom). Several prominent interactions were traced and averaged over the MD simulations. With MAO-A (Figure S72), there are two strong and highly abundant (over 95% of the MD simulations time) hydrogen bonds between the flavone hydroxyl group and Asn 181, and Tyr 444. These two hydrogen bonds are in the negative free energy

region of the water density calculations. Interrupting these interactions with bulkier and hydrophobic substituents would decrease binding to MAO-A. At the same position of MAO-B, there is one strong hydrogen bond with Thr 174 and π-π stacking with Tyr 398 (Figure S73). Modifying acacetin to have small hydrophobic groups at this position (R$_1$) should not alter MAO-B activity. In general, acacetin has stronger hydrogen bonds and more polar contacts with MAO-A, and more hydrophobic contacts with MAO-B (Figures S72-73).
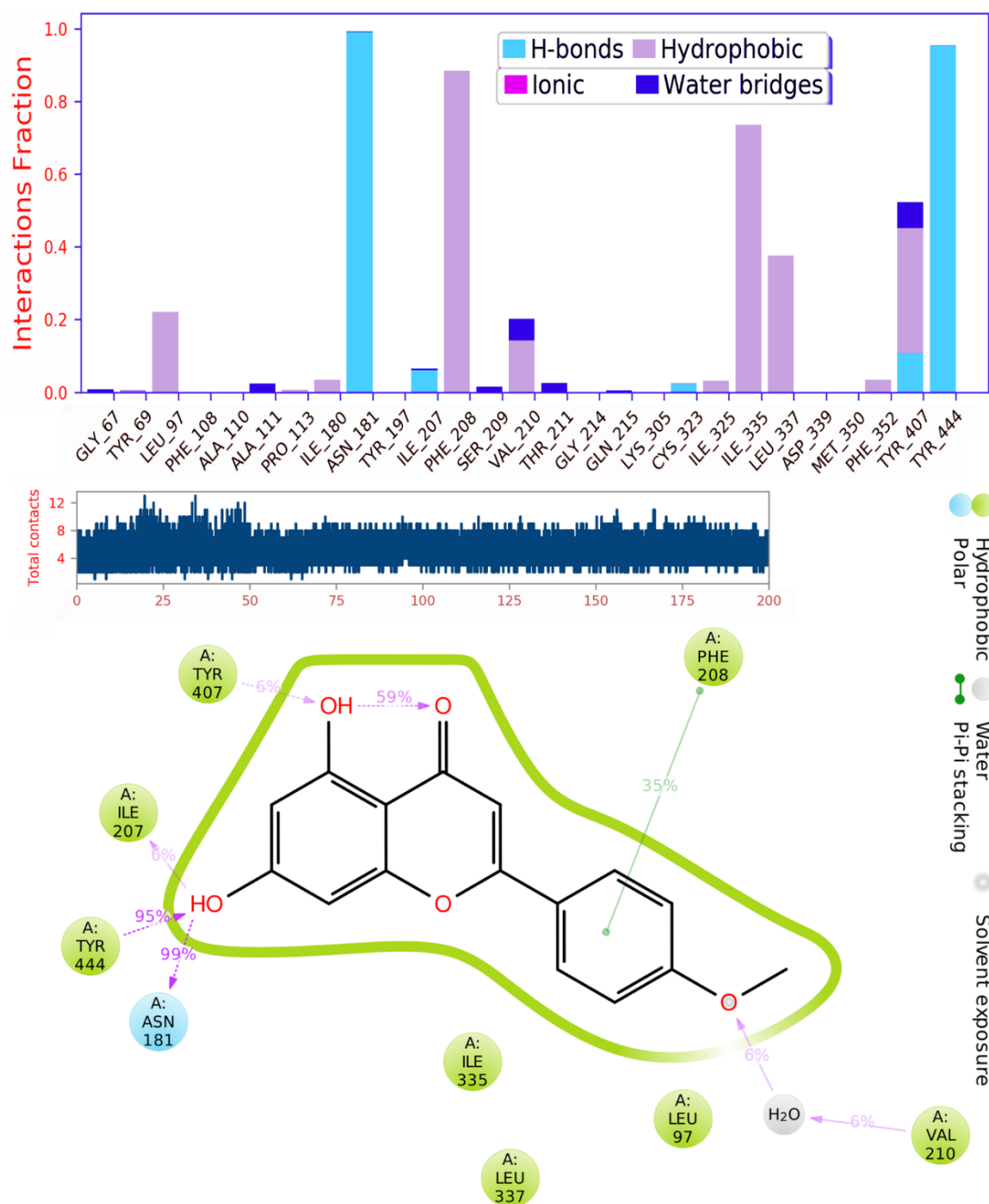
Figure S72 Interaction profile of acacetin in MAO-A.

Protein-Ligand Contacts
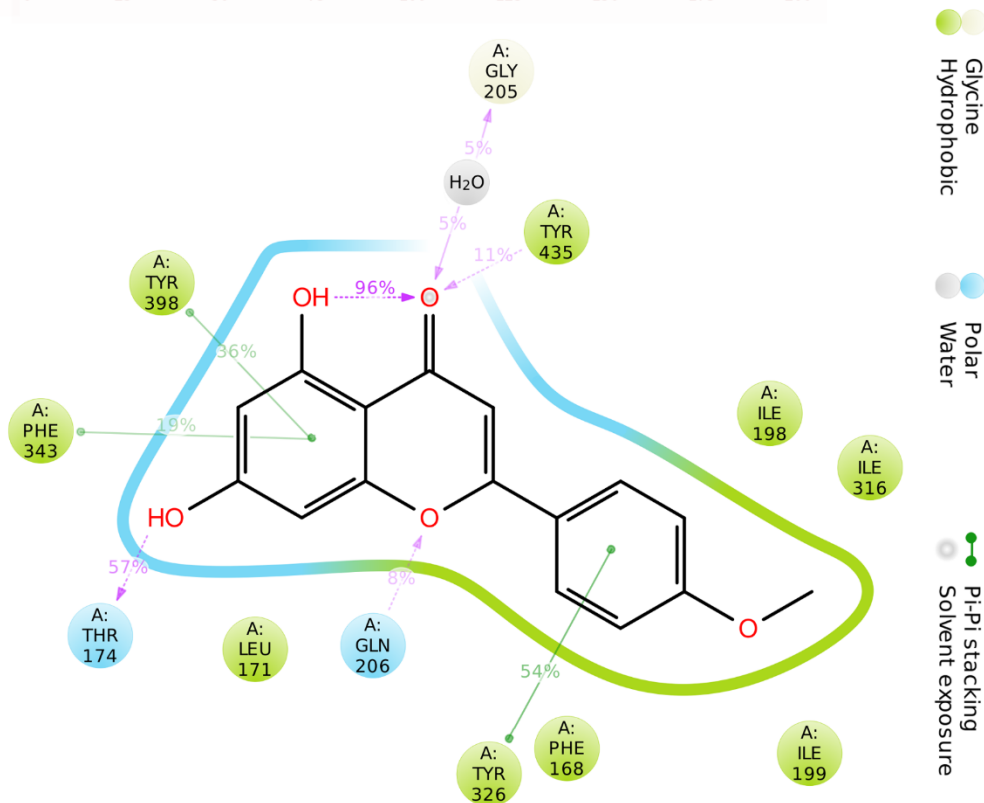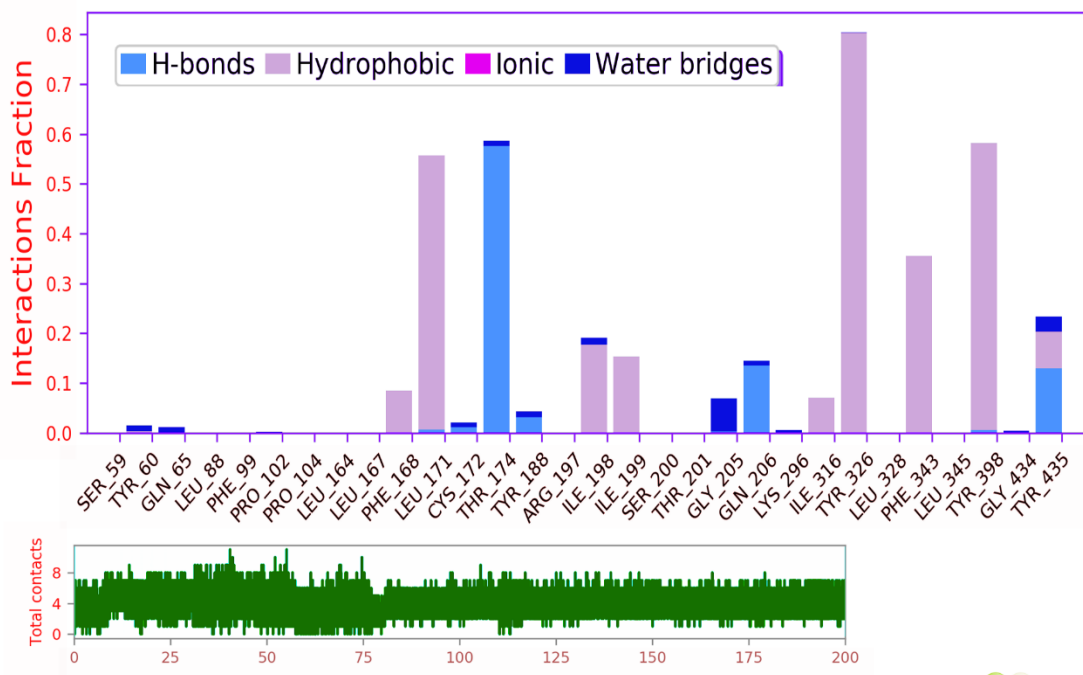
Figure S73. Interaction profile of acacetin in MAO-B.
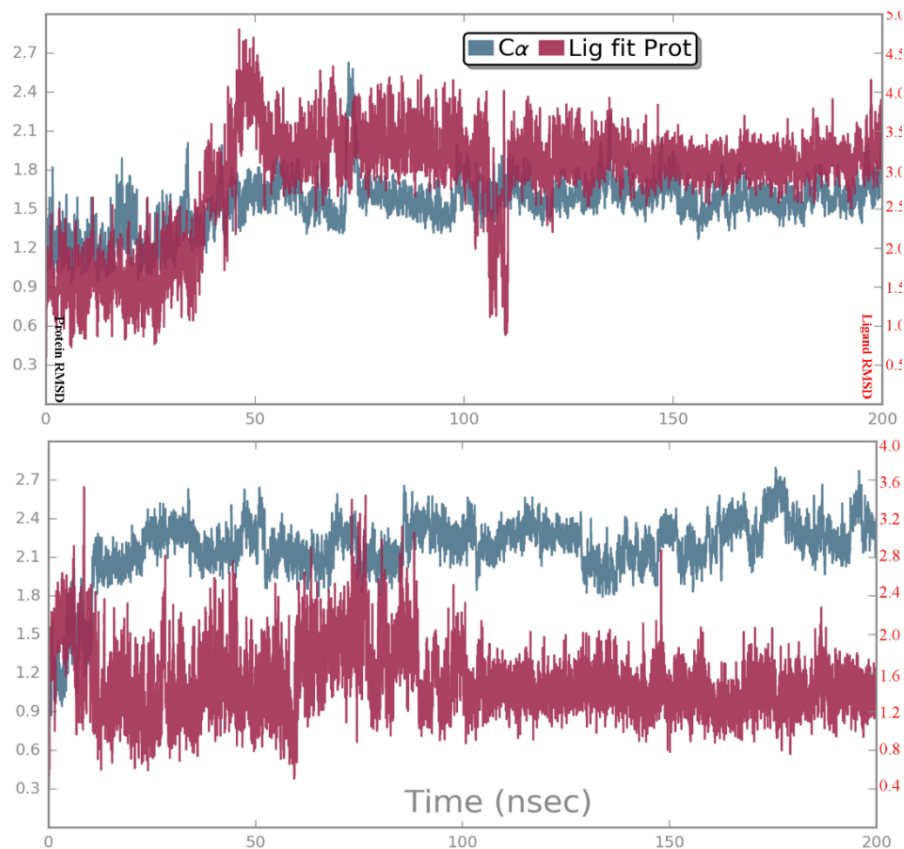
Figure S74. Protein and ligand RMSD. Top: RMSD of pose 1. Bottom: RMSD of pose 2 for acacetin 7-*O*-methyl ether.
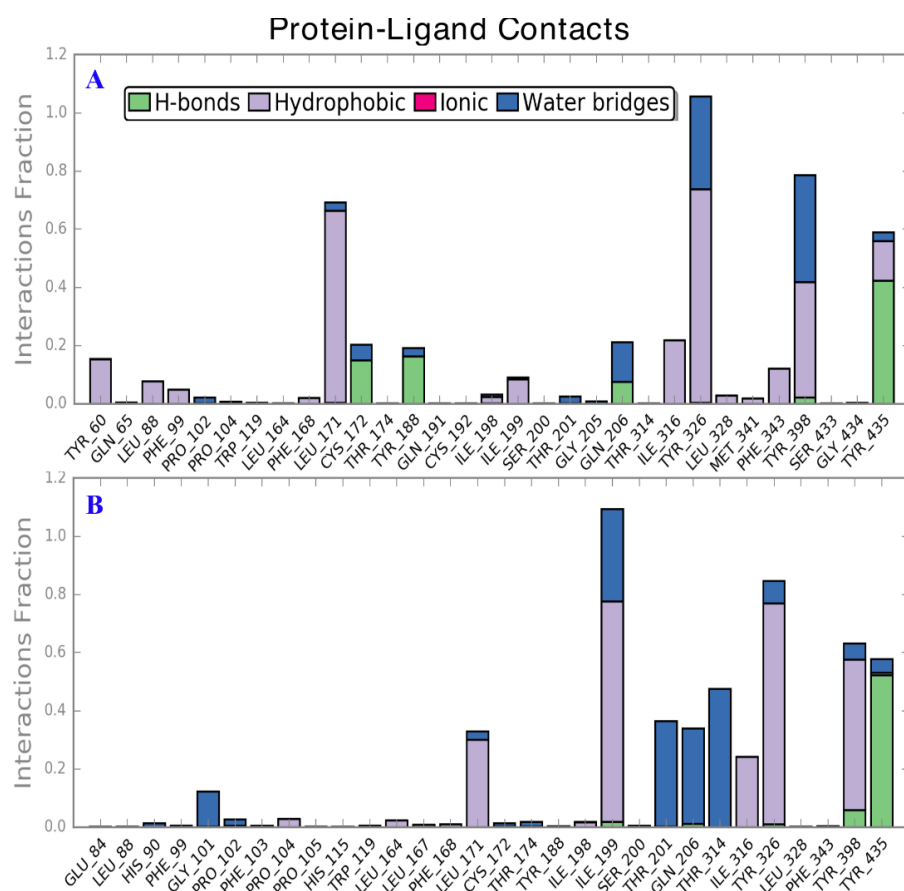
Figure S75. Protein-ligand contacts and their interaction fractions for pose 1 (A) and pose 2 (B) for acacetin 7-*O*-methyl ether.
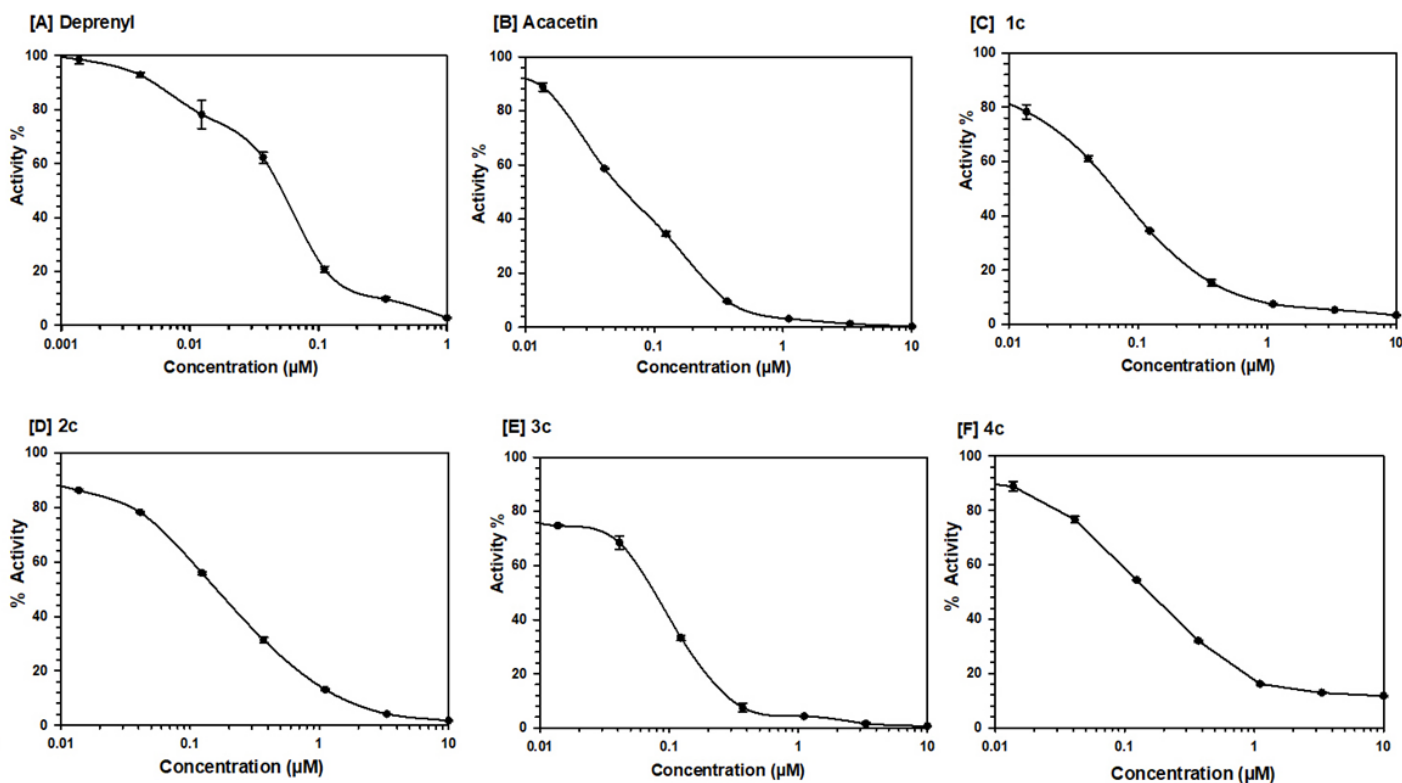
Figure S76. Dose-response profile for in vitro inhibition of recombinant human MAO-B by deprenyl, acacetin, and potent acacetin 7-*O*-methyl ether analogs (**1-4**) **c** (% activity vs concentration).
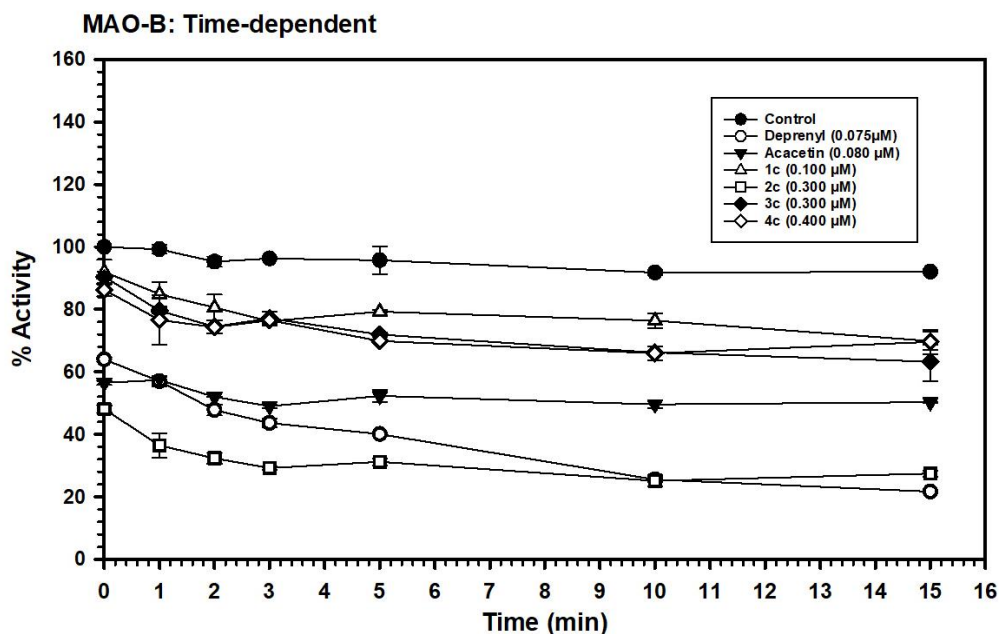
Figure S77. Time-dependent inhibition of recombinant human MAO-B by Deprenyl (0.075 μM), acacetin (0.080 μM), **1c** (0.100 μM), **2c** (0.300 μM), **3c** (0.300 μM), and **4c** (0.400 μM). Each point represents mean ± S.D. of triplicate values.

Table S1. Docking scores of acacetin 7-*O*-methyl ether analogs

Compound	MAO-A Docking score [kcal/mol]	MAO-B Docking score [kcal/mol]
1c	-3.511	-15.243
2c	-3.650	-15.102
3c	-2.732	-15.663
4c	-4.661	-15.545
5c	-5.434	-16.172
6d	-5.871	-15.451
7d	-3.221	-14.912
8d	-4.761	-16.084
Acacetin	-6.2	-8.1
Acacetin 7-*O*-methyl ether	-6.7	-8.9

Table S2. ADME Predictions for Acacetin Analogs

Compound	MW	SASA	QPlogPo/w	QPlogS	% Human oral absorption	PSA	#N and O	Rule of five	Rule of three
1c	326.348	618.778	4.020	-5.166	100.000	70.522	5	0	0
2c	326.348	611.087	3.963	-5.183	100.000	70.582	5	0	0
3c	340.375	640.381	4.359	-5.575	100.000	69.728	5	0	0
4c	322.317	592.458	3.835	-4.913	100.000	70.872	5	0	0
5c	338.359	637.061	4.249	-5.512	100.000	70.886	5	0	0
6d	325.363	621.141	3.834	-5.322	100.000	75.690	5	0	0
7d	325.363	612.923	3.797	-5.337	100.000	75.196	5	0	0
8d	337.374	639.249	4.059	-5.646	100.000	76.089	5	0	0
Acacetin	284.268	513.480	2.461	-3.824	87.477	85.418	5	0	0
Acacetin 7-*O*-methyl ether	298.295	537.958	3.141	-3.960	100.000	71.054	5	0	0
Harmine	212.251	444.308	3.082	-3.550	100.000	33.445	3	0	0
Deprenyl	187.284	454.187	2.993	-1.854	100.000	5.098	1	0	0
Clorgyline	272.174	547.929	4.044	-3.558	100.000	12.399	2	0	0

*MW: Molecular Weight; SASA: Solvent Accessible Surface Area; QPlogPo/w: Predicted octanol / water partition coefficient (Recommended values –2.0 to 6.5); QPlogS: Predicted aqueous solubility (log S Recommended values –6.5 to 0.5); PSA: Polar Surface Area.